

**APPLICATION OF REMOTE SENSING TECHNOLOGY AND ECOLOGICAL  
MODELING OF FOREST CARBON STOCKS IN MT. APO NATURAL PARK,  
PHILIPPINES**

A Dissertation

by

LIGAYA RUBAS LEAL

Submitted to the Office of Graduate and Professional Studies of  
Texas A&M University  
in partial fulfillment of the requirements for the degree of

DOCTOR OF PHILOSOPHY

Chair of Committee, J. Richard Conner  
Committee Members, Sorin Popescu  
Robert Washington-Allen  
Sergio Capareda  
Head of Department, Kathleen Kavanagh

May 2015

Major Subject: Ecosystem Science and Management

Copyright 2015 Ligaya Rubas Leal

## ABSTRACT

This dissertation work explored the application of remote sensing technology for the assessment of forest carbon storage in Mt. Apo Natural Park. Biomass estimation is traditionally conducted using destructive sampling with high levels of uncertainty. A more accurate and non-destructive method for assessment of biomass level is imperative to characterize remaining forest cover. This research study aimed to: 1) examine the vegetation profile and estimate species-specific biomass of Mt. Apo Natural Park, 2) develop an algorithm to assess biomass in plot-level using a terrestrial lidar system (TLS), and 3) generate landscape-level biomass estimates using interferometric synthetic aperture radar (IFSAR). This research endeavors to provide answers to these questions: 1) how the 3 tropical allometries compare in estimating field collected species-level biomass and carbon stocks in three management zones?, 2) what are the significant terrestrial laser scanning-derived metrics to assess plot-level biomass?, and 3) to what degree of uncertainty can IFSAR estimate biomass at the landscape level? Field data was gathered from 1382 trees, covering 52 local species during fieldwork in July and August 2013. Twenty-six plots (30 m x 30 m) were sampled on three management zones: multiple use, strict protection and restoration. Local insurgency problems restricted the research team from sampling additional plots. Destructive sampling was not permitted inside the protected area, thus requiring biomass to be estimated via the use of referenced biomass from 3 allometric equations by relating tree height, diameter-at-

breast height, and wood specificity volume. A vegetation profile across the park was generated using a canopy height map (CHM).

Results showed that resampled IFSAR products can be used to characterize biomass and carbon storage at the landscape level. This research has demonstrated the adoption of IPCC's Tier 2, a combination of field and remote sensing data in the assessment of available biomass levels in a tropical forest. The maps created can assist in providing information for biomass and carbon level in MANP for monitoring, reporting and verification in compliance with REDD requirements. Furthermore, this study can provide helpful information regarding policy implications for reforestation and afforestation activities.

## **DEDICATION**

Dedicated especially to my late Father, Clyde Romero Rubas, for his keen interest in my research.

I also dedicate this to my loving mother, Mrs. Cecilia Caldito Rubas, for her unceasing prayers, and words of love and wisdom.

My grand family: Beverly & Armand, Hazel & Armando, Lotis & Noel, Ramil, Lucille, Aurea, Clyde II, Aveline, Adriane & Arven Clyde.

Love and gratitude to my husband, Arturo Leal, and our forthcoming baby girl.

## **ACKNOWLEDGEMENTS**

I would like to thank my committee chair, Dr. Conner, and my committee members, Dr. Popescu, Dr. Washington-Allen, and Dr. Capareda, for their guidance and support throughout the course of this research. Thank you also for pooling your research funds to acquire the IFSAR data.

Special thanks to Dr. Conner for believing in me, and supporting me throughout my Ph.D. education.

Thanks to the TAMU funding to defray some fieldwork expenses: 2013 Harry Wayne Springfield Research Award and 2013 OGAPS Research Grant.

Thanks to my friends: Sasa, Ryan, Tony, Tan, and Fred, for the technical help in my times of need.

Thanks also to my Professors, the department faculty and staff for making my time at Texas A&M University a great experience.

I also want to extend my gratitude to the Department of Environment and Natural Resources (Regions XI and XII), which provided the research permit, and to the Philippine National Police of Region XII for providing the security escorts. Thanks also to my research assistants for the invaluable support during the rigorous fieldwork

activities. My research team members are: Beverly Rubas, Clyde Rubas II, Clark Rubas, Chadney Anastacio, Aurea Rubas, Harold Rubas, and Armand Atang.

I am also grateful for the assistance and kindness extended to us by the Energy Development Corporation, and for allowing us entry into the EDC sampling plots.

Finally, thanks to my loving parents and siblings for their encouragement and to my husband for his prayers, patience and love.

Above all, praise and honor to our Lord Almighty, whom all things come. I am so blessed.

## NOMENCLATURE

AGB	Aboveground Biomass
ALOS	Advanced Land Observing Satellite
AVHRR	Advanced Very High Resolution Radiometer
CGIAR	Consultative Group on International Agricultural Research
CO <sub>2</sub> Eq.	Carbon Dioxide Equivalent
DENR	Department of Environment and Natural Resources
ETM	Enhanced Thematic Mapper
GLC 2000	Global Land Cover 2000
GHG	Greenhouse Gas
GWP	Global Warming Potential
JAXA	Japan Aerospace Exploration Agency
JERS-1	Japan Earth Resource Satellite -1
ICRAF	International Council for Research in Agroforestry
IFSAR	Interferometric Synthetic Aperture Radar
IPCC	Intergovernmental Panel on Climate Change
IUCN	International Union of Conservation of Nature
ISODATA	Iterative Self-Organizing Data Analysis Technique
LANDSAT	Land Satellite
LGU	Local Government Unit

LIDAR	Light Detection and Ranging
LULUCF	Land-use, Land-use Cover and Forestry
MAFI	Mt. Apo Foundation, Inc.
MODIS	Moderate Resolution Imaging Spectroradiometer
NIPAS	National Integrated Protected Area System
PAMB	Protected Area Management Board
RADAR	Radio Detection and Ranging
REDD	Reducing Emissions from Deforestation and Degradation in Developing Countries
SPOT	Satellites Pour l'Observation de la Terre/Earth Observing Satellite
UNFAO	United Nations Food and Agriculture Organization
UNFCCC	United Nations Framework Convention on Climate Change
USGS	US Geological Survey
USEPA	US Environmental Protection Agency



## TABLE OF CONTENTS

	Page
ABSTRACT .....	ii
DEDICATION .....	iv
ACKNOWLEDGEMENTS .....	v
NOMENCLATURE .....	vii
TABLE OF CONTENTS .....	ix
LIST OF FIGURES .....	xii
LIST OF TABLES .....	xiv
CHAPTER	
I INTRODUCTION .....	1
1.1. Carbon Balance and International Agreements .....	1
1.1.1. Global Carbon Cycle .....	1
1.1.2. Greenhouse Gas Emissions & Carbon Sequestration.....	3
1.1.3. International Agreements on GHG Emissions.....	3
1.1.4. Intergovernmental Panel on Climate Change (IPCC).....	4
1.1.5. Global Forest Resource Assessment (FRA) .....	7
1.1.6. Tropical Forest Deforestation and Degradation.....	8
1.1.7. Tropical Deforestation and Biodiversity Hotspots .....	9
1.1.8. Protected Areas .....	11
1.2. Carbon Dynamics in the Philippines .....	12
1.2.1. The Study Area: Mount Apo Natural Park .....	13
1.2.2. Dissertation Rationale.....	16
1.2.3. Limitations of the Study .....	18
1.2.4. Organization of the Dissertation .....	18
II VEGETATION PROFILE AND BIOMASS ESTIMATES IN MT. APO NATURAL PARK .....	20

CHAPTER	Page
2.1. Introduction.....	20
2.1.1. Rationale.....	23
2.1.2. Objectives.....	24
2.1.3. Hypothesis .....	24
2.2. Review of Related Literatures .....	25
2.3. Data and Methods .....	27
2.3.1. Data Acquisition .....	27
2.3.2. Modelling for Referenced Biomass .....	29
2.3.3. Data Processing Flowchart .....	31
2.4. Results and Discussions.....	32
2.4.1. Habitat Type.....	33
2.4.2. Tree Height and Stem Diameter.....	34
2.4.3. IVI Index .....	37
2.4.4. Species-specific Biomass .....	38
2.4.5. Plot-level Biomass.....	40
2.5. Conclusions.....	42
III ASSESSMENT OF TROPICAL FOREST BIOMASS USING TERRESTRIAL LIDAR SYSTEM .....	45
3.1. Introduction .....	45
3.1.1. Rationale.....	46
3.1.2. Objectives.....	46
3.2. Review of Related Literatures .....	47
3.3. Data and Methods.....	50
3.3.1. Data Acquisition.....	50
3.3.2. Scan Pre-processing and Registration.....	51
3.3.3. Vegetation Height Metrics.....	52
3.3.4. Height and DBH Stem Maps.....	54
3.3.5. Field Biomass Generation .....	55
3.3.6. Data Processing Flowchart .....	56
3.4. Results and Discussions.....	56
3.4.1. Height Histograms .....	57
3.4.2. Scan Registration .....	58
3.4.3. Referenced Biomass .....	59
3.4.4. Biomass Estimation I.....	59
3.4.5. Biomass Estimation II.....	61
3.5. Conclusion .....	63

CHAPTER	Page
IV TROPICAL FOREST BIOMASS ACCOUNTING USING IFSAR SYSTEM.....	66
4.1. Introduction .....	66
4.1.1. Rationale .....	67
4.1.2. Objectives .....	67
4.2. Review of Related Literatures .....	68
4.3. Materials and Methods .....	70
4.3.1. SAR Data Acquisition .....	70
4.3.2. Methods .....	72
4.3.3. Data Processing Flowchart .....	74
4.4. Results .....	75
4.4.1. CHM Distribution Map.....	75
4.4.2. Biomass Modeling.....	76
4.4.3. IFSAR Height Calibration .....	82
4.4.4. Management Zone Mapping.....	83
4.4.5. Biomass and Carbon Mapping.....	83
4.4.6. Uncertainty Analysis.....	84
4.5. Discussion.....	85
4.6. Conclusion .....	90
V CONCLUSIONS .....	92
REFERENCES.....	95
APPENDIX A – FIGURES.....	123
APPENDIX B - TABLES .....	152
APPENDIX C – PRE-RESEARCH ACTIVITIES.....	175

## LIST OF FIGURES

FIGURE	Page
1-1 Location of MANP research site in the Philippines .....	123
1-2 Habitat map of Mt. Apo Natural Park.....	124
1-3 Vegetative cover map of Mt. Apo Natural Park .....	125
1-4 Management zone map of Mt. Apo Natural Park .....	126
2-1 Location of 26 study plots inside Mt. Apo Natural Park .....	127
2-2 Data processing flowchart for biomass estimation .....	128
2-3 Frequency distribution of tree height by management zones .....	129
2-4 Frequency distribution of stem diameter by management zones.....	130
2-5 IVI Index for top 20 ecologically important species .....	131
2-6 IVI index by management zone .....	132
2-7 Distribution of number of tree species or plot heterogeneity .....	133
3-1 Sampling plot design.....	134
3-2 Sayaban Elementary School DBH stem map.....	134
3-3 Sayaban Elementary School height stem map .....	135
3-4 Data processing flowchart for terrestrial laser scan data .....	136
3-5 Height histogram of Sayaban Elementary School (multiple use zone) .....	137
3-6 Point cloud image of Sayaban Elementary School (multiple use zone) .....	137

FIGURE	Page
3-7 Height histogram of Matiaw 1 (restoration zone).....	138
3-8 Point cloud image of Matiaw 1 (restoration zone).....	138
3-9 Height histogram of Lake Venado 2 (strict protection zone).....	139
3-10 Point cloud image of Lake Venado 2 (strict protection zone) .....	139
3-11 Regression model for maximum height from field and TLS data .....	140
3-12 Regression model for mean height from field and TLS data.....	140
4-1 Flowchart for IFSAR image and data processing .....	141
4-2 IFSAR CHM distribution map.....	142
4-3 Areas within the restoration zone .....	143
4-4 Areas within multiple use zone.....	143
4-5 Areas within strict protection zone .....	144
4-6 Scatterplot chart showing the empirical models to relate maximum IFSAR height and field-derived height .....	145
4-7 Mt. Apo management zone map overlaid with study plots .....	146
4-8 Mt. Apo biomass map measured in Mg ha <sup>-1</sup> .....	147
4-9 Mt. Apo forest and non-forest carbon map .....	148
4-10 Mt. Apo carbon stocks on management zone map .....	149
4-11 Comparing Philippines forest carbon values from this study to published materials.....	150
4-12 Global canopy maps from Saatchi et al (2011) and Baccini et al (2012) .....	150
4-13 PDF approximation for AGB residuals.....	151

## LIST OF TABLES

TABLE		Page
1-1	Compiled results of the total estimated carbon stocks in the Philippines. A compilation by Gibbs et al. (2007).....	152
1-2	Scientific papers examined on carbon storage in selected areas in the Philippines.....	152
2-1	Profile of study plots by land cover type .....	153
2-2	Classification of the study plots by management zone .....	153
2-3	Distribution of study plots by elevation and habitat type .....	153
2-4	Descriptive statistics by management zone .....	153
2-5	Test for Normality for height and DBH.....	154
2-6	Frequency distribution for 52 local tree species .....	154
2-7	Species-specific biomass estimates for ten leading species.....	155
2-8	Actual mean biomass by DBH class .....	156
2-9	Plot-level mean biomass .....	157
2-10	Carbon stock estimates by management zone .....	158
2-11	Carbon stock estimates by land cover type.....	158
3-1	Selected studies on uncertainties of tropical AGB estimation.....	159
3-2	Classification of field plots by management zone .....	159
3-3	Point cloud registration results.....	159
3-4	Lidar point cloud data of each plot .....	159
3-5	List of regression variables .....	160

TABLE	Page
3-6	Lake Venado 1 plot biomass using quadratic-mean-stem-diameter .... 161
3-7	Referenced biomass from three allometric equations ..... 162
3-8	Plot-level carbon stock estimates by management zone ..... 162
3-9	Summary of regression results using percentile heights ..... 163
3-10	GLM model regression results using percentile heights (Brown, 1997) ..... 164
3-11	GLM model regression results using percentile heights (Chave et al., 2005) ..... 165
3-12	GLM model regression results using percentile heights (Ketterings et al., 2001) ..... 166
3-13	Summary of regression results using normalized height bins ..... 167
3-14	Stepwise regression results using normalized height bins (Brown, 1997) ..... 167
3-15	Stepwise regression results using normalized height bins (Chave et al., 2005) ..... 168
3-16	Stepwise regression results using normalized height bins (Ketterings et al., 2001) ..... 168
4-1	Selected papers on biomass estimation in tropics using SAR technology ..... 169
4-2	Intermap’s STAR-3i technical specifications ..... 169
4-3	Specifications of Intermap’s core products ..... 169
4-4	2013 IFSAR Product Accuracy ..... 170
4-5	Relating field height and CHM-derived height by management zones ..... 170
4-6	Regression variables for 5 modelling tiers ..... 170
4-7	Regression results using standard least squares in JMP software ..... 171

TABLE	Page
4-8	Regression results using stepwise regression in JMP statistical software..... 171
4-9	Standard least squares regression model using calibrated IFSAR cubic convolution..... 172
4-10	Average biomass values in management zones ..... 172
4-11	Compilation of results for the total estimated carbon stocks in the Philippines (Gibbs et al., 2007)..... 172
4-12	Scientific paper examined on carbon storage in selected areas in the Philippines..... 173
4-13	Comparison of methods for global carbon maps ..... 173
4-14	Hypothesis tests for distribution comparison of residuals and AGB residuals ..... 174
4-15	Hypothesis tests for normality of distribution for residuals..... 174



## CHAPTER I

### INTRODUCTION

Why are ecologists interested in carbon? We can cite two reasons, first, half the dry weight of plants and animals, including humans, is carbon and secondly, carbon in the form of carbon dioxide (CO<sub>2</sub>) is the leading greenhouse gas released to the atmosphere from human activities.

#### 1.1. Carbon Balance and International Agreements

##### 1.1.1. Global Carbon Cycle

The carbon cycle is a complex system of biological, chemical and physical processes. In plants, carbon is brought into the terrestrial biosphere through photosynthesis. Carbon accumulation occurs in the net primary production (NPP), measured as the difference between photosynthesis and respiration. NPP quantifies the conversion of atmospheric CO<sub>2</sub> into plant biomass (Running *et al.*, 2004). Carbon is released back to the atmosphere through respiration, decomposition, fires, and some human land use practices (Foley and Ramankutty, 2003).

The amount of carbon stored in the terrestrial biosphere is the result of the balance between NPP, and carbon losses through decomposition, land use, fires and other disturbances. There is a net sink of carbon when carbon accumulated through net primary productivity exceeds the amount of carbon released to the atmosphere. A net

source occurs when more carbon is released to the atmosphere through respiration, fire, land use and disturbances than is accumulated via NPP.

The global carbon cycle has focused on the imbalance in the carbon budget or the missing carbon. Houghton et al. (1998) developed an equation for the global carbon balance:

Atmospheric increase

$$\begin{aligned} &= \text{fossil fuel} + \text{net emissions from changes in land use} \\ &- \text{oceanic uptake} - \text{residual terrestrial sink} \end{aligned} \quad (\text{Eq. 1})$$

In 1980s, the average annual emissions of 7.1 Pg C were higher than the 5.3 Pg C average annual accumulation of carbon in the atmosphere. The average annual emissions of 7.1 Pg C come from  $5.5 \pm 0.5$  Pg from combustion of fossil fuels, and  $1.6 \pm 0.7$  Pg C for changes in land use. The average annual accumulation of 5.3 Pg C carbon comes from  $3.3 \pm 0.2$  Pg of carbon uptake from the atmosphere, and  $2.0 \pm 0.8$  Pg C yr<sup>-1</sup> of annual oceans uptake. An additional sink of 1.8 Pg C yr<sup>-1</sup> is required for balancing the carbon budget.

The global carbon cycle considered regrowth of forests following previous disturbance, CO<sub>2</sub> fertilization and nitrogen fertilization as contributing to the missing sink (Houghton et al., 1998). The atmospheric CO<sub>2</sub> increases more rapidly in warm years, and less rapidly in cool years, which implies a positive feedback of climate-carbon system.

### 1.1.2. Greenhouse Gas Emissions & Carbon Sequestration

Greenhouse gases trap infrared radiation in the form of heat in the atmosphere. The United States Environmental Protection Agency (EPA) listed carbon dioxide as the major greenhouse gas (GHG) emitted in 2012 (Hofmann et al., 2006). Other greenhouse gases are methane (CH<sub>4</sub>), nitrous oxide (N<sub>2</sub>O), and fluorinated gases. CO<sub>2</sub> enters the atmosphere through the burning of fossil fuels, solid waste, wood products, vegetation respiration, and cement manufacturing. During forest clearing and forest fires, the stored above- and belowground carbon in biomass and litter is released to the atmosphere. Forest clearing, mostly in the tropics, is a major source of CO<sub>2</sub> emitted to the atmosphere (Canadell et al., 2007).

CO<sub>2</sub> is sequestered from the atmosphere through photosynthesis. A metric measure, carbon dioxide equivalent, was adopted by US-EPA to compare the emissions from various GHGs based upon their global warming potential (US-EPA, [www.epa.gov](http://www.epa.gov)). Carbon dioxide equivalents are expressed as “million metric tons of carbon dioxide equivalents” (MMTCO<sub>2</sub> Eq).

### 1.1.3. International Agreements on GHG Emissions

There are two leading international agreements that address the issue of greenhouse gas emissions in the atmosphere: the United Nations Framework Convention on Climate Change (UNFCCC) and the Kyoto Protocol ([www.unfccc.org](http://www.unfccc.org)). Both agreements have focused on assessing land cover changes and have initiated activities to address data and monitoring shortcomings. Whereas, the UNFCCC did not explicitly

stipulate levels to which member- countries should agree to reduce GHG emissions, the Kyoto Protocol specifically stated that emissions should be reduced by at least 5% below the 1990 levels by 2008-2012. The Kyoto Protocol had two commitment periods: 2005-2012 and 2012-2020. In 2012, the Protocol was ratified by other Annex I countries, excluding Canada and Unites States of America.

The UNFCCC is an international environmental treaty negotiated at the United Nations Conference on Environment and Development in 1992. The treaty's objective was to "stabilize GHG concentrations in the atmosphere at a level that would prevent dangerous anthropogenic interference with Earth's climate system". Among its first tasks was the establishment of national inventories of GHG emissions and removals. These national inventories were used to create the 1990 benchmark levels by the Annex I, or developing countries. UNFCCC also provides a common global framework to combat global warming, and the conversion of forests as the major source of GHG emissions (Grainger and Obersteiner, 2010).

#### 1.1.4. Intergovernmental Panel on Climate Change (IPCC)

The Intergovernmental Panel on Climate Change (IPCC) is the leading international body for the assessment of climate change. It was created in 1988 by two UN organizations, the World Meteorological Organization (WMO) and the United Nations Environment Programme (UNEP) (IPCC, [www.ipcc.ch](http://www.ipcc.ch)). IPCC is a scientific body under the auspices of the United Nations, with 195 country-members. Its mandate

is “to review and assess the most recent scientific, technical and socio-economic information produced worldwide relevant to the understanding of climate change”.

The UNFCCC adopted a collaborative initiative called Reducing Emissions from Deforestation and Forest Degradation in developing countries (REDD) (Gibbs et al., 2007, Asner et al., 2009). This program promotes the informed and meaningful involvement of all stakeholders, including indigenous peoples and other forest-dependent communities in national and international REDD implementation. UN-REDD estimated that deforestation and forest degradation, through agricultural expansion, conversion to pastureland, infrastructure development, fires and destructive logging contribute approximately 20% of global greenhouse emissions. REDD is designed as a mechanism to create financial value for the carbon stored in forests. It offers incentives for developing countries to reduce emission levels from forested lands. REDD promotes the role of conservation, sustainable management of forests and enhancement of forest carbon stocks.

IPCC provided guidelines to UNFCCC in support of the REDD implementation. These guidelines aimed to assist countries in developing carbon assessment methodologies (IPCC, 2006). There were five carbon pools identified by IPCC (2003a) to be monitored for deforestation and degradation. These carbon pools are: aboveground biomass, belowground biomass, litter, dead wood and soil organic carbon. The most practical method is to monitor aboveground biomass (CIFOR, 2008).

IPCC (2003a and 2006) following suggestions from Brown (1997) provides the guidelines for conducting REDD assessments. REDD countries will need to identify: (1) the aerial extent (in hectares) of deforestation and forest degradation, (2) for degradation, the proportion of forest biomass lost, (3) location (by forest type) where deforestation or degradation occurred, (4) the carbon content of each forest type, and (5) the process of forest loss which affects the rate and timing of emissions (IPCC 2003a and 2006). Biomass refers to the total amount of aboveground living organic matter in trees, expressed as oven-dry tons per unit area. Aboveground biomass is found in the components of trees, shrubs, palms, and saplings. Belowground biomass is found in dead plant mass such as fine litter and wood. Root biomass is estimated to be 20% of the aboveground forest carbon stocks (Houghton et al., 2001; Achard et al., 2002). Dead wood or litter carbon stocks are assumed to be 10-20% of the aboveground forest carbon stocks in mature forests (Harmon and Sexton, 1996; Houghton et al., 2001; Achard et al., 2002). The most direct way to measure aboveground forest biomass is by harvesting the trees, drying and weighing the carbon stored. The carbon is measured using a bomb calorimeter or absorption spectroscopy methods. Carbon content was estimated at 50% of the dry biomass by Westlake (1966), and 42%-55% of dry biomass by Chapin et al. (2011). Forests usually store more carbon than any of the other ecosystems, and are considered as natural brakes on climate change (Gibbs et al., 2007).

The IPCC (2003b) outlined three tiers for estimating GHG emissions: Tier 1 makes use of biome-averages that provide rough approximations that can be readily used to estimate the nation's carbon stocks, Tier 2 involves combining ground-based tree

measurements such as tree diameters and heights to estimate forest carbon stocks, and Tier 3 utilizes high-resolution methods, including ecosystem modeling, that are repeated through time and are specific for each country (Penman et al., 2003, IPCC 2006). Tiers 2 and 3 make use of satellite or airborne remote sensing instruments to estimate tree volume and other forest characteristics to estimate the biomass and carbon stocks of forests (Gibbs et al., 2007, Goetz et al., 2009). The accuracy of forest biomass and carbon stock estimates increases from Tier 1 to 3, thus reducing measurement uncertainties (Asner et al., 2009).

#### 1.1.5. Global Forest Resource Assessment (FRA)

The United Nations Food and Agriculture Office (FAO) publishes the Global Forest Resource Assessment (FRA) every five to ten years, initiating the first survey in 1947. This assessment provides a comprehensive accounting of aboveground carbon stocks for tropical forests and how they are changing. The most recent publication is FRA 2010. There are two primary sources of data for the FRA: Country Reports prepared by national correspondents and remote sensing analyses conducted by FAO, with national focal points and regional partners (DeFries et al., 2002, Grainger, 2008). FRA 2010 reported that 13 million ha of global forests were converted to other uses between 2000 and 2010. Most of these forest losses were in the South American and African tropics. Countries in Asia, on the other hand, had adopted afforestation activities and registered a net gain of 2.2 million ha in the same period.

Baccini et al. (2012) reported that the FRA national estimates were primarily derived from ground-based forest inventories. They provided some criticism of the FRA 2010 effort including that the majority of existing forest inventories are not current, many countries do not undertake forest inventories or have obsolete inventories, and that national estimates were biased towards the timber volume of commercial tree species (Baccini et al., 2012). They recommended that high quality information on the spatial distribution of carbon stocks is needed in order to reduce the uncertainty in estimates (Baccini et al., 2012, Mitchard et al., 2013).

#### 1.1.6. Tropical Forest Deforestation and Degradation

The tropical rainforest biome covers about 6% of the Earth's surface (Myers, 1988). These rainforests are mainly located around the equator. The average temperature is between 20°C and 35° C. These areas receive more than 200 cm of rainfall per year (Chapin et al., 2011). Tropical forests are among the most carbon-rich ecosystems in the world (Drake et al., 2002). Forests provide ecosystem services like habitat, biodiversity, climate regulation, water source, and carbon sequestration and economic services including merchantable resources like timber, fuel, and forage. Natural resources, like forests, are faced with providing both commercially-derived values and non-market values associated with many other ecosystem services. They have a large potential to sequester carbon primarily through reforestation, agroforestry and conservation of existing forests (Brown et al., 1996). Deforestation and degradation directly impacts the largest pool of carbon stored in the aboveground living biomass of trees. UN-FAO has



estimated that tropical deforestation and forest degradation accounts for 20% of global anthropogenic CO<sub>2</sub> emissions to the atmosphere (Olander et al., 2008). These resources are being destroyed at rapid rates with the highest conversion rates in Southeast Asia (Achard et al., 2002, FAO 2003). This rapid loss of tropical forest in Southeast Asia is the primary concern of this dissertation, particularly carbon dynamics in the Philippines.

#### 1.1.7. Tropical Deforestation and Biodiversity Hotspots

Like most forest cover in the equatorial regions, the Philippines has moist tropical forests, where a hectare of land contains at least 300 plant species (Bagarinao 1988). Bagarinao (1988) reported that the country has 12,000 species of flowering plants, pteridophytes, bryophytes, algae, and fungi, of which 3,500 species are considered endemic, and large varieties are grown as ornamentals. Mittermeier et al. (2004) state that there is a minimum estimate of 6,091 and 588 endemic plants and vertebrates, respectively in the Philippines. These figures are approximately 3.8% of the global total of endemic species (Myers et al., 2000).

The Philippines government's Department of Environment and Natural Resources (DENR) presently reports an extremely high habitation of 52,177 species of flora and fauna, with greater than 50% of these endemic species (DENR, [www.denr.gov.ph](http://www.denr.gov.ph)). The second largest and rarest eagle in the world lives in the Philippines rainforests in the forest canopy of large trees and is also listed as "Critically Endangered" on the International Union for the Conservation of Nature's (IUCN) Red List: the Philippine eagle (*Pithecophaga jefferyi*). However, Lewis (1986) reported that

the population of this eagle is declining due to forest degradation and road network construction. McNeely et al. (1990) indicated that the Philippines' forest cover is regarded as one of the world's "biodiversity hotspots". A region must meet two strict criteria to be able to qualify as a biodiversity hotspot: firstly, a region must have at least 1,500 vascular plants as endemics and secondly, the region must have 30% or less of its original natural vegetation (Myers 1988, 1990, and 2003, Pressey et al., 1993, Ginsberg 1999, Prendergast et al., 1999, Mittermeier et al., 1999, Myers et al., 2000, Mittermeier et al., 2004). The Philippines is one of 34 hotspots in the world that represent 2.3% of the land surface and supports > 50% of the world's endemic plant species (Heaney et al., 2004 in Mittermeier et al., 2004). According to Olsen's biogeographic classification (Olsen et al., 2001), the Philippines tropical forest is designated Tropical and Subtropical moist broadleaf forest where 297, 179 km<sup>2</sup> of the original forest has been reduced by 93% to 20,803 km<sup>2</sup> or only 7% of its forests remains (Heaney et al., 2004 in Mittermeier et al., 2004). Revilla (1997) reported that at the time of the island's discovery by Europeans in 1521, 90% of the country was covered with lush tropical rainforest, equivalent to 27 million hectares. By 1900, the forest coverage had been reduced to 21 million hectares, and by 1996, there was only 6.1 million ha remaining (Revilla 1997). Revilla (1997) further stated that in the 1990s, deforestation was reducing the forest cover at rates ranging from 190,000 to 200,000 hectares per year. Lasco et al. (2001) reported that major causes of deforestation were attributed to shifting cultivation, permanent agriculture, ranching, logging, fuel-wood gathering and charcoal-making. This loss of forest totaling over 25 Gt C has led to Conservation International (CI)

ranking the “World’s 10 Most Threatened Forest Hotspots” including the Philippines as the 4<sup>th</sup> ranked hotspot in the world (Jensen, 2003; Myers, 2003). This reduction and observed fragmentation of the southern Asian tropical forests has led to reduction in habitat, endangerment, and extinction of fauna and flora (Brooks et al., 1997 and 1999).

#### 1.1.8. Protected Areas

In 1992, the Philippines government adopted a conservation strategy through implementation of the National Integrated Protected Area System (NIPAS), assisted by a \$20 million grant from the Global Environment Facility (GEF) (Heaney et al. 2004 in Mittermeier et al., 2004). Under this protection are the remaining natural forests types, which consist mainly of old-growth dipterocarp, mossy, secondary forest, pine and mangroves. These forests types, however, are open access, and most are located in highly inaccessible areas. The poor accessibility poses problems for monitoring, and thus protection is not enforced to the utmost level.

The NIPAS Act of 1992 has identified 240 protected areas in the Philippines. These protected areas are administered by the Department of Environment and Natural Resources - Biodiversity Management Bureau. These protected areas cover a total area of 35,700 square kilometers or 11.9% of the country. However, if protection is considered in IUCN categories I to IV then only 6% of the country is protected (Heaney et al., 2004). Protected areas are managed according to their classifications. There are 14 classifications, to wit: national parks, natural parks, natural monuments, protected landscape, protected landscape and seascape, protected seascape, game refuge and bird sanctuaries, resource reserves, managed resource protected areas, marine reserves,

watershed forest reserves, natural biotic areas, wildlife sanctuaries, and wilderness areas. Verburg et al. (2006) described that in certain locations in the Philippines, hotspots of deforestation and forest degradation overlap with the protected areas. These deforestation activities happened in spite of different national policies implemented to reduce illegal logging and agricultural expansion.

### 1.2. Carbon Dynamics in the Philippines

The Philippines is endowed with tropical rainforests that could help mitigate climate change through carbon sequestration. In the Philippines, various studies have been conducted in selected forest sites aimed at estimating carbon storage (Table 1-1). Han et al. (2010) piloted a study using destructive sampling approach in 2007-2008 at Mt. Makiling Forest Reserve in Luzon Island. Their study aimed to compare the carbon storage and flux between a 60-year old secondary natural forest stand and a large-leafed mahogany plantation. Their results showed that the total carbon storage in aboveground biomass, litter layer and soil of the secondary forest stand was 313.12 Mg C ha<sup>-1</sup>, which is 1.7 times larger than the carbon storage of the large-leafed mahogany plantation, estimated at 185.28 Mg C ha<sup>-1</sup>. Soil respiration rate and bacteria count in the secondary forest is higher than in the mahogany plantation especially during the wet season, which contributes to higher carbon emissions.

Lasco et al. (2004) also conducted a non-destructive sampling at a similar study site in 1992-1996. They reported that the secondary forest could store 418 Mg C ha<sup>-1</sup>. In the southern part of the country, Lasco et al. (2006) studied the effects of selective logging on carbon stocks of Dipterocarpaceae forests on fixed plots using a

chronosequence of 1-21 years after logging. They found that unlogged forests had average carbon stocks of 258 Mg ha<sup>-1</sup>, of which 34% was in soil organic carbon (SOC). After logging, the above-ground carbon stocks declined by 50%, while changes in SOC showed no apparent relationship with number of years after logging. Table 1-2 lists selected research findings on estimates of tropical forest aboveground biomass and carbon density.

UN-REDD was implemented in the Philippines with a primary partnership involving the Department of Environment and Natural Resource (DENR). The UN-REDD Philippines Initial National Programme started with a budget of \$500,000 US (UN-REDD, [www.un-redd.org](http://www.un-redd.org)). Its time frame is from January to December 2011. During this time, DENR established the social and environmental safeguards, set-up a harmonized methodology for reference baselines, and established a technical working group mandated to use a national monitoring, reporting and verification (MRV) approach.

#### 1.2.1. The Study Area: Mount Apo Natural Park

The Mt. Apo Natural Park (MANP) primary conservation area totals 54,974.87 hectares. It is located on Mindanao Island in southern Philippines at 7° 0'30" N latitude, 125° 16 '33" E longitude, with geographic coordinate system of WGS 84, and projection of UTM 51 N. Figure 1-1 shows the location of MANP research site in the Philippines. MANP is bounded by two governmental administrative regions: Region XI, which lies on the north and south portions of the park, and Region XII, which borders the western

side. Various local government units (LGU) also oversee MANP's administration including Davao City in the north, Davao del Sur in the east, and Cotabato in the western portion of MANP. Figure 1-2 shows the habitat map of MANP with an elevations range from 600 to 2,954-m, and mean monthly temperature ranges from a low of 26.4° C during January to 27.9° C during April. Monthly relative humidity ranges from 78% during March and April, to 82% during June and July. Annual precipitation ranges from 1,135 mm to 4,489 mm, with a mean of 2,500 mm.

MANP is a landscape of steep inclines and craggy boulders on soils that developed from volcanic parent material that supports lush forests and mossy swamps. MANP is geothermically active with a number of hot spring spa concessions in the park, as well as an active energy development program by the Department of Energy of the Philippines. MANP includes 2 volcanoes: Mt. Apo at 2,954 m asl, which last erupted in 1640 (Kellman, 1970) with most of the lava being deposited on the western slope and the extinct volcano Mt. Talomo (2,674 m). MANP is the major watershed for two regions of Southern Mindanao (Region XI) and Central Mindanao (Region XII), with 19 major rivers originating from the volcanic formations (Mt. Apo Natural Park Management Plan, 2000).

Mt. Apo is also home for six indigenous peoples from the tribes of Bagobo, Manobo, Ubo, Ata, K'lagan and Tagacaolo. A total of 25,252 individuals from 39 village (or barangay) communities live inside the park (MAFI-c, [www.mafi.org.ph](http://www.mafi.org.ph)). One-third of this population belongs to the indigents, and the remaining are migrants from other islands in the Philippines. The indigenous people consider Mt. Apo as a

sacred ground and a place for worship, and the burial ground of their great forefather, Apo Sandawa. Politically, some communities still maintain the traditional Tribal Councils or Council of Elders.

A vegetation cover map of MANP is presented in Figure 1-3. The remaining natural forests types consist mainly of old-growth Dipterocarpaceae, Bryophytes, pines and mangroves. MANP is populated with trees mostly from the Dipterocarpaceae family, including *Shorea astylosa* commonly called Yakal, which is an endemic listed as “critically endangered” on the IUCN Red List (Ramos et al., 2012).

Mount Apo Natural Park (MANP) was declared as a National Park on May 9, 1936, by President Manuel L. Quezon by virtue of Presidential Proclamation No. 59 (MAFI-a, [www.mafi.org.ph](http://www.mafi.org.ph)). From 1936, numerous land use policies were adopted along with the turn-over of leadership in the Philippine government. Amendments were adopted in 1983 converting over half of the park including forested areas into alienable and disposable areas, to include agricultural use (Lewis, 1988). Large areas inside the park were destroyed due to human settlements and agricultural activities (Lewis, 1988). In 1984, IUCN declared Mt. Apo as one of the world’s most threatened protected natural areas, drawing international attention. The 1983 amendments were revoked in 1985 during the term of Pres. Corazon C. Aquino, under Proclamation 853, reverting portions of alienable and disposable areas back to forested area (Lewis, 1988). The Mount Apo Protected Area Act of 2003, or Republic Act 9237, was legislated in 2004. Mt. Apo is listed as a natural park, and was established in 2007 as a World Heritage Site. Natural parks are defined in NIPAS Act (1992) as “relatively large areas not materially altered

by human activity where extractive resource users are not allowed and maintained to protect outstanding natural and scenic areas of national or international significance, educational and recreational use”. Figure 1-4 shows the management zone map of MANP. Based on the NIPAS Act, a national government strategy was implemented to divide the natural park into zones with 30,000 ha assigned as strict protection zone, 26,000 ha as managed reserved zone, and 7,800 ha for built-in or multiple use zones.

### 1.2.2. Dissertation Rationale

This dissertation attempts to provide an estimation of the forest cover, biomass, and carbon stocks remaining in MANP (Figure 1-1), despite the agricultural and urban pressures existing in the area. I will also map the spatial distribution of forest biomass and carbon content at IPCC tier 2 at the species, plot, and landscape spatial scales.

At the landscape spatial scale a tree canopy height, biomass, and carbon maps of MANP will be created using 2013 commercial airborne radar imagery. Forest carbon stocks will be compared in the three management zones: multiple use, strict protection, and restoration (Figure 1-4).

This research endeavors to provide answers to the following questions:

1. How do three different allometric equations developed for tropical forests by Brown (1997), Ketterings et al. (2001) and Chave et al. (2005) compare in estimating field collected species-level biomass and carbon stocks across management zones in MANP? What is the uncertainty of this method?



2. Can algorithms be developed for using Terrestrial Laser Scanning (TLS) technology to assess plot-level biomass and what is their uncertainty?
3. To what degree of uncertainty can Interferometric Synthetic Aperture Radar (IFSAR) estimate biomass at the landscape level?

This research offers innovation in the following manner:

1. Chapter II will use an IPCC Tier 2 approach, by combining field data in developing species-specific biomass estimates. In compliance with REDD guidelines, this study also attempts to assess carbon stocks by forest type. The field data will also quantify the frequency of occurrence of two endangered species inside the MANP. Chapter II will also present the estimation of the referenced biomass values using three allometric equations, which will be used all throughout the dissertation. The referenced biomass will be used in lieu of the biomass data from a destructive sampling approach, which is the approach used in many previous studies.
2. Chapter III will use an IPCC Tier 2 approach using field data and high-resolution TLS data to develop an algorithm for the plot-level biomass and carbon stock estimates.
3. Chapter IV will use an IPCC Tier 2 approach to estimate and map the spatial distribution of tree heights, biomass, and carbon stocks using field data and airborne IFSAR.

### 1.2.3. Limitations of the Study

This research conducted a one-time inventory of local field and airborne remote sensing data of MANP from July to August 2013. Consequently, this is an IPCC Tier 2 approach (IPCC, 2006). An IPCC Tier 3 approach requires repeated observations over time which is not the case of this study. Nevertheless, I hope to provide a baseline approach for assessing biomass and carbon stocks at various scales in MANP. Security problems in Region XI forested area also posed restrictions on the research team's ability to cover additional sampling areas. A total of 26 plots were sampled, stratified on the MANP's management zones, forest types and elevation ranges.

In order to generate a referenced biomass for the MANP, 3 tropical allometric equations were considered, relating field-derived H and DBH attributes, and published data on wood density. Other published biomass estimation studies used a destructive sampling approach to derive oven-dried biomass. This destructive sampling approach, however, was not allowed inside the MANP, which is a protected area. These tropical allometric equations also has its pros and cons, which will be discussed in Chapter II.

### 1.2.4. Organization of the Dissertation

Chapter II will address question 1 by inventorying the forest characteristics of the study area: Mt. Apo Natural Park (MANP). This study will characterizes the structure, composition, biomass, and carbon stocks of the commercial hardwood trees in tropical plant communities present in the lowland, midland and upland areas of MANP. Three tropical allometric equations that were developed by Brown (1997), Ketterings et al.

(2001) and Chave et al. (2005) will be compared for species-specific biomass and carbon stocks using tree mensuration metrics. This study will also compare the impacts of three primary land uses and land cover types on these vegetation characteristics.

Chapter III will address question 2 and seeks to develop algorithms for calculation of plot-level biomass and carbon stocks using terrestrial laser scanning data (TLS). TLS produces three-dimensional (3D) over- and understory information. A new referenced biomass algorithms may be developed by comparing the outcomes of using three tropical allometric equations developed by Brown (1997), Ketterings et al. (2001) and Chave et al. (2005).

Chapter IV will address question 3 by producing landscape-level biomass, carbon, and tree height estimates using interferometric synthetic aperture radar (IFSAR). Canopy height mapping (CHM) will show the park-level distribution of forested and non-forested areas. A digitized land management map will also be created, showing biomass and carbon storage per zone.

Finally, Chapter V will provide a summary of the findings of the three essays. Recommendations were also provided and key points for future research efforts are suggested.

**CHAPTER II**  
**VEGETATION PROFILE AND BIOMASS ESTIMATES**  
**IN MT. APO NATURAL PARK**

2.1. Introduction

Mt. Apo National Park was created by Proclamation No. 59 on May 9, 1936, and amended by Proclamation No, 35 on May 8, 1966. The Mt. Apo Foundation, Inc. (MAFI) reports that this national park originally covered an aggregate area of 76,900 hectares. Since 1966, numerous land use policies have been adopted along with many changes of leadership in the Philippine Government. Amendments were adopted converting forested areas into alienable and disposable areas, to include agricultural use. During 1960s, there was a considerable deforestation in Mt. Apo due to establishment of coffee plantations (Meher-Homji, 1991). The Philippine Government, in 1983, reclassified over half of the park for agricultural use. However, this reclassification was revoked in 1985 (Lewis, 1988). In 1984, the International Union of Conservation of Nature (IUCN) declared Mt. Apo as one of the world's most threatened protected natural areas, drawing international attention. Large areas inside the park were destroyed due to human settlements. Ramos et al. (2012) described Mt. Apo as populated with trees mostly from the dipterocarpacea family, including *Shorea astylosa*, which is included in the IUCN Red List of threatened species. Large areas inside the Mt. Apo Natural Park were also degraded due to agricultural activities.

On June 17, 1986, prior government amendments were revoked during the term of Pres. Corazon C. Aquino, under Proclamation 853, reverting portions of alienable and disposable areas back to forested areas. On September 24, 1996, Mt. Apo Natural Park was declared by Pres. Fidel V. Ramos, through Proclamation No. 882, a protected area. Republic Act 9237, or the Mt. Apo Protected Area Act of 2003, was signed into law declaring an area of 54,974 ha as effective park area, with peripheral areas designated as buffer zones (MAFI-a, [www.mafi.org.ph](http://www.mafi.org.ph)). On December 18, 2003, the Association of Southeast Asian Nations (ASEAN) declared Mt. Apo National Park as one of only two ASEAN Natural Heritage Parks in the country (ASEAN, [www.asean.org](http://www.asean.org)). MANP was recognized for its effort to meet United Nation's Millennium goals on the environment with respect to reducing biodiversity loss. The other ASEAN Natural Heritage Park is Mt Iglit in Mindoro, Philippines. This park is the home of endangered tamaraw.

In December 2009, the UNESCO National Commission of the Philippines submitted MANP for inclusion in the UNESCO World Heritage list. MANP remains in the Tentative List, and must comply with UNESCO's Operational Guidelines before it can be included in the World Heritage List. To be in the World Heritage List, the site must show its justification of outstanding universal value. Among the justifications submitted include: (1) Mt Apo belongs to the 15 biogeographic zones in the Philippines considered to have the highest land-based biological diversity in terms of flora and fauna per unit area (UNESCO, [www.unesco.org](http://www.unesco.org)), (2) Mt. Apo is considered to be one of the richest botanical mountains in the region hosting hundreds of rare, endemic and threatened species of flora. Mt. Apo is the habitat for endemic species. It was estimated

to have eight hundred (800) vascular and non-vascular plant species that were collected between 300 meters asl and 1000 meters asl. Among the identified floral species are: 629 species, 42 of which are endemic and 18 species are considered at risk, including the *Vanda sanderiana* (Waling-Waling) which is recognized as the "Queen of Philippine Orchids" and recommended by plant enthusiasts as the Philippine National Flower. Endemics were identified at each forest formation, between 300 meters asl and 1000 meters asl. These include members of the genera *Pipturus*, *Sauravia* and *Poikilospermum*. *Humalanthus populneus*, *Elephantopus spicatus*, *Piper apoanum* and *Vanda sanderiana* are possibly extinct in the wild. Endemic at mild altitudes include the endangered *Lithocarpus submonticolus* and *Peperonia elmeri*. In the upper montane forest, the endemic species are *Cypholopus microphyllus* and *Nepenthus copelandi*. Thirty-seven (37) species were highly valued, such as, the endangered *Agathis philippinensis* (Almaciga) and dipterocarps, such as the rare *Vatica manggachapoi* (Narig) and *Shorea palita* (Lauan) (MAFI-b, [www.mafi.org.ph](http://www.mafi.org.ph)).

Aside from the floral species, MANP is also the habitat for a total of 227 vertebrate species. These fauna species belong to 59 families of amphibians, reptiles, birds and mammals. There were 118 species of butterflies belonging to 69 families recorded in the area. There are 272 species of birds, wherein 111 (40%) are endemic to Mount Apo. The Bird Life International (BI) identified 2 species that were classified in the critical endangered list (BI, [www.birdlife.org](http://www.birdlife.org)). One endemic but critically endangered bird species is *Pithecophaga jefferyi* (Philippine Eagle), whose remaining population is believed to be only around 500 (UNESCO, [www.unesco.org](http://www.unesco.org)). The

Philippine eagle, the second largest eagle in the world, is of outstanding universal value for science and conservation. Its nesting and feeding areas are located in dipterocarp forests including closed canopy forests. The Philippine eagle is not found elsewhere in the world. It symbolizes environmental preservation, and represents the country as the national bird.

Mt. Apo is also home for six indigenous peoples from the tribes of Bagobo, Manobo, Ubo, Ata, K'lagan and Tagacaolo. A total of 25,252 individuals from 39 village (or barangay) communities live inside the park (MAFI-c, [www.mafi.org.ph](http://www.mafi.org.ph)). One-third of this population belongs to the indigents, and the remaining are migrants from other islands in the Philippines. The indigenous people consider Mt. Apo as a sacred ground and a place for worship, and the burial ground of their great forefather, Apo Sandawa. In terms of political structure, some communities still maintain the traditional Tribal Councils or Council of Elders.

#### 2.1.1. Rationale

The rationale of this research is to assess forest carbon stocks in one of the world's threatened protected natural areas. Mt. Apo is home for endangered flora and fauna, but noise of chainsaw operations were heard inside the MANP during the fieldwork activities in August 2013 in the Camp Baroring area. Logging bans were implemented by the government, but strict monitoring and enforcement may be lacking. As a UN-REDD partner country, the Philippines is duty-bound to be active in monitoring deforestation and degradation activities inside protected areas, like Mt. Apo Natural Park.

This research uses innovative technologies in compliance with UN-REDD guidelines to identify carbon content by forest type. An IPCC Tier 2 approach is used. Tree mensuration metrics were used to estimate species-level biomass, including endangered tree species identified by IUCN. These endangered species include: *Agathis philippinensis* (Almaciga) and Dipterocarps, such as the rare *Vatica manggachapoi* and *Shorea palita* (Lauan).

### 2.1.2. Objectives

The objectives of this study are to:

1. Characterize the structure, composition, and biomass stocks of the hardwood tropical trees in plant communities present in the lowland, midland and upland areas in the Mt. Apo Natural Park.
2. Compare the allometric equations for deriving biomass from tree mensuration metrics. The 3 tropical allometric equations will further be assessed on its pros and cons, and will be evaluated to be used as bases for reference biomass estimation in the succeeding essays.
3. Compare the impacts of three primary land management zones: the multiple use (MU), strict protection (SP) and restoration (R) zones, on these characteristics.

### 2.1.3. Hypothesis

Considering probable recovery from open access agricultural policies of the 1980s, we hypothesize that the SP conservation areas will have the greatest species diversity, the tallest plants, the greatest diameter-at-breast height (DBH), and the highest importance value relative to the other two land uses. We further hypothesize that the



restoration sites will be intermediate between the SP and MU sites, with the MU sites being the most disturbed. We also hypothesized that the general tropical allometric equation developed by Chave et al. (2005) will show the most accurate biomass estimation, compared to the allometry developed from commercial hardwood samples by Brown (1997) and site-specific equation by Kettering et al. (2001).

## 2.2. Review of Related Literatures

Various estimates of total carbon for the Philippines have been published that have used compiled harvest data and forest inventory. Gibbs et al. (2007) reported national-level forest carbon stocks in developing countries using default values published by IPCC. Table 1-1 listed these compiled results of the total estimated carbon stocks in the Philippines. These carbon stock estimates range from 765 to 2503 Mt C ha<sup>-1</sup> with high uncertainty levels coming from biome-averages.

Drake et al. (2002) reported that tropical forests are among the most carbon-rich ecosystems in the world. Brown (1996) also stated that tropical forests have a large potential to sequester carbon primarily through reforestation, agroforestry and conservation of existing forests. However, Achard et al. (2002) reported that these resources are being destroyed at rapid rates, with the highest conversion rates in Southeast Asia. Knowledge of carbon pools and storage with net primary production of tropical forest is based primarily on a small number of studies. Hertel et al. (2009) observed that most tropical studies are from South and Central America, while precise data from Southeast Asia and Africa are rare.

In the Philippines, various studies have been conducted in selected forest sites aimed at estimating carbon storage. Table 1-2 lists scientific papers examined on carbon storage in selected areas in the Philippines. First, Han et al. (2010) piloted a study using a destructive sampling approach in 2007-2008 at Mt. Makiling Forest Reserve on Luzon Island. Their study aimed to compare the carbon storage and flux between a 60-year old secondary natural forest stand and a large-leafed mahogany plantation. Their results showed that the total carbon storage in aboveground biomass, litter layer, and soil of the secondary forest stand was 313.12 Mg C ha<sup>-1</sup>, which is 1.7 times larger than the carbon storage of the large-leafed mahogany plantation, estimated at 185.28 Mg C ha<sup>-1</sup>. Soil respiration rate and bacteria count in the secondary forest was higher than in the mahogany plantation especially during the wet season, which contributes to high carbon emissions. Second, Lasco et al. (2004) also conducted a non-destructive sampling of a similar study site in 1992-1996. They reported that secondary forest can store 418 Mg C ha<sup>-1</sup>. Finally, in the southern part of the country, Lasco et al. (2006) studied the effects of selective logging on carbon stocks of dipterocarp forests on fixed plots using a chronosequence of 1-21 years after logging. They found that unlogged forests had average carbon stocks of 258 Mg C ha<sup>-1</sup>, of which 34% was in soil organic carbon (SOC). After logging, the above-ground carbon stocks declined by 50%, while changes in SOC showed no apparent relationship with number of years after logging.

Various studies were conducted using limited sampling plots. Ribeiro et al. (2008) published a study on aboveground biomass and leaf area index mapping for the Niassa Reserve, northern Mozambique. Fifty circular plots were established in

homogeneous areas of vegetation within the 23,000 km<sup>2</sup> conservation area. In another study, Ribeiro et al. (2013) conducted a study of vegetation dynamics and carbon stock density in miomo woodlands in Niassa National Reserve, the 14<sup>th</sup> largest protected area in the world. Their team established 50 permanent sampling plots over the protected area of 42,000 km<sup>2</sup>. Plot selection was largely limited due to accessibility issues. However, the plots were almost evenly distributed across the vegetation gradient.

### 2.3. Data and Methods

#### 2.3.1. Data Acquisition

The study team secured a research permit from the Mt. Apo Protected Area Management Board (PAMB) prior to conducting any fieldwork. The PAMB is composed of representatives from various stakeholders including, national and local government units, civic organizations, and tribal communities residing within the park. Aside from closely coordinating with PAMB, written communications were sent and courtesy visits were also made to the 5 local government units that surround MANP. These local government units are: three cities of Davao, Digos and Kidapawan, and two municipalities of Magpet, and Makilala.

Field sampling was conducted in July and August 2013. Twenty-six 30-m diameter forest stands were established in July and August 2013, in a manner similar to Ribeiro et al. (2013). The location of 26 study plots inside MANP is presented in Figure 2-1. The center of the plot was geographically referenced using a Garmin III plus Geographic Positioning System (GPS) unit. A Kestrel 3500 weather unit was also used to provide information on altitude, temperature, wind speed, and relative humidity.

Finally, a compass was employed initially to locate directions to guide where to place the scan targets.

#### 2.3.1.1. Structure

Stems taller than breast-height of 1.37 m with a diameter-at-breast-height (DBH) >5 cm were recorded using a DBH tape. Tree height, and canopy diameter were measured using a Laser Technology TruPulse laser hypsometer, and canopy cover using a concave spherical densiometer, and basal area index (BAI) using factor prism were also measured for all trees.

#### 2.3.1.2. Flora and Species Composition and Distribution

Individual species for hardwood trees were identified by local names with the help of a native guide. Local names for tree species were identified to family name by the technical staff of the Watershed Management Department of the Energy Development Corporation (EDC, [www.energy.com.ph](http://www.energy.com.ph)). Species and family names were identified using the manual on collection of plants in a 1-hectare sampling plot in EDC by Amoroso (2013), and from an interactive outpost of Co's Digital Flora of the Philippines ([www.philippineplants.org](http://www.philippineplants.org)). Information for wood densities was collected from the website of World Agroforestry Center ([www.worldagroforestry.org](http://www.worldagroforestry.org)).

This study utilized the importance value index (IVI) to provide a synthetic measure of species composition and distribution within a stand, between each land use, and across the entire park (Kunwar and Sharma, 2004). Importance values rank species within a stand based on three criteria. These criteria include relative frequency, which measures how commonly a species occurs relative to the total number of species,

relative abundance or density which is the total number of individuals of a species relative to the total number of individuals for all species, and lastly, relative dominance measures the total amount of forest area occupied by a species relative to the area occupied by all the species. Each criterion for a particular species was computed as:

$$RF = [\text{Frequency (species } i) / \text{Sum of frequencies of all species}] \times 100 \quad (\text{Eq. 2})$$

$$RD = [\text{Density (species } i) / \text{Sum of densities of all species}] \times 100 \quad (\text{Eq. 3})$$

$$RDo = [\text{Total basal area (species } i) / \text{Sum of basal areas of all species}] \times 100 \quad (\text{Eq. 4})$$

Where RF is Relative Frequency, RD is Relative Density, and RDo is Relative Dominance and

$$RF + RD + RDo = IVI \quad (\text{Eq. 5})$$

The computation for stock density or basal area is:

$$BA (i) = (\pi/40000) D^2 (i)/A \quad (\text{Eq. 6})$$

Where  $i$  is the local species name = 1,2,...,52,  $D$  is the DBH, and  $A$  is the area of the plot = 0.071 ha. The maximum importance value for any one species is 300. These IVI indices were then ranked for comparison between species and between three land management zones identified by the Mt. Apo Foundation, Inc (MAFI-e, [www.mafi.org.ph](http://www.mafi.org.ph)). The three management zones are shown in Figure 1-4. These land management zones are the multiple use (MU), strict protection (SP) and restoration (R) zones.

### 2.3.2. Modelling for Referenced Biomass

Both species-specific and plot-level aboveground biomass was estimated using three allometric equations developed by Brown (1997), Ketterings et al. (2001), and

Chave et al. (2005) respectively. Biomass was estimated for the ten leading species, as identified from IVI results. Plot-level biomass, based on the same 3 equations, was also calculated showing mixed species wood densities.

Brown (1997) developed an allometric equation using the destructive sampling method for tropical forests in Kalimantan, Indonesia and other tropical areas. The equation related oven-dried biomass with stem diameter. Height was omitted as it was observed to be related to site-specific stem diameter (Ketterings et al., 2001). Brown's data was collected by various investigators from different tropical forest areas at different times (Basuki et al., 2009). The data covers 170 sample trees, with a DBH range of 5 to 148 cm. Brown's method was used in the FAO 2005 Forest Assessment of the Philippines to estimate plot to country-level forest biomass stocks (Saket et al., 2005). A limitation for this model is that it is based on old forest inventories, with 1970s or earlier. These national forest inventories covered sites where there are viewed to have large commercial values, e.g., closed forest, and with little regard to open, drier forests or woodlands, where people extract other non-timber resources. The range of DBH is from 10-80 cm.

Chave et al. (2005) developed a pantropical model that included tropical forests in America, Asia and Oceania. This model was developed using time-series data from 1950 to 2005 from 27 study sites producing 2,410 tree samples from mixed species with a DBH range of 5 to 156 cm. These tree samples represent areas from young, secondary and old-growth forest types.

Ketterings et al. (2001) established a site-specific allometric equation using destructive sampling in mixed secondary forest in Sumatra, Indonesia. This study utilized 29 trees from 14 genera with a DBH range from 7.6 to 48.1 cm.

Tree biomass equals the product of the volume and the density. Wood density (WD) was estimated in Ketterings et al. (2001) with an average of  $0.60 \text{ kg dm}^{-3}$  (range of  $0.53 - 0.67 \text{ kg dm}^{-3}$ ). A comparable spread was also observed in other mixed tropical forests. Brown et al. (1995) in their study of Amazonian forest estimated a WD average of  $0.67 \pm 0.09 \text{ kg dm}^{-3}$  ( $0.52-0.80 \text{ kg dm}^{-3}$ ). Brown (1997) estimated an average of  $0.71 \text{ kg dm}^{-3}$  from 428 species in Asia. Brown and Lugo (1984) showed a global average for tropical forests of  $0.62 \text{ kg dm}^{-3}$ . Uhl et al. (1988) in their study of 30 common tree species conducted in Paragominas, Para State, Brazil reported a value of  $0.71 \text{ kg dm}^{-3}$ .

### 2.3.3. Data Processing Flowchart

The collected field data was processed to estimate species-level biomass. Figure 2-2 shows the data processing flowchart for biomass estimation. The primary data on tree metrics [DBH and height (H)] were processed to estimate biomass. Secondary data and land-use map graphics were acquired with permission from the Mt. Apo Foundation, Inc. (MAFI) website ([www.mafi.org.ph](http://www.mafi.org.ph)) and used to characterize management zones and vegetation profiles.

A hypothesis test using Chi-squared distribution was performed to check if the H and DBH samples across three management zones came from the same reference data. An importance value index was also computed for the 52 species. A third tree metric, wood density data, was also gathered from the World Agroforestry Center. These

statistical metrics were considered to compute for a referenced biomass that will be further used in the succeeding chapters. The aboveground biomass (AGB) was estimated based on the three tropical-designed allometric equations from Brown (1997), Ketterings et al. (2001), and Chave et al. (2005). Two levels of biomass estimation was computed: a species-level and a mixed species or plot-level.

#### 2.4. Results and Discussions

A total of 1,382 individual trees belonging to 52 local species were recorded. These samples were found in the 26 plots. These study plots were mostly located in the north and west side of the Mt. Apo Natural Park. Our research group attempted to enter the eastern side, or the Davao City portion, but we were strongly advised by the Philippine Army to defer this field visit due to the reported presence of communist rebels in the mountain area. The group also did not attempt to go to the southern side, Bansalan and Sta. Cruz, for similar security reasons. Added to this reason is that the vegetation cover in the southern multi-use management zone of MANP is mostly covered with coconut plantations.

A profile of study plots by land cover type is presented in Table 2-1. Eleven plots were mapped inside the closed-canopy forest, with a total of 32 species sampled. Open canopy forests were represented in 9 plots, containing 27 species. There were also 6 plots sampled inside the cultivated areas, with 21 species.

Table 2-2 lists the classification of the study plots by management zone. Thirteen stands were sampled within the multiple use (MU) management zone. These plots were located in Sayaban, Kidapawan City (N=2), Bongolanon, Magpet (N=4), New Israel,



Makilala (N=3) and Kapatagan, Digos City (N=4). A total of 34 species within 638 individual trees were sampled.

Seven stands were established within the strict protection (SP) zone. A total of 465 individual trees belonging to 28 species were measured. These sampling plots were located in Lake Venado (N=2), Makadak (N=3) and EDC reforestation sites (N=2).

Six stands were also established in the restoration (R) zone that were located in Agco (N=2) and Matiaw (N=4) areas. A total of 279 individual trees were measured that belonged to 23 species.

#### 2.4.1. Habitat Type

The habitat map for the park is shown in Figure 1-2. Distribution of the study plots by elevation range and habitat type is provided in Table 2-3. The park is classified into five distinct habitats. Lowland forest or lowland evergreen is located at elevation range of 600-1200 masl. This forest type is covered by multi-strata rainforest with closed canopy ranging from 10-20 m high. This area is also covered by secondary forest and open cultivated and denuded areas. Five plots were sampled falling in the lowland evergreen forest. These plots were located in Sayaban, Kidapawan City, and New Israel, Makilala.

Montane or low montane ranges from 1200-1500 masl, where vegetative structure is relatively lower in stature. Ten plots were located in the lower montane habitat site. These plots were located in Agco, Kidapawan City, Bongolanon, Magpet, and Sitio Matiaw, Kidapawan City.

Mossy forest or high montane is located in elevation ranges from 1500-2500 masl which are characterized by high density of epiphytes, mosses and liverwort. Eleven study plots were established in the upper montane area. These plots are located in Lake Venado, Makadak, and Kapatagan, Digos City.

Summit area is found in elevation greater than 2500 masl on steep walls. This area is mostly occupied with tall grasses. No sampling plots were established in this area due to absence of hardwood trees species.

All the study plots were distributed as either an open canopy, with mature forest covering <50 percent, or a closed canopy forest, with mature forest covering >50 percent. The southern part of the park (Sta. Cruz, Davao del Sur) is mostly dominated with coconut plantations, while areas in Bansalan are mostly cultivated areas.

#### 2.4.2. Tree Height and Stem Diameter

Tree heights and stem diameters differed across management zones. Table 2-4 showed the descriptive statistics by management zone, detailing tree height, stem diameter, elevation range and number of species per zone. The multiple use zone has H range of 2.1-35 m, DBH range of 9.5-293 cm, and has the most number of species, totaling to 34 distinct local species. The strict protection zone has H range of 2.3-27.1 m, DBH range of 6.5-441 cm, and contains 28 species. The restoration zone has H range of 2-38.4m, DBH range of 9-432 cm and has the least number of species, with only 23 species. The restoration zone contained both the tallest tree (Agoho) and the biggest tree with largest DBH (Tinikaran).

Figure 2-3 provides a look at the frequency distribution of tree height by management zones. Tree heights were categorized by height size class of < 2 m to the maximum height class of 35-40 m. The over-all height distribution were: <2 m, 3 trees, 2-5 m, 147 trees, 5- 10 m, 660 trees, 10-15 m, 309 trees, 15-20 m, 162 trees, 20-25 m, 55 trees, 25-30 m, 23 trees, 30-35 m, 13 trees, and 35-40 m, 5 trees. All of the management zones listed 1 tree having a height of < 2 m. Each class size shows the topmost number of trees per management zone. Trees with height range of 2-5 m and 5-10 m are mostly found in the strict protection zone. However, as height increases to the class sizes of 20-25 m, 25-30 m, and 30-35 m, most of the tallest trees are found in the multiple use zone. Agoho (H=38.4 m), which is a pine tree, is the tallest tree found in the restoration zone. This observation may be attributed to the species diversity (N=34) that promotes tree growth and height.

The frequency distribution for stem diameters by management zone is found in Figure 2-4. Trees were classified by stem diameter class size, from 5-10 cm, to a maximum class size of 401-500 cm. The over-all DBH distributions were: 5-10 cm, 7 trees, 11-50 cm, 824 trees, 51-100 cm, 346 trees, 101-150 cm, 116 trees, 151-200 cm, 32 trees, 201 - 250 cm, 20 trees, 251-300 cm, 10 trees, 301-400 cm, 3 trees, and 401-500 cm, 2 trees. The two largest trees were found in the strict protection zone (Tinikaran, DBH= 441 cm) and the restoration zone (Ulayan, DBH = 432 cm). Trees with stem diameters of 2-5 cm, and 5-10 cm, were mostly found in the strict protection zone. However, wider stem diameters from 10-15 cm, and up to the class size of 30-35 cm, were predominantly found in the multiple use zone.

A Chi-squared procedure to test for normality of distribution was applied. Table 2-5 shows the result of the test for normality for H and DBH. These hypothesis tests aim to ascertain if the distribution for H and DBH across the management zones come from the same reference distribution. For H distribution, a test value of 0.9872 shows that it failed to reject the null hypothesis that the samples come from the reference distribution. A similar conclusion can be derived for the DBH distribution at a test value of 0.8980 at a 95% confidence interval.

The collected local tree species were ranked based on their frequency. Table 2-6 shows the frequency distribution for 52 local tree species. An important finding can be gleaned from these results related to the 2 endangered species. *Agathis philippinensis* (Almaciga) was only sampled in 3 out of the total of 1,382 trees. These sampled Almaciga trees were only mapped in the closed-canopy forest. On the other hand, a higher frequency of occurrence is observed in *Shorea palita* (Lauan), where 59 trees were mapped. Lauan trees were found in all three land cover types. However, Lauan trees made up only 4% of the total trees.

The results from the MANP fieldwork were compared to the results of field study conducted by Lasco et al. (2004) in the northern side of the country, in Mt. Makiling Forest Reserve. They measured trees with DBH range from 5-166 cm, and height range from 2.5-24 m. MANP trees are bigger in DBH, with range of values from 6.5 – 441 cm. MANP trees are also taller, with H range from 2-38.4 m.

### 2.4.3. IVI Index

Figure 2-5 shows the results for the IVI index for the top 20 ecologically important species, based on the species frequency from the total of 52 species. The top 5 ecologically-important tree species, based on IVI index, were: Tinikaran (IVI=67), Ulayan (IVI=61), Tapol (IVI=57), Philippine Cedar (IVI= 55), and White lauan (IVI=46). The next 10 ecologically-important species are: Kalingag (IVI=44), Madsum (IVI=43), Abo-abo (IVI=35), Asik-asik (IVI=34), Indang (IVI=33), Manok (IVI=26), Alingatong (IVI=25.4), Basikong (IVI=25), Angelo (IVI= 24.5), and Mahogany (IVI=23). The last 5 ecologically-important species are: Agoho (IVI=21.1), Tambis (IVI=21), Banti-banti (IVI=20), Balingos (IVI=18), and Malatambis (IVI=17).

The results shown in Figure 2-5, however differ when the IVI index is computed according to management zone. Philippine cedar (IVI= 26) is the topmost ecologically important tree species in the multiple use zone, while Agoho (IVI=31) is the leading tree species in the restoration zone. For the strict protection zone, Tinikaran (IVI=71) is the most important tree species.

A similar study was conducted by Arsenio et al. (2011) on the vegetation of Mt. Maculot, in Pampanga, northern part of the Philippines. They used IVI as a tool in identifying measures for biodiversity conservation for the 61 species belonging to 51 genera and 28 families. Their results showed that the tree species with the highest importance value index were: *Canarium asperum* Benth (Burseraceae) (IVI=22.71), *Diplodiscus paniculatus* Turcz. (Malvaceae) (IVI=21.91), *Bischoffa javanica* Bl.

(Phyllanthaceae) (IVI=20.94), and *Palaquium philippinense* (Perr). C.B. Rob. (Sapotaceae) (IVI=15.72).

#### 2.4.4. Species-specific Biomass

The allometric equation developed by Brown (1997) for tropical forest is:

$$\text{TAGB} = \exp(-2.134 + 2.53 \ln(\text{DBH})) \quad (\text{Eq. 7})$$

where TAGB is total above-ground biomass in kg tree<sup>-1</sup> and DBH is in cm.

Kettering et al. (2001) developed an equation of:

$$\text{TAGB} = r p^{\text{avg}} (\text{DBH})^{2+c} \quad (\text{Eq. 8})$$

where r is a parameter that is constant over wide range of geographical areas, p<sup>avg</sup> is the average wood density for the study area, and c is the parameter estimated by relating DBH and H. Ketterings et al. (2001) used these values: r is 0.11, p<sup>avg</sup> is 0.604 g cm<sup>-3</sup>, and c is 0.397.

Chave et al. (2005) generated an allometric equation of:

$$\text{AGB} = \exp(-2.977 + \ln(pD^2H)) = 0.0509 \times pD^2H \quad (\text{Eq. 9})$$

where p is the species-specific wood density (g cm<sup>-3</sup>), D=DBH (cm) and H is height (m).

Of the 52 species, there were 31 hardwood species which only had fewer than 10 tagged trees. There are also 11 species for which the number of sampled trees was between 10-35. This limited number of observations for 42 species restricts the estimation of species-level biomass. Table 2-7 shows the species-specific biomass estimates for the top 10 species, based on the frequency of occurrence.

Results using the Brown (1997) equation showed the highest biomass level in kg tree<sup>-1</sup>, as it only considered DBH as its independent variable. When additional variables

were added to the equation, like wood density and H, the equation provided a more comparable range, as shown by the biomass estimates between Ketterings et al. (2001) and Chave et al. (2005).

Wood densities for the top 10 tree species are also shown in Table 2-7. Range for WD is 0.51-0.77 g cm<sup>-3</sup>. Wood densities for Tapol and Asik-asik adopted the average WD of 0.71 g cm<sup>-3</sup> from Brown (1997).

Tinikaran (N=319 trees) has the highest number of trees in the sampled plots with DBH range of 12-441 cm, and H range of 2.3-25.2 m. *Leptospermum flavescens* or Tinikaran is an indigenous forest species in MANP. Average biomass levels were estimated as: 7,391.6 kg tree<sup>-1</sup> by Brown (1997) equation, 2,070.3 kg tree<sup>-1</sup> by Ketterings et al. (2001) equation, and 1,623.8 kg tree<sup>-1</sup> using Chave et al. (2005) equation. Figure 2-6 shows the IVI index by management zones. This figure displays that some species were found in all zones, while others are only found in a specific zone. Species like Almaciga, Malatambis, Nato, Kalisaw were only found in the SP zone. Agoho is only found in R zone. Tambis, Bay-ang and Kape are only found in MU zone.

Most of these local trees are endemic to the park, and thus there are only a few species-specific biomass estimates available in the literature. Han et al. (2010) using the destructive sampling method, reported carbon storage of 313 Mg C ha<sup>-1</sup> for a natural forest stand in Mt. Makiling Forest Reserve, Philippines and carbon storage of 185 Mg C ha<sup>-1</sup> for a mahogany plantation. Lasco et al. (2004) also conducted a study in the same area using non-destructive sampling, and reported carbon storage of 418 Mg C ha<sup>-1</sup>. Another study by Lasco et al. (2006) in a selectively logged Dipterocarpaceae forest in

Surigao del Sur, Philippines, estimated carbon stocks of 258 Mg C ha<sup>-1</sup>, and 34% of soil organic carbon.

The results for the species-specific biomass estimates supported the findings in IVI ranking. The top ten species with the highest biomass were also the ten top ecologically important species, with the exception of Mahogany (IVI rank=15).

The number of species in each plot provided information on the species heterogeneity. Figure 2-7 showed the pie chart distribution of the number of species per plot. Nine plots contained 1-5 species, 11 plots have 6-10 species, 4 plots have 11-15 species, and 2 plots have the heterogeneity of 16-20 species. A closer inspection relating plot heterogeneity and biomass level did not support direct correlation. Biomass was largely related to the DBH and H attributes of the species.

#### 2.4.5. Plot-level Biomass

Biomass was also estimated for mixed species by plot level. Table 2-8 presented the actual mean biomass by DBH class size. For small DBH class size of 5-50 cm, Brown (1997) exhibited the largest biomass estimate compared to the two equations. As DBH class size increases, Chave et al. (2005) consistently showed the intermediate biomass estimates, and the most accurate values. Estimates from Brown (1997) tends to show at least 2x bigger than Chave et al. (2005) values. Over-all, Chave et al. (2005) showed the intermediate estimates across all class sizes, and is the most accurate biomass estimate. The allometric equations developed by Ketterings et al. (2001) is site-specific, and Brown (1997) is biased to commercial timber.



Plot-level mean biomass is shown in Table 2-9. Plot-level information is provided on the total number of trees sampled, number of species present, DBH range, and H range. Biomass levels were compared using the similar three allometric equations considered in estimating species-specific biomass. A similar observation was noted with the species-specific biomass estimates, regarding the highest biomass amounts using Brown (1997) equation. Brown (1997) tend to show at least 2x higher than Chave's estimates. Biomass estimates using the Ketterings et al. (2001) and Chave et al. (2005) equations showed comparable figures. Chave et al (2005) showed the best estimate. Plots from Antapan and Lake Venado 2 showed the highest level of biomass. These plots also showed the highest range of DBH, with trees measuring up to 432 cm and 441 cm, respectively. Plots with at most 2 species, Sayaban Elementary, Godi-godi 1, Makadak 1 and Makadak 3, did not show high biomass values. The high number of species per plot, like in the case of Coong-Matiaw (N=104), Makadak 2 (N=93), and Sayaban High School (N=89), also did not show high plot biomass storage. This plot biomass characterization suggested that high biomass storage is mostly attributed to the DBH.

Table 2-10 shows the carbon stock estimates by management zones. Carbon content is 50% of the biomass values (Westlake, 1966). The mean carbon stocks were estimated using the three tropical allometries. In terms of species frequency, the MUZ has the most number of trees species (N=34). The SPZ has the second highest number of 28 tree species, while the RZ has the least number of 23 tree species. MUZ, despite having the highest number of plots, and most heterogeneous species, showed the 2<sup>nd</sup> largest carbon content. On the other hand, RZ with the smallest plots and number of

species, showed the highest carbon content, with mean of 2,721 kg C tree<sup>-1</sup>. Carbon estimates generated from Chave et al. (2005) equation showed the intermediate values and the most accurate estimation. Relating to the plot biomass information in Table 2-9, RZ contain Plot Antapan, which has the highest biomass storage.

Finally, carbon stocks by land cover type are presented in Table 2-11. Thirty-seven plots from the closed-canopy forest contain the highest number of species sampled (N=37). Twenty-seven plots from the open-canopy forest contained 27 species. Six plots from the cultivated area have 21 species. The equation from Chave et al. (2005) also showed the intermediate carbon values. The highest carbon storage is found in the closed-canopy forest with mean value of 3,142 kg C tree<sup>-1</sup>. This result is consistent to the hypothesis established.

## 2.5. Conclusions

This study aimed to provide a profiling for the various types of plant communities present in the lowland, midland and upland areas in the park. The results showed that smaller trees with stem diameters of 2-5 cm, and 5-10 cm, were mostly found in the strict protection zone. However, wider stem diameters from 10-15 cm, and up to the class size of 30-35 cm, were predominantly found in the MUZ. In terms of height attributes, most of the tallest trees were found in the multiple use zone. Over-all, these findings showed that MU zone contained the highest species diversity, which rejected the hypothesis set for the SP zone. However Tinikaran, an indigenous forest species, and has the highest importance index, is dominant in the SP zone. R zone has the least number of species, but contained the highest biomass, with the biggest DBH of

432 cm in Plot Antapan, and also has the tallest tree, Agoho (H= 38.4 cm), a pine tree from Plot Matiaw 3. Half of the sampled plots represent areas in the MU zone. Additional plots can be mapped in areas from SP and R zones, when security issues can be settled, to allow further collection of field data. Plot biomass results suggested that high heterogeneous mix of species do not support high biomass storage. Large DBH as in the case of two plots, Antapan and Lake Venado 2, with DBH of 432 and 441 cm, contributed to the highest biomass content.

IVI was also used as an index of ecosystem importance and as a quantifier for vegetation studies. From the 52 listed species, the results for the top 10 highest species-specific biomass also supported the findings in IVI ranking. The IVI results also showed low frequency of occurrence for the 2 endangered species, *Agathis philippinensis* (Almaciga) and *Shorea palita* (Lauan). The findings implied a stark reduction of these species inside the protected area.

Most of these 20 species, which were developed into species-level biomass, have limited existing literature to be used for comparison in terms of species-specific biomass estimates. The existing local species with biomass estimates include mahogany and Dipterocarpaceae.

The 3 tropical allometric equations have shown how referenced biomass can be estimated. Brown (1997) equation exhibited large biomass values, usually at least 2x bigger than Ketterings et al. (2001) and Chave et al. (2005). This big difference is attributed to the fact that FAO used national inventories which were mainly based on commercial hardwood timber volumes, mostly with large DBH. Another allometry

developed by Ketterings et al. (2001) tended to show the smallest biomass values among the three equations. This is attributed to the fact that this equation was developed in a site-specific forest condition in Indonesia, where constant parameters were used: a) to reflect geographical area ( $r = 0.11$ ), b) average wood density for the study area ( $\rho^{\text{avg}} = 0.604 \text{ g cm}^{-3}$ ), and c) fixed parameter estimated by relating DBH and H ( $c=0.397$ ). Chave et al. (2005) has shown to be the best estimation approach in both the species-level and plot-level biomass estimation. This equation was developed from pan-tropical forest zones, and has considered wide variations for DBH and H, and species-specific wood density information. In the succeeding essays, these three allometric equations will be continued to be assessed in generating referenced biomass, and relating to various remotely-sensed biomass metrics.

Management zoning also provided insights on plot heterogeneity, which were helpful to promote species dynamics and growth structure. Ground-based forest inventory will further be validated using remote sensing approach to help quantify carbon stocks in inaccessible forested areas. It is also recommended to add permanent field plots to other areas that were considered critical areas during the 2013 fieldwork. These plots can help characterize vegetation dynamics in this uncovered portion of MANP. These biomass data will be beneficial for the Mt. Apo's forest inventory, as well as in monitoring, reporting and verification activities in line with the REDD program. These results will be considered as a first step for monitoring species-level carbon stocks and vegetation dynamics over time.

## **CHAPTER III**

### **ASSESSMENT OF TROPICAL FOREST BIOMASS USING TERRESTRIAL LIDAR SYSTEM**

#### **3.1. Introduction**

Measurement and quantification of forest structure is a vital step in developing a better understanding of how forest ecosystems work (Drake et al., 2002). The ability to estimate forest biomass is an important step in estimating the amount of carbon in terrestrial vegetation pools, and relating its significance to global carbon cycle studies. The terrestrial LiDAR system (TLS) offers the benefit of extracting forest structural metrics at the plot-level, which are cost-effective compared to rigid field measurements. These vertical structures can be used to estimate above-ground carbon storage (Lefsky, 2010). LiDAR remote sensing provides the technological capability to assess woody plant structures at a high-level of detail, thereby allowing more accurate estimates of biomass over large geographic areas.

TLS technology provides objective and consistent, though not necessarily unbiased measurements due to the influence of scanner parameters, scan resolution, speed and pulse duration (Pueschel, 2013). To increase accuracy in the extraction of tree metrics, the attempt to scan objects should be scanned from multiple locations to reduce the problem on shadowing, or occlusion of background objects by foreground objects. Basic inventory tree metrics that have shown accuracy in extraction are: tree location,

stem density and diameter-at-breast-height. Other important metrics, however, such as tree height and stem volume, have not so far been retrieved with high accuracy.

### 3.1.1. Rationale

This essay displays the application of Tier 2 approach as required by the Intergovernmental Panel on Climate Change (IPCC). A high-resolution TLS data will be added to the field measurements in developing an algorithm for the plot-level biomass. In compliance to the Reducing Emissions from Deforestation and Degradation (REDD) guidelines, the carbon content will also be assessed by forest type (Olander *et al.*, 2008).

This research attempts to provide an answer to this question: how can TLS technology be helpful in developing a plot-level biomass model? TLS-extracted height metrics will be related to reference biomass using ecological models.

### 3.1.2. Objectives

The primary objective of this study is to develop algorithms to determine above-ground biomass (AGB) at the plot level from terrestrial LiDAR data. Its specific objectives include:

1. Relating referenced AGB values from three allometric equations to TLS variables;
2. Identifying meaningful TLS variables in estimating plot-level AGB;

3. Demonstrating the effect of multiple scan locations on the accuracy of extracting individual tree metrics like height and stem diameter. and
4. Characterizing carbon content by management zone.

### 3.2. Review of Related Literatures

Tropical forests are among the most carbon-rich ecosystems in the world (Drake et al., 2002). They have a large potential to sequester carbon primarily through reforestation, agroforestry and conservation of existing forests (Brown, 1996). However, these resources are being destroyed at rapid rates (Achard et al., 2002) with the highest conversion rates in Southeast Asia. Knowledge of carbon pools and storage with net primary production of tropical forest is based primarily on a small number of studies, mostly from South and Central America while precise data from Southeast Asia and Africa are rare (Hertel et al., 2009). Table 3-1 shows selected studies on uncertainties of tropical AGB estimation using airborne and GLAS LiDAR. After extensive review, no studies were found that were done in tropics using TLS in biomass estimation.

Monitoring forests is crucial to ensure social, environmental and economic sustainability (Chen et al., 2007). Non-LiDAR technologies are capable of providing spatial and temporal results only in two dimensional formats. LiDAR is an active sensor, which emits a series of laser pulses, and measures the distance to the targets by knowing the speed of light and the time the signal takes to travel to and from a system (Lefsky et al., 2002). Unlike optical remote sensing, LiDAR remote sensing provides detailed information on the horizontal and vertical distribution of vegetation in forests, and it can generate three dimensional point cloud data with high spatial resolution and accuracy.

To obtain accurate understory information, terrestrial laser scanning (TLS) can produce better results compared to airborne LiDAR and traditional methods (Loudermilk et al., 2009).

Individual tree segmentation has significant implications in forestry (Li et al., 2012; Chen et al., 2007). This means that after trees are accurately segmented, tree structural attributes can be determined such as tree height, crown diameter, canopy-based height, basal area, DBH, wood volume, biomass and species type. Popescu and Wynne (2004) used a local maximum filtering technique to locate and measure individual trees. Bienert et al. (2006) showed how DBH and profiles along the stem can be determined using fitting circles. Popescu et al. (2003) showed that measuring individual tree crown diameter with LiDAR will also assess its influence on estimating forest volume and biomass.

Tree-level AGB was modelled for loblolly pines and hardwoods in East Texas using TLS data by Srinivasan et al. (2014). The significant variables for estimating AGB for loblolly pines were DBH, height variance, and interquartile distance. For hardwood species, volume and crown width showed better modeling results. Temporal change was also showed for trees between 2009 and 2012 using TLS data.

Ku et al. (2012) developed an algorithm for measuring plot-level woody biomass in mesquite trees in Texas. They showed that the height bin model is more robust compared to percentile heights. Their biomass map was up-scaled to regional scales



using digital ortho-rectified quarter quads (DOQQ) multispectral imagery, which covers larger areas than the terrestrial LiDAR data.

Drake et al. (2002) used large-footprint LiDAR technology to estimate above-ground biomass at plot level over the La Selva Biological Station, a tropical wet forest site in Costa Rica. Their study used QMSD as an index and reported an accuracy of  $R^2 = 93\%$ , compared to a basal area index with  $R^2 = 72\%$ . Their study confirmed the ability of LiDAR instruments to estimate important structural attributes, including biomass in a tropical forest.

Several factors such as light interception and  $\text{CO}_2$  fluxes are controlled by the three-dimensional arrangement of forest canopy elements. A significant parameter in the indirect estimation of true leaf area index is gap fraction. Stand-level directional gap fraction distributions were determined from TLS datasets and provided similar results when compared with gap fraction measurements obtained from hemispherical photographs (Danson et al., 2007). Crown density is another attribute which is used to measure tree health. It provides information on the amount of plant material, such as leaves and branches that obstructs skylight from shining through the tree crown. In addition, various metrics derived from TLS point cloud will be useful for inventory analysis and time series analysis, specifically tree growth and yield.

Setting up scanner parameters and data filtering has a direct effect on the accuracy of detecting stems, stem diameter and volume extraction from phase-shift TLS (Pueschel, 2013). This study demonstrated that scan speed, pulse duration, (i.e. noise

compression) and data filtering only have marginal influence on stem detection rates as well as on DBH and stem volume accuracies. This means that scans can be acquired with low scan quality and corresponding short scan times without significantly losing parameter estimation accuracy.

### 3.3. Data and Methods

#### 3.3.1. Data Acquisition

Sixteen circular plots at 30 m x 30 m diameter were scanned during the fieldwork in July 2013. These plots were stratified across the management zones, covering the vegetation gradient in MANP. The presence of local insurgency activity prevented the research team from sampling additional plots. FARO Laser Scanner Focus 3-D (FARO 2010 copyright) was placed in five different scan locations per plot: center, north, east, west and south. Figure 3-1 shows the sampling plot design. Four scanning targets made of volleyballs mounted on 2 m long polyvinyl chloride (PVC) pipes were positioned at each of the four sides. The scanner was mounted on a tripod at an average height of 1.48 m above ground. Each scan runs for 6 to 9 minutes. FARO Laser Scanner Focus 3-D was used with its high-speed 3D laser scanner for detailed measurement. FARO scanner 120 is a touch-operated screen that produces images of complex environments in only a few minutes. This scanner emits a laser beam from a rotating mirror out towards the scanned area. It then distributes the laser beam at a vertical range of 305° and a horizontal range of 360°. This laser beam is then reflected back to the scanner by objects in its path. The laser emits pulses of 905 nm at 1 cm posting and 120 m range. Its multi-

sensory capability enables it to level each scan with an accuracy of  $0.015^\circ$  and a range of  $\pm 5^\circ$ . The scanner can detect the heights relative to a fixed point via an electronic barometer and adds it to the scan. Its electronic compass gives the scan an orientation.

A geographic positioning system (GPS Garmin III plus) was used at the center tree to record the plot location. A laser hypsometer provided measurements of horizontal distance, tree height and azimuth. A spherical densiometer was used to measure canopy cover and its complement, the gap fraction. A Kestrel weather unit was also employed to provide information on elevation, temperature and relative humidity. A prism was used to estimate forest basal area. Finally, a compass was used initially to locate directions to guide where to place the scan targets.

All hardwood trees with at least 5 cm diameter within the circular plot were tagged using a standard stick of 1.34 m. Individual species for hardwood trees were identified by local names with the help of a native guide. Diameter-at-breast-height (DBH), height, and canopy width were measured for all trees with  $DBH > 5$  cm. Canopy cover and basal area index were also recorded for the plot. These study plots were stratified into three management zones. Table 3-2 displays classification of field plots by management zone.

### 3.3.2. Scan Pre-processing and Registration

Directional raw FARO laser scans (FLS) were registered using FARO SCENE software. Pre-processing was applied to detect spheres used as scanning targets. Scans were registered with the use of at least three reference objects per scanned image.

Correspondence view was generated and registration results with weighted statistics were shown. An option was chosen to level scans according to inclinometer. The value tension describes the discrepancy in the global coordinate system between the position and orientation of the two corresponding reference objects in at least two scans. Values close to zero indicate a good registration result. Table 3-3 shows the point cloud registration results.

Registered scans were exported as point cloud and saved as XYZ format. These ASCII data were then transformed into txt file format using SURFER software (Golden Surfer 9 copyright). SURFER is a full-function 3-D visualization, contouring and surface modeling program. Its interpolation engine transforms ASCII data into more useful 3-D surface mapping. Table 3-4 shows the plot-level LiDAR point cloud data density and height statistics.

### 3.3.3. Vegetation Height Metrics

The transformed ASCII files were then imported into the Quick Terrain Modeler (QTM, Applied Imagery copyright). QTM is a three-dimensional point cloud terrain visualization software package designed for processing LiDAR data. Above-ground level (AGL) analysis was applied with grid sampling of 1 meter and registered using a global coordinate system of Universal Traverse Mercator (UTM) with zone of 51N. AGL analysis is a powerful tool within the QTM software that enables it to convert the absolute elevations into relative heights. This tool removes ground and facilitates extraction of vertical heights to every point cloud.

A circular plot was extracted using LASTools software to show a 15 m plot boundary. This process begins with an acquisition of the coordinates for the center tree. The point clouds from the circular plot were clipped below an elevation of 2 m.

The resulting image provides the plot vegetation with height above 2 m. This vegetation height model was then processed in FUSION software to extract percentile heights and normalized bin heights. FUSION software enables command line programs designed specifically for LiDAR data processing.

There were two sets of height metrics generated from the model. Table 3-5 lists the regression variables. The first set consists of point cloud statistics related to mean height, maximum height, height standard deviation, and percentile heights. The second set of height metrics is the normalized height metrics. Height bins were classified as 2-5 m, 5-10 m, up to 40-45 m. Normalized height bin (NHBin) metrics are derived as:

$$\text{NHBin}(i) = \frac{\text{Returned points for bin } (i)}{\text{Sum of all total returned points}} \quad \text{for } i = 5, 10, \dots, 45 \quad (\text{Eq. 10})$$

Regression modelling was employed to relate the above-ground biomass derived using three tropical allometric equations, to the height statistics. Two types of regression models were chosen to evaluate the goodness of fit. Generalized linear model (GLM) using maximum likelihood estimation was considered to assess the relationship between these predictor variables. This method estimates the parameters of a statistical model, with the assumption that tree heights are normally (Gaussian) distributed with some unknown mean and variance. The second regression model used is stepwise

regression. A forward selection was chosen that automatically adds variables that improve the model fit. A variance inflation factor (VIF) was also derived for the significant parameters in the stepwise regression to detect the presence of multicollinearity in the data.

#### 3.3.4. Height and DBH Stem Maps

Height and DBH stem maps were plotted on a Cartesian plane for each plot. The reference tree is the center tree with (0,0) coordinates. Trees within the plot are mapped using the azimuth and horizontal distance information.

These stem maps provide an aerial display of the location for each tree within a plot with reference to the center tree. In the first step of the mapping process, an adjusted angle was computed which is the difference between  $360^\circ$  and angle ( $\emptyset$ ) for a specific tree. Then polar coordinates were computed using the adjusted angle and its relation to the angle size of a tree, multiplied with a constant factor to convert degrees to radians.

$$\text{Adjusted Angle} = 360^\circ - \emptyset \quad (\text{Eq. 11})$$

$$\text{Polar Coordinates} = (\text{Adjusted Angle} + 270^\circ) \times 0.0174532925 \quad \text{or} \quad (\text{Eq. 12})$$

$$\text{Polar Coordinates} = (\text{Adjusted Angle} - 90^\circ) \times 0.0174532925 \quad (\text{Eq. 13})$$

Figure 3-2 shows Sayaban Elementary School DBH stem map. It is a sample of a DBH stem map from a mahogany tree plantation inside a multiple use zone. Figure 3-3 displays Sayaban Elementary School height map.

### 3.3.5. Field Biomass Generation

Biomass density is estimated based on the biomass per average tree of each DBH class multiplied by the tree density in the class. Trees in each plot were classified based on DBH class. The DBH classes are: 5 - 50 cm, 51 - 100 cm, 101 - 150 cm, 151 – 200 cm, 201 – 250 cm, 251 – 300 cm, and above 300 cm. Tree density was computed as the number of trees present per plot based on each DBH class. The midpoint of each class was computed based on the quadratic-mean-stem-diameter (QMSD). Brown (1997) suggested the use of QMSD as a better choice, as compared to the average DBH, particularly for wide diameter class. QMSD is defined as the DBH of a tree of average basal area in the class. This is derived by first computing for the basal area (BA) of the average tree. Then QMSD is derived as 2 times the square root of BA divided by  $\pi = 3.1416$ .

$$\text{Basal area of average tree} = \frac{(\text{BA of the diameter class})}{(\text{Number of trees in the DBH class})} \quad (\text{Eq. 14})$$

$$\text{QMSD} = 2 \times \left\{ \sqrt{\left( \frac{\text{BA}}{\pi} \right)} \right\} \quad (\text{Eq. 15})$$

After computing the midpoint of the DBH class, tree biomass was calculated using the three tropical allometric equations adopted in Chapter II. Then biomass of all trees was computed as the product of tree density and QMSD per DBH class. Total above-ground biomass per plot ( $\text{Mg plot}^{-1}$ ) was computed as the summation of all biomass of trees in all DBH class. Table 3-6 shows Lake Venado 1 plot biomass using QMSD calculation.

### 3.3.6. Data Processing Flowchart

Image processing for the terrestrial laser scan data is shown in Figure 3-4. This shows how the TLS point cloud data was pre-processed and merged using FARO SCENE software. LASTools were also utilized to generate 30 m diameter plot extraction using the center scan coordinates. Above-ground analysis and ground removal was applied using QTM software to exclude any below-ground point cloud data. Vegetation height above 2 m was extracted for height bin analysis using the Cloud Metrics tool in FUSION software. Point cloud statistics were also derived for the percentile heights. These TLS variables were related to reference AGB, derived in Chapter II. Two sets of regression analysis were applied to relate tree metrics to reference AGB. These estimation approaches are generalized linear model/ maximum likelihood estimation, and a stepwise regression.

## 3.4. Results and Discussions

Permanent plots were sampled covering 697 hardwood trees from three types of management zone: multiple use, restoration and strict protection. Table 3-2 shows the classification of field plots by management zone and land cover type.

Nine plots were sampled from the multiple use (MU) zone, which includes areas in Sayaban, Kidapawan City, Bongolanon, Magpet, and New Israel, Makilala. Five plots represent restoration (R) zone, which are found in the Lake Agco and Matiaw areas in Kidapawan. Two plots were sampled from the strict protected (SP) zone in the upper montane areas. These plots represent the western and peak areas of the park. There were



no plots established in the northern portion of the park due to inaccessibility and presence of insurgency problems.

In terms of land cover classification, 10 plots were sampled from closed-canopy forest and 6 plots from cultivated area. No plots were scanned in open-canopy forest.

#### 3.4.1. Height Histograms

Figure 3-5 shows a height histogram of Sayaban Elementary School. The x-axis displays the height (m) and y-axis shows the frequency of trees per height classification. It represents point clouds height distribution of a plot from a MU zone. This histogram showed that mahogany trees display a more homogeneous height distribution with most trees around 20 m tall. This plantation area shows that mahogany are almost all at the same height. Figure 3-6 shows point cloud image of Sayaban Elementary School. It is an image of mahogany plantation with an inset of height legend.

Figure 3-7 displays height histogram of Matiaw 1. This is an example of a height distribution from a plot in a restoration zone. The histogram shows a varied height distribution, with most trees at 10 – 13 m tall. Figure 3-8 shows a point cloud image of Matiaw 1. This plot contains 7 types of hardwood species.

A height histogram for Lake Venado 2 is shown in Figure 3-9. This plot shows the presence of multi-stemmed trees found in the upper montane type. This site is inside a strict protection zone with 4 hardwood species. Tree heights are mostly lumped in the

lower height at 6 m tall, with few taller trees. Figure 3-10 shows a point cloud image of Lake Venado 2.

#### 3.4.2. Scan Registration

Scan merging showed higher deviation results with a range from 0.02 to 3.16. These results indicate that target scans or reference objects were not accurately detected during point-cloud registration. The four targets were not all detected at all times from the center scan. There were also instances where only 1 target is detected from any directional scan.

To remedy this issue, similar-looking objects (e.g. branches, hanged backpacks), were identified between scans to allow point cloud registration. Initial attempts were made to do tree-level AGB analysis, but an inspection of these point clouds discouraged us from further work on this research objective. Therefore, we directed our efforts to doing plot-level AGB estimation.

Height metrics derived from LiDAR data were generated and related to the field data. Figure 3-11 shows the regression model for maximum height. This model shows an  $R^2 = 64\%$  for the maximum heights for the two observations. However, a better model fit was generated when relating mean heights between field and TLS. Figure 3-12 shows the regression model for mean height. The regression model shows a higher  $R^2 = 88\%$ . These results may suggest that TLS may not be able to detect point clouds in upper canopies, or those that can be occluded by other under-canopy dense vegetation. This

study also shows that the use of terrestrial LiDAR technology can capture accurate understory information.

#### 3.4.3. Referenced Biomass

Table 3-7 presents the referenced biomass from three allometric equations. The plot-level biomass computed using the QMSD approach by Brown (1997) are shown for the 16 plots. Information for each plot also contains range of values for DBH and H, as well as mean biomass computed from three tropical equations. Higher values for mean biomass are shown for plots with high range for DBH values. Two examples are Antapan (DBH range= 21 – 432 cm) and Lake Venado 2 (DBH range= 6.5 – 441 cm). Biomass values from Chave et al. (2005) provided intermediate values between Brown (1997) and Ketterings et al. (2001).

Biomass values were converted to carbon content by a factor of 0.5 (Westlake, 1966). Table 3-8 displays plot-level carbon stock estimates by management zone. Biomass values calculated from Chave et al. (2005) showed that the strict protection zone has the highest carbon storage (mean C =173 Mg C plot<sup>-1</sup>).

#### 3.4.4. Biomass Estimation I

A summary of regression results using percentile heights is shown in Table 3-9. Three allometric equations were compared using linear and logarithmic models to evaluate how the independent variables relate to AGB. The generalized linear model use maximum likelihood estimation (GLM/MLE) to fit the model. It is a non-linear

estimation method. The test statistics of MLE follows a chi-square distribution. For non-linear models, indices such as minimum Akaike Information Criterion corrected (AICc), minimum deviance, minimum Pearson value, or maximum likelihood function can be used to compare model validity. In this case, the model with lower AICc was chosen to depict goodness of fit. AICc is defined as AIC with a correction factor for finite sample size or when there is a large number of parameter (k). This study considered a small number of observations, with n=16 and k=8. AICc is expressed as:

$$AICc = AIC + \frac{2k(k+1)}{n-k-1} \quad (\text{Eq. 16})$$

Table 3-10 shows the GLM model regression results using percentile heights from the Brown (1997) equation, Table 3-11 shows the GLM model regression results from Chave et al. (2005) and Table 3-12 displays the GLM model regression results from Ketterings et al. (2001).

Results of the logarithmic model from using the Brown (1997) allometric equation shows the model is valid at  $\alpha = 0.05$  level. Five independent variables also proved to be significant: mean height, and percentile heights at the of 25<sup>th</sup>, 50<sup>th</sup>, 75<sup>th</sup> and 95<sup>th</sup> levels. The final equation for the predictive model is written as:

$$AGB = \exp(3.56) \times \text{meanH}^{68.9} \times \text{Per25H}^{-11.08} \times \text{Per50H}^{-17.09} \\ \times \text{Per75H}^{-15.71} \times \text{Per95H}^{-11.18} \quad (\text{Eq. 17})$$

Chave et al. (2005) allometric equation showed that the MLE model is significant at  $\alpha = 0.10$ . There were two regressors that were significant at  $\alpha = 0.05$  level. These

are percentile heights at the 50<sup>th</sup> and 95<sup>th</sup> levels. Equation 18 shows the final equation for the predictive model.

$$AGB = \exp(5.51) \times \text{Per50H}^{-12.0} \times \text{Per95H}^{-9.98} \quad (\text{Eq. 18})$$

The final equation from Ketterings et al. (2001) showed that the logarithmic model is significant at  $\alpha = 0.10$  level. There are also five independent variables showing to be significant at  $\alpha = 0.05$  level. These are mean height, percentile heights at the 25<sup>th</sup>, 50<sup>th</sup>, 75<sup>th</sup> and 95<sup>th</sup> levels. The final equation is written as:

$$AGB = \exp(3.27) \times \text{meanH}^{58.13} \times \text{Per25H}^{-9.16} \times \text{Per50H}^{-14.95} \\ \times \text{Per75H}^{-13.13} \times \text{Per95H}^{-9.79} \quad (\text{Eq. 19})$$

#### 3.4.5. Biomass Estimation II

The second biomass estimation approach displays the statistical relationship between normalized height bins to AGB. Unlike the GLM/MLE model, standard least square is a linear model which uses stepwise regression to fit the model. The test statistic is an F-test, where information for Regression Sum of Square (SSR) and Total Sum of Square (SST) are given, enabling the computation of  $R^2$ . The index  $R^2$  explains the linear relationship between dependent and independent variables.

The summary of the regression results using normalized height bins are shown in Table 3-13. In this case, stepwise regression showed a better model performance for relating height bins in predicting AGB level. The  $R^2$  level for each model are at mid-50%

level, which may suggest that there are other unexplained factors that were not captured with these given independent variables.

Table 3-14 shows the stepwise regression results using normalized height bins from Brown's (1997) equation. Table 3-15 shows the stepwise regression results from Chave et al. (2005). Lastly, Table 3-16 presents stepwise regression results from Ketterings et al. (2001).

Results from an analysis of variance (ANOVA) for the Brown (1995) allometric equation showed that the model is valid at  $\alpha = 0.05$  level. The significant predictors are NHBin25 and NHBin 30. Both independent variables have  $VIF = 2.18$ , implying an absence of any multicollinearity issues. The final equation is written as:

$$AGB = 4396.79 x 2651839.9 NHbin25 x - 6336060 NHBin30 \quad (\text{Eq. 20})$$

ANOVA results from the Chave et al. (2005) allometric equation showed that the model is valid at  $\alpha = 0.05$  level. The only significant predictor is NHBin25 with  $VIF=2.21$ . The final equation is written as:

$$AGB = 2608.39 x 613949.8 NHbin25 x - 948818.8 NHBin30 \quad (\text{Eq. 21})$$

The ANOVA results from the Ketterings et al. (2001) equation also showed that the model is valid at  $\alpha = 0.05$  level. Like the Brown (1997) equation, NHBin25 and NHBin30 are significant predictors with  $VIF=2.18$ , implying absence of data multicollinearity issues. The final equation is written as:

$$AGB = 1593.9 x 652758.41 NHbin25 x - 1542118 NHBin30 \quad (\text{Eq. 22})$$

The predictive models generated provided an insight on how percentile heights and normalized height bins relate to estimating plot-level AGB. It may be easier for the user to identify height bins at 5 m interval, than using percentile heights. The use of wood density information from allometries developed by Chave et al. (2005) and Ketterings et al. (2001) would provide additional variability in addition to height and DBH information.

The regression models relating reference AGB to TLS height metrics had identified significant variables useful for biomass estimation. Variables selection techniques like GLM/MLE and stepwise regression also were useful in presenting how TLS height variables predict AGB. The various algorithms presented will be helpful in assessing carbon at plot-level.

### 3.5. Conclusion

Tropical forests are among the most carbon-rich ecosystems in the world, with the ability to sequester carbon through reforestation, agroforestry and conservation of existing forests. Mt. Apo Natural Park contains the hardwood tree species that has massive diameter sizes of  $\geq 300$  cm.

A referenced biomass was used to relate to the TLS-derived metrics. These referenced biomasses were computed using the 3 tropical allometric equations from Brown (1997), Ketterings et al. (2001) and Chave et al. (2005). Destructive sampling was not permitted in the MANP protected area. To compute plot biomass with large

DBH intervals, Brown (1997) suggested using quadratic-mean-stem-diameter for each DBH class to be used as a midpoint tree.

The allometric equations considered in this study reported a good modeling fit with the DBH classes. The predictive models generated provided an insight on how percentile heights and normalized height bins relate to estimating plot-level AGB. It was recommended to identify height bins at 5 m interval, than using percentile heights. Stepwise regression showed a good model fit in relating height bins to referenced biomass. The use of wood density information from allometries developed by Chave et al. (2005) and Ketterings et al. (2001) would provide additional biomass information, in addition to height and DBH information.

Far-flung areas limit the accessibility for doing field inventory inside this park. Local insurgency restricted the research team's access the northern portion of the park. The use of terrestrial LiDAR technology captured accurate understory information which are helpful in extraction of tree metrics. The algorithms developed are beneficial for future research work to extrapolate the biomass levels to landscape and park-level, using available multispectral or radar imagery.

This study demonstrated the biomass modeling study to be conducted in this national park. In compliance to REDD requirements, this study also characterized carbon content by management zone and forest types. These results will provide important insights to various stakeholders, both government and civic organizations, who are keepers of this cultural heritage for effective land-use management. The results



generated showed the ecological importance of these hardwood species, and their significance in storing carbon stocks. These research results will be used to generate a baseline carbon stocks information for MANP, which is considered as an important forest ecosystem in the country.

## CHAPTER IV

### TROPICAL FOREST BIOMASS ACCOUNTING USING IFSAR SYSTEM

#### 4.1. Introduction

Synthetic aperture radar (SAR) is an active sensing technology. SAR emits and records the reflection of microwave radio energy. Airborne SAR systems collect data from a very high altitude. Interferometric synthetic aperture radar (IFSAR or InSAR) provides a reliable three-dimensional remote sensing of forest structure. This 3D measurement provides an indicator of the effectiveness of the important forest ecological process of carbon cycling. Balzter et al. (2007) stated that forest canopy height is a critical parameter used in quantifying terrestrial carbon pools stored in vegetation and predicting timber yield for forest management. To generate canopy height, IFSAR uses polarimetric separation of scattering phase centers derived from interferometry. A canopy height model (CHM) derives its sensitivity to forest vertical structure from the differences in the signals received by two radar receivers. Wijaya and Gloaguen (2009) stated that IFSAR complements optical remote sensing to enhance vertical-structure estimates and measurements of biophysical quantities such as aboveground biomass.

IFSAR is an active microwave sensor that can operate at night, through cloud cover, through light rain, snow and dust. This technology is useful and cost-effective for mapping through the smoke of a forest fire, rain clouds, during a flood or at night. IFSAR products include digital surface model (DSM), digital terrain model (DTM) and

orthorectified radar imagery (ORI). DSM is a topographic model of the earth's surface. This model includes natural terrain features like vegetation and cultural features such as buildings and roads. DSM provides the accurate elevation needed for geo-referencing all subsequent layers. DTM is a topographic model of the bare earth that has had vegetation, buildings and other cultural features digitally removed. This model can enable users to infer terrain characteristics that were possibly hidden in the DSM. ORI is a grayscale image of the earth's surface that has been corrected to remove geometric distortions, accentuating topographic features far more than is possible with aerial photography (Intermap Product Handbook, version 4.4).

#### 4.1.1. Rationale

This study was designed to answer this research question: To what degree of accuracy can IFSAR estimate forest biomass at the landscape level? IFSAR X-band is often the shortest wavelength range (2.4-3.8 cm) which has partial penetration into canopy. Tighe and Barker (2000) noted that forests, comprised of individual trees of varying heights, trunk diameters, branches and leaves, are subjected to multiple and volume scattering as the radar penetrates the canopy. The IFSAR system, through STAR-3i Technology, offers a promising tool for deriving high-resolution digital elevation models and a good method for mapping topography.

#### 4.1.2. Objectives

The objectives of this paper are five-fold. First, it aims to present a method for canopy height mapping (CHM). The CHM layer will be calibrated with field height data to establish a linear relationship. This calibrated CHM layer leads to the second

objective, which is to examine the influence of calibrated IFSAR height in estimating biomass. Three interpolation techniques will be compared to derive radar backscatter values for biomass modelling. The third objective aims to use an un-calibrated CHM layer and compare backscattered variables from three resampling techniques. The fourth objective is to test whether multispectral data from Landsat 8 and ORI improve biomass estimation. The last objective is to characterize carbon storage across the three management zones.

#### 4.2. Review of Related Literatures

Derivation of forest canopy height models is vital in generating the spatial extent of a forest carbon pool using dual-wavelength SAR interferometry. Balzter et al. (2007) adopted a coherent microwave model to produce an estimate of terrain elevation. They compared IFSAR and LIDAR-derived CHMs for a test-specific site. Their paper also discusses a limitation of PolInSAR, where it relies on sufficient scattering phase center separation at each level in deriving accurate canopy height estimates. Balzter et al. (2007) reported that wavelength-dependent penetration depth into the canopy is known to be strong, which would potentially offer a better method to do height separation.

Saatchi et al. (2007) reported the use of multi-frequency polarimetric SAR in estimating distribution of forest biomass and three major fuel load parameters: canopy fuel weight, canopy bulk density and foliage moisture content. These radar estimates were in high agreement with field-based fuel measurements. Saatchi et al. (2007) created a biomass map at 1 km resolution which showed 11 biomass classes with 88% overall accuracy. They estimated total biomass of 86 Pg C (range 69-102 Pg C) in the Amazon

basin. Biomass estimates from Saatchi et al. (2007) are comparable to the estimates computed by Houghton et al. (2001). The biomass levels estimated by Houghton et al (2001) are within a range of 39-93 Pg C.

Table 4-1 lists selected papers on biomass estimation in tropics using SAR technology. Most of the studies I read used destructive field sampling methods to calculate biomass using allometric equations. Shimada and Isoguchi (2002) stated that the accessibility of JERS-1 SAR mosaics of Southeast Asia using L-band SAR has triggered research on biomass modeling in the region. Wijaya and Gloaguen (2009) combined SAR images and Landsat ETM data for land-cover classification using parametric and non-parametric methods, and estimated biomass using field data and SAR backscatter as a predictor over the tropical forest in Indonesia. Wijaya and Gloaguen (2009) found that data fusion between Landsat and SAR data and textures resulted in the highest classification accuracy of 90.55% and Kappa of 0.89, using the support vector machine technique. They initially observed a problem with low correlation between AGB and radar backscatter, and ended up using a non-parametric method for biomass modeling.

ALOS PALSAR data was used in a study by Morel et al. (2011) to estimate aboveground biomass in forests and oil palm plantations in Malaysia. Field data were integrated with ALOS PALSAR imagery to discriminate plantation from forest stands. Their research group predicted AGB using regression analysis of HV-polarized data. Precipitation effects on backscatter data changed the HV prediction and further suggested the use of multi-temporal SAR data.

Misbari and Hashim (2014) used IFSAR data over Malaysian forest to estimate total aboveground biomass. They applied a Gamma filter technique that improved total AGB estimation by 30%. They showed that IFSAR technology was able to sense sub-canopy structure of the forest with penetration through clouds for precise biomass estimation. The authors also related DBH and backscatter on IFSAR image and reported a high correlation with  $R^2 = 0.6411$ . Misbari and Hashim (2014) created a biomass model following Chave et al. (2005) allometry. Their biomass model showed a high accuracy result with  $R^2 = 0.9139$ .

#### 4.3. Materials and Methods

##### 4.3.1. SAR Data Acquisition

Airborne Interferometric Synthetic Aperture Radar (IFSAR or INSAR) is being used as an accurate and reliable 3-D mapping tool (Intermap Product Handbook, version 4.4). It is enabled by cost-effective sensor positioning and an orientation solution that uses Global Positioning System (GPS) and Inertial Navigation System (INS) technologies. The STAR-3*i* system is a commercial implementation of an airborne, single-pass across track IFSAR system, owned by Intermap Technologies since 1997 (Li et. al, 2002) . The STAR-3*i* system comprises an X-band SAR interferometer onboard a LearJet 36. Two antennae are mounted to a solid invar frame with a 1 m baseline.

Intermap STAR-3*i* technology offers a number of capabilities and advantages. First, IFSAR is an active microwave sensor and can operate in various environments e.g., at night, through cloud cover, through light rain, snow or dust. It generates first

surface DEMs, and terrain models or bare-Earth DEMs. IFSAR also generates high-resolution orthorectified radar imagery along with DEMs. Large-area mapping can also be done in a short-time frame due to its weather independence, fast data acquisition and high level of production automation. Lastly, this STAR-3i technology is very competent to generate high-resolution and highly accurate mapping data for large areas. Details on Intermap's STAR-3i technical specifications are shown below in Table 4-2. Specifications of Intermap's core products are provided in Table 4-3.

Intermap Technologies mapped the study area in July 2013, while the group was conducting forest inventory. Table 4-4 shows the description for the 2013 IFSAR product accuracy. The IFSAR core data purchased include Type II products for DSM and DTM, with 1 m vertical and 2 m horizontal RMSE accuracy. ORI has a 2 m RMSE and an improved pixel size of 0.625 m.

Hagberg et al. (1995) described radar interferometry as using the difference in phases between two radar images acquired from slightly different locations. These phase differences were used to generate information relating the elevation angle to an imaged point. Sensors emitting pulses with short wavelength (X-band) measures the canopy surface, or DSM. However, sensors with longer wavelength (L-band) collect information about the sub-canopy and terrain features, or DTM. Andersen et al. (2006) stated that the difference between the canopy elevation (X-band) and underlying terrain elevation (L-band) results in a canopy height model (CHM). CHM represents a spatially-explicit

description of canopy structure over a defined area of interest. These canopy structures refer to volume, height, biomass, and canopy fuel density.

#### 4.3.2. Methods

IFSAR data is compiled in the band-interleaved by line (.bil) file extension. These were manually renamed to float format, and then converted to raster format. Projection was defined to a coordinate system of Universal Transverse Mercator (UTM) with Zone 51 North. A CHM raster was generated as the difference between DSM and DTM. Twenty-six circular field plots were geo-located in the 5 m CHM raster using center scan GPS information. Then a 15 m radius was calculated to buffer the study plot. Each plot contains an area of 707 m<sup>2</sup>. Individual plot CHM was extracted by mask in ArcGIS model builder. Area-based statistics were computed from the 5 m CHM plots using zonal statistics. These statistics include percentile heights from 25<sup>th</sup>, 50<sup>th</sup>, 75<sup>th</sup>, 90<sup>th</sup> and 95<sup>th</sup> levels, maximum, minimum and standard deviation. Variance textural indices were also computed from CHM and ORI raster. Rasters for slope, elevation and aspect were derived from DTM. Average pixel values for these three raster surfaces were then computed from 5 m IFSAR products.

These IFSAR products were also resampled to 26.6 m<sup>2</sup> to capture the circular plot in a pixel. Equation 23 shows the computation, where A is the area of a plot and radius (r) = 15 m.

$$A = \pi r^2 = 26.6 \text{ sq m} \quad (\text{Eq. 23})$$



Three interpolation methods were investigated: nearest neighbor (NN), bilinear (BI), and cubic convolution (CC). Similar sets of parameters from the 5 m IFSAR were extracted from the resampled IFSAR products. IFSAR maximum height for all study plots were calibrated to field plots. The regression equation was used to do height calibration. The new IFSAR calibrated height were processed into resampling techniques (NN, BI and CC). A similar set of backscattered values were extracted.

Landsat 8 imagery acquired on June 19, 2014 over Mt. Apo Natural Park was downloaded from the USGS Earth Explorer website (USGS, [www.earthexplorer.usgs.gov](http://www.earthexplorer.usgs.gov)). Landsat 8 acquires global moderate resolution measurements of the Earth's terrestrial regions in the visible, near-infrared, short-wave and thermal infrared. It has various capabilities and applications of new science opportunities, which include agriculture, land cover, disturbance and change, surface reflectance, albedo, temperature, evapotranspiration and drought. The Landsat address for MANP is Path 112 and Row 55. Six Landsat 8 bands were stacked in one layer and projected to UTM Zone 51 N. These band names are band 2 (Blue), band 3 (Green), band 4 (Red), band 5 (Near-Infrared), band 6 (SWIR1) and band 7 (SWIR2). Three parameters were extracted from the stacked Landsat 8 image. First, principal correlation analysis (PCA) was applied and PC1, or the first component was chosen as a model predictor with the highest factor loading of 0.9688. Two indices like normalized difference vegetation index (NDVI) and simple ratio (SR) were also calculated. Vegetation indices for NDVI and SR are computed as:

$$\frac{\text{NIR} - \text{Red}}{\text{NIR} + \text{Red}} = \text{NDVI} \quad (\text{Eq. 24})$$

$$\frac{\text{NIR}}{\text{Red}} = \text{SR} \quad (\text{Eq. 25})$$

A management zone map was downloaded from Mt. Apo Foundation, Inc. (MAFI, [www.mafi.org.ph](http://www.mafi.org.ph)). This downloaded map was digitized to re-create the park boundaries. The resulting biomass map was then extracted by mask using the management zones polygons. Biomass levels were estimated by management zone map. Predicted biomass was compared to reference biomass values. Residuals were processed for uncertainty analysis using a software package, Simulation and Econometrics to analyze Risk (SIMETAR).

#### 4.3.3. Data Processing Flowchart

A flowchart for the IFSAR image and data processing is shown in Figure 4-1. IFSAR 2013 images were pre-processed and geo-referenced using field plots coordinates. Three IFSAR products were utilized, DSM, DTM and ORI. A CHM 5 m raster was generated as the difference between DSM 5 m and DTM 5 m. A 15-m buffer was created using the center scan coordinates for the 26 field plots. There were a total of 5 AGB models considered for this analysis. The 5 m IFSAR metrics derived constitute the 1<sup>st</sup> AGB model. The 2<sup>nd</sup> AGB model consists of un-calibrated metrics derived from resampled ORI and CHM layers. In this 2<sup>nd</sup> model, ORI 0.625 m was resampled into a 26.6 m<sup>2</sup> using three interpolation techniques. Similar to Model 1, a 15 m CHM raster

was also created. The metrics derived in the 2<sup>nd</sup> model were not calibrated to the field data.

The 3<sup>rd</sup> AGB model involved the calibration between IFSAR height and the field data height. The plot metrics derived include CHM 26.6 m<sup>2</sup> from the three resampling methods and ORI texture. The 4<sup>th</sup> model considered the Landsat 8 with 30 m data. This multispectral data was resampled using NN to 26.6 m<sup>2</sup>. The last AGB model involved the hybrid of Landsat 8 resampled and IFSAR un-calibrated metrics. Referenced AGB values were taken from Chapter III, following the quadratic-mean-stem-diameter approach by Brown (1997). The estimated biomass was overlaid on the digitized management zone to characterize forest biomass. A 0.5 conversion factor was applied to derive a forest carbon map.

An uncertainty analysis was also conducted using the AGB residuals, computed as the difference between the predicted and observed biomass. A simulation analysis was applied to determine the uncertainty level.

#### 4.4. Results

##### 4.4.1. CHM Distribution Map

Figure 4-2 shows an IFSAR CHM distribution map. Field plots were labeled based on the land use types. Plots in the restricted zone (RZ) have a higher range for minimum CHM values (5 - 14 m), the strict protection zone (SPZ) has a 1 - 10 m range, while the multiple use zone (MUZ) has a range of 0 - 10 m. In terms of maximum CHM

range, MUZ has the highest range of 10 - 29 m. In terms of the mean CHM range, RZ has the highest range of values of 12-18 m.

Results from the forest inventory covering 26 plots showed that the minimum tree height is 2 m. This information was considered to classify the CHM values of 0 - 2 m as open or non-forested areas. The non-forested areas constituted 73,192 pixels, or 7.9% of the entire park. These non-forest areas were masked in the CHM map.

Figure 4-3 to Figure 4-5 exhibit examples of orthorectified imageries, displaying areas falling within these three management zones. Figure 4-3 presents an area within the restoration zone. The geothermal plant, Energy Development Corporation/Philippine National Oil Company, is visible in the image. This geothermal plant occupied 701 ha. This company also supports reforestation projects in the identified restoration areas. The reforested areas were mostly covered with a young teak plantation *Leptospermum flavescens* or locally called as Tinikaran, which is an indigenous forest species. Figure 4-4 displays an area within the multiple use zone. The imagery shows the dominance of rectangular plots. These areas are vegetable plots planted with cabbage, carrots, and potatoes. Other bigger areas were planted with exportable Cavendish bananas. An example of an area within the strict protection zone is shown in Figure 4-5. It is located in the upper montane. The imagery shows the closed canopy cover.

#### 4.4.2. Biomass Modeling

Maximum tree heights per plot were computed from the results of the field inventory conducted in July 2013. Measurements derived from IFSAR CHM maximum

heights, were compared to the referenced field data. Table 4-5 showed the results relating field height and CHM-derived height by management zone. Figure 4-6 displays the scatterplot chart showing the empirical models to relate maximum IFSAR height and field-derived height. Height comparisons were done on two levels: by management zone and aggregated zones. A limited number of field samples (26 plots) were obtained due to safety concerns, as discussed in Chapter II. However, the research team believed the sampled plots represent the vegetation gradient in the MANP. For the multiple use zones, 13 plots showed that field height tended to be under-estimated by 5.18 m with IFSAR-derived height when the coefficient is close to 1. For coefficients larger than 1, IFSAR CHM heights would always under-estimate the field heights, as observed in the strict protection, restoration and aggregated zones.

An index, the coefficient of determination ( $R^2$ ), indicated how well data fit a statistical model. In general, the  $R^2$  results in Table 4-5 signified an over-all good fit for explaining the variability in the field height data by the independent variable, the IFSAR height. The multiple use zone has a  $R^2 = 0.68$ , the strict protection zone has a  $R^2 = 0.85$ , the restoration zone has a  $R^2 = 0.91$ , and the over-all zone has a  $R^2 = 0.75$ . Another index, the root mean square error (RMSE) measures the difference between values predicted by the model and the values actually observed. RMSE provides a measure of model accuracy. RMSE values for each zone are: 3.86 m (MUZ), 3.33 m (SPZ), 2.09 m (RZ), and 4.30 m (All zone). The lowest RMSE coincided with the restoration zone for which only a few plots ( $n = 6$ ) were sampled.

NDVI is a numerical indicator that uses the visible and near-infrared bands of the electromagnetic spectrum (Jensen, 2007). NDVI is an index to quantify green vegetation. The value range is between -1 to 1, where healthy vegetation generally falls between values of 0.20 to 0.80. Sampled plots from the multiple use zone exhibited higher NDVI values, with a range of values from 0.20 to 0.52. Plots from the restoration zone showed a range of NDVI values of 0.13 to 0.30, while plots from the strict protection zone had the lowest NDVI values with a range from 0.08 to 0.10.

Another vegetation index is the simple ratio. Simple ratio (SR) describes the ratio of light that is scattered in the NIR range to that which is absorbed in the red range (Jensen, 2007). The range of values is from 0 to more than 30, where healthy vegetation falls between values of 2 to 8. Plots from the multiple use zone also exhibited the highest SR value range from 1.5 to 3.2. The restoration zone has SR values from 1.3 to 1.9, while the strict protection zone has the lowest range of SR values from 1.18 to 1.20.

Table 4-6 shows the regression variables for 5 modelling tiers. The dependent variable used was AGB, expressed as Mg plot<sup>-1</sup>. Table 4-7 contained the regression results using standard least squares (SLS) regression in JMP software. An output from the SLS regression listed all independent variables, irrespective of any significant effects on the model. In comparison, Table 4-8 presents the regression results using stepwise regression. Stepwise regression is a variable selection procedure that uses both forward and backward selection techniques. All candidate variables were evaluated using some

cut-off probability and tolerance levels. The final model generated from stepwise regression reports variables that meet the cut-off probability.

Regression results reported these four indices to evaluate the model accuracy:  $R^2$ , F-statistics, root mean square error (RMSE), and variance inflation factor (VIF).  $R^2$  measures the goodness-of-fit of linear regression.  $R^2$  values denote how the independent variables explain the variability in the model. F-stat is used to determine if the variances between the means of two populations are significantly different.

VIF quantifies the severity of multicollinearity in regression analysis. Multicollinearity occurs when two or more predictors are highly correlated. If multicollinearity is severe it affects calculations regarding individual predictors. A VIF index greater than 10 is used as rule of thumb for detecting severe multicollinearity (JMP 8 User Guide, 2008).

#### 4.4.2.1. First AGB Model (IFSAR 5 m)

The 1<sup>st</sup> model related metrics derived from 5 m IFSAR to AGB plot level. From the standard least squares regression result, the 5 m IFSAR model showed an  $R^2 = 0.85$ , F-stat = 0.0004 and RMSE = 398 Mg plot<sup>-1</sup>. The significant variables at  $\alpha = 0.05$  level, are percentile heights from the 25<sup>th</sup>, 50<sup>th</sup> and 75<sup>th</sup> levels. The VIF index, however, displayed values greater than 10, suggesting that these variables are correlated. From stepwise regression results, it showed that IFSAR 5 m shows  $R^2 = 0.32$ , F-stat = 0.0123 and RMSE = 365 Mg plot<sup>-1</sup>, and VIF index of less than 10.

#### 4.4.2.2. Second AGB Model (IFSAR 26.6 m<sup>2</sup> un-calibrated)

The 2<sup>nd</sup> biomass model related plot AGB to un-calibrated and resampled IFSAR metrics. These IFSAR metrics are not calibrated to the field height data. The three resampling techniques applied were nearest neighbor, bilinear and cubic convolution. In theory, nearest neighbor assignment does not essentially alter the value of the input cells. This technique will determine the location of the closest cell center on the input raster and assign the value of that cell to the pixel on the output raster.

Bilinear interpolation uses the average value of the four closest input cell centers to determine the value on the output raster. This resampling approach results to a smoother-looking surface compared to the nearest neighbor. Lastly, cubic convolution is similar to bilinear assignment except that the weighted average is computed from the 16 nearest input centers and their values. The output surface will tend to have sharpened edges, since more cells are involved in the computation of the output value.

The resampled IFSAR modelling results from the use of cubic convolution had the highest  $R^2 = 0.434$  and the lowest  $RMSE = 283 \text{ Mg plot}^{-1}$  as shown in Table 4-7. From the stepwise regression in Table 8, the cubic convolution approach generated a  $R^2 = 0.395$ , and  $RMSE = 272 \text{ Mg plot}^{-1}$ .

BI also showed comparable results with the CC technique. NN, on the other hand, showed the lowest  $R^2$  and highest RMSE level. All three resampling techniques did not present any issues of multicollinearity.



#### 4.4.2.3. Third AGB Model (IFSAR 26.6 m<sup>2</sup> calibrated)

The 3<sup>rd</sup> biomass model exhibited the relation between AGB and the three resampling methods applied to calibrated IFSAR heights. The results from standard least squares regression depicted in Table 4-7 show that the cubic convolution technique had the highest  $R^2 = 0.434$  and lowest  $RMSE = 283 \text{ Mg plot}^{-1}$ .

The stepwise regression results in Table 4-8 showed smaller values for both indices, but also indicated that CC has the best modeling performance. BI showed a close performance results with CC, and NN showed the least-likely modeling indices. All the three resampling techniques did not present issues of multicollinearity.

#### 4.4.2.4. Fourth Model (Landsat 26.6 m<sup>2</sup>)

The 4<sup>th</sup> model showed the relationship between plot AGB and Landsat metrics. The metrics are from the resampled Landsat image using NN technique. As reported in Table 4-7, this model had the lowest  $R^2 = 0.09$  and a relatively high  $RMSE = 327 \text{ Mg plot}^{-1}$ . Similar results are exhibited in Table 4-8 for this model with a  $R^2 = 0.12$  and  $RMSE = 314 \text{ Mg plot}^{-1}$ . The VIF index from the two regression methods showed the presence of multicollinearity. In this case, Landsat variables were not considered for further analysis.

#### 4.4.2.5. Fifth Model (Landsat 26.6 m<sup>2</sup> and IFSAR 26.6 m<sup>2</sup> un-calibrated)

The 5<sup>th</sup> model displayed the relationship between plot AGB and the combination of Landsat and IFSAR metrics. These statistical metrics were derived using the

resampling techniques from the 4<sup>th</sup> model and the three resampling styles applied in the 2<sup>nd</sup> model. Results reported in Table 4-7, reveal that the CC method presented the highest  $R^2 = 0.40$  and a  $RMSE = 323 \text{ Mg plot}^{-1}$ . The stepwise regression results reported in Table 4-8 show that the NN approach had the highest  $R^2 = 0.31$  and a  $RMSE = 318 \text{ Mg plot}^{-1}$ .

#### 4.4.3. IFSAR Height Calibration

The regression results using the calibrated IFSAR height displayed a small difference compared to the results using the un-calibrated IFSAR heights. The comparison between the two regression methods showed that standard least squares, reported in Table 4-7 has higher model accuracy results, compared to the stepwise regression reported in Table 4-8.

An inspection of the three resampling techniques between the 2<sup>nd</sup> and 3<sup>rd</sup> biomass model revealed identical values for  $R^2$  and  $RMSE$ . The difference can be seen in F-statistics. The F-statistics indicated that CC in calibrated IFSAR contained the most robust biomass model. The biomass equation developed from calibrated IFSAR CC-standard least squares regression model is written as:

$$AGB = -46.90 - 14.71 (\text{slope}_{CC}) + 8.40 (\text{ORI}_{\text{stddev}_{CC}}) \quad (\text{Eq. 26})$$

The biomass model from the un-calibrated IFSAR model, using IFSAR CC-standard least squares regression is written as:

$$AGB = -52.86 - 14.75 (\text{slope}_{CC}) + 8.42 (\text{ORI}_{\text{stddev}_{CC}}) \quad (\text{Eq. 27})$$

#### 4.4.4. Management Zone Mapping

The digitized management zone map is shown in Figure 4-7. The map shows that the Mt. Apo Natural Park consists of the strict protection zone (45.9%), the multiple use zone (51.5%), and the restoration zone (2.6%). This profile is translated to areas covered as: strict protection (25,201 ha), multiple use zone (28,340 ha) and restoration zone (1,434 ha).

#### 4.4.5. Biomass and Carbon Mapping

IFSAR metrics derived using the CC spatial interpolation method and calibrated IFSAR were used in developing the final biomass model. The IFSAR 5 m model showed a higher  $R^2$  values, but in order to generate an up-scaled biomass for the entire park, the resampled image was considered. Table 4-9 shows the standard least squares regression model using calibrated IFSAR cubic convolution. Surface rasters for aspect and ORI layer were considered in generating the biomass map. The MANP biomass map measured in  $\text{Mg ha}^{-1}$  is shown in Figure 4-8. The computed biomass for the entire park has a range of values from 0 - 3,019  $\text{Mg ha}^{-1}$ . A conversion factor of 50% was applied to the biomass values in order to derive the carbon content. Figure 4-9 displays the MANP forest and non-forest carbon map. Non-forested areas displayed carbon storage lower than 225  $\text{Mg C ha}^{-1}$ . Forested areas displayed carbon values ranging from 225 to 1,509  $\text{Mg C ha}^{-1}$ .

Figure 4-10 display the MANP carbon stocks on management zone map. RZ contains the lowest range of carbon from 2.5 to 1,212  $\text{Mg C ha}^{-1}$ . SPZ has the 2<sup>nd</sup> highest

carbon storage, ranging from 2.5- 1,478 Mg C ha<sup>-1</sup>. MUZ has the highest carbon stocks, with values ranging from 2.5 to 1,509.5 Mg C ha<sup>-1</sup>. Table 4-10 also presents information on the average biomass values per management zone. The table shows that despite having the smallest area of 2.6% in the entire MANP, RZ contained the highest average biomass per hectare of 1,616 Mg ha<sup>-1</sup>. The lowest average biomass of 94 Mg ha<sup>-1</sup> is found in MUZ.

#### 4.4.6. Uncertainty Analysis

An uncertainty analysis was implemented to assess the error and the uncertainty of the error of predicted AGB. We applied the empirical model from the cubic convolution technique relating it to AGB. We then compared the model's predicted (from IFSAR 26.6 m<sup>2</sup> pixel) AGB to the ground reference (observed) value. The remote sensing model prediction error for each plot was computed as the difference between the predicted and observed AGB value. This is also referred to as the AGB residuals. In simulation, the residuals are used to quantify the unexplained risk for a random variable. A bootstrapping sampling technique was used to calculate confidence interval (CI). Bootstrapping is a statistical technique that approximates the sampling distribution by simulating data from a model, and treating the simulated data like the real data. A univariate distribution containing the prediction errors of 26 plots were further simulated using a Gaussian kernel approach. The iteration was run for 500 samples. The CI characterizes a probability density function (PDF) about the mean error value.

Figure 4-12 presents the PDF approximation for AGB residuals. The PDF shows a unimodal distribution about the mean error value of  $0.428 \text{ Mg ha}^{-1}$ . The uncertainty of the error was reported as a 95% CI. The mean error is within the 20% of average of 3 allometric equations used in the reference biomass estimation. REDD requires that uncertainty errors to be 20% or less of the difference between predicted and observed AGB residuals.

Two levels of hypothesis testing were applied at 95% CI to the distribution of AGB residuals. The 1st hypothesis test is the distribution comparison of the two data series. The first series is the AGB residuals. The second series is the iterated data from 500 samples. The 2<sup>nd</sup> hypothesis test is for the normality of distribution of AGB residuals.

#### 4.5. Discussion

The availability of three-dimensional IFSAR data over Mt. Apo Natural Park has provided a new means to estimate forest biomass. IFSAR offered an improved technology for tropical forests, continually faced with issues of dense cloud cover, and complex forest structure. Airborne SAR technology used differences in phase shift, which enables the generation of a canopy height model from two sensors of varying wavelengths. The short wavelength sensor measured the canopy elevation while the longer wavelength sensor provided information on sub-canopy and terrain features. The CHM map showed a spatially-explicit description of the canopy structure (e.g., biomass, height) across this park. The classification of vegetation based on CHM range also

provides information on the distribution of forested and cultivated areas. This paper showed that IFSAR core products offer new sources of aerial-based metrics. These metrics, like textural measurements, surface rasters and heights, contributed to more accurate estimates of AGB. The CHM map also provided significant input in preparing a management zone map using the support vector machine classifier. The biomass pixel<sup>-1</sup> revealed that the restoration zone contains the highest biomass storage in the park, at 1,616 Mg ha<sup>-1</sup>. The strict protection zone constituted 45.9% of the park area, but average biomass is at 118.6 Mg ha<sup>-1</sup>. The multiple use zone showed the lowest average biomass at 94.8 Mg ha<sup>-1</sup>. The multiple use zone was also adjacent to non-forested areas, which make up 7.9% of the pixels in the park. In this study, non-forested areas were classified as having CHM values lower than 2 m. This was a conservative estimate and assumption, as canopy cover estimates from the ground were not considered. It is likely that other forested areas were susceptible to human encroachment like small patches of farming activities. It was likewise observed during the field work that sounds from chain saw machines were heard inside the park, close to sampled plot in Baroring, Kapatagan.

Landsat 8 multispectral data was tested on its ability to improve biomass estimation. The Landsat derived metrics however showed problem of multicollinearity, as shown by high VIF index. The orthorectified image was also considered for biomass modeling, where it showed as a significant input for the final biomass model. The final biomass model, developed from CC interpolation, showed a  $R^2 = 0.43$ , from two IFSAR metrics: slope and ORI, using standard least squares regression. This result means that 43% of the AGB variability is explained by IFSAR variables. It implies that there are

other factors, which were not accounted for in this model that could potentially improve the biomass estimation. Increasing the sample size can also be considered as a means of improving the accuracy of the AGB estimation. In this study, only 26 plots were sampled due to the insurgency issues surrounding the research site. This insurgency concern limited the research team's ability to gather additional reference data. In a study conducted by Montesano et al. (2014), they illustrated how airborne and spaceborne SAR models explained proportions of variability in AGB. Airborne SAR (UAVSAR) models explained 60 - 89% of AGB variation with a large number of observation,  $N = 113$ . However, ALOS PALSAR with a bigger number of observations ( $N = 607$ ) reported lower  $R^2$  values, which implied that PALSAR explained 13–46% of AGB variation.

Gibbs et al. (2007) compiled results of the total estimated carbon stocks in the Philippines, shown in Table 4-11. Their group divided the methods used for carbon mapping from compiled harvest data and from forest inventory. The range of carbon values from compiled harvest data is from 765 – 2,503 Mt C. These figures were taken from these following reports. Olson et al. (1983) and Gibbs (2006) reported 869 Mt C. Houghton (1999) and DeFries et al. (2002) reported 765 Mt C. IPCC (2006) reported 2,503 Mt C. Meanwhile, for the forest inventory data, the range of C values is from 1,213- 1,530 Mt C. These values are reported by Brown (1997), Achard et al. (2002), Achard et al., (2004) at 1,213 Mt C, and Gibbs and Brown (2007a,2007b) at 1,530 Mt C. Results from forest inventory data showed higher carbon levels compared to the harvest data. This range of carbon values from 765 – 2,503 Mt C represents various types of

forest areas over the entire country. MANP is located in the southern part of the Philippines, but climatic conditions are similar throughout the country. MANP has the highest altitude which can be compared in the upper range of carbon values.

The derived carbon stocks levels from this study in Mt. Apo are also comparable with the studies conducted in the Philippines. Table 4-12 lists the scientific papers examined on carbon storage in selected areas in the Philippines. Han et al., (2010) reported carbon storage of 313 Mg C ha<sup>-1</sup> from a natural forest stand, and 185.28 Mg C ha<sup>-1</sup> from mahogany plantations in the Mt. Makiling Forest Reserve. The location of Mt. Makiling is in the northern part of the country. Lasco et al., (2004) also conducted a study in the same forest location, and reported carbon storage of 418 Mg C ha<sup>-1</sup>. Another study by Lasco et al. (2006) showed carbon storage of 258 Mg C ha<sup>-1</sup> for a selectively logged forest in Surigao del Sur. The forest from Surigao del Sur is located in the southern portion of the country, found on the same island as MANP. Figure 4-11 compares the Philippine forest carbon values from this study to published materials. This graphical presentation compares the range of carbon levels, with standard errors, of this study to Gibbs et al. (2007) and two studies from Lasco et al. (2004, 2006).

The results for carbon storage derived on this study were compared to the global canopy maps. Mitchard et al (2013) compared two carbon maps generated by Saatchi et al. (2011) and Baccini et al. (2012). Both studies showed a carbon storage of 300 Mt C ha<sup>-1</sup>. The global canopy carbon maps from Saatchi et al (2011) and Baccini et al (2012) is shown in Figure 4-12. Both studies of Saatchi et al. (2011) and Baccini et al. (2012)



showed similarities in methodologies: 1) both carbon maps were generated from LiDAR GLAS footprints, and 2) allometric equation from Chave et al (2005) were considered. The differences include quality of spatial resolution, number of calibration points, and choice of modelling algorithm. Table 4-13 presents the comparison of methods for global canopy maps.

Uncertainty analysis for AGB residuals was conducted using bootstrapping sampling technique. This technique is used for advanced simulation problems and assume that past deviates or errors can be resampled an infinite number of times. The bootstrapping technique uses samples from a known distribution with replacement. A PDF approximation for the AGB residuals is shown in Figure 4-13. The PDF graph displays simulation results. The mean of the AGB residuals is shown in the chart. It shows that a unimodal distribution about the mean error value of  $0.428 \text{ Mg ha}^{-1}$  at 95% CI. Lower and upper quantiles are also shown in the PDF graph.

A Gaussian kernel estimator was used to smooth the data. The uncertainty error value of  $0.428 \text{ Mg ha}^{-1}$  was within the 20% of the uncertainty between the predicted and observed AGB residuals. The hypothesis test for distribution comparison of residuals and AGB residuals is shown in Table 4-14. This 1<sup>st</sup> hypothesis test shows that at 95% confidence level, the test failed to reject the null hypothesis that the means are equal. These data means refer to the distributions from AGB residuals and the iterated 500 samples from bootstrapping simulation.

Table 4-15 reports the hypothesis test for normality of distribution for residuals. This 2<sup>nd</sup> hypothesis test for the normality distribution of AGB residuals showed that the test failed to reject the null hypothesis that the distribution is normally distributed. The normality tests are: Shapiro-Wilks, Anderson-Darling, Cramer-von Mises, and Chi-Squared. Twenty bins or intervals were set for the chi-squared test.

#### 4.6. Conclusion

This study has demonstrated how IFSAR products (DSM, DTM and ORI) can be used to characterize biomass and carbon in a landscape level. This research undertaking presented an application of remote sensing technology to assess available biomass levels, which are usually extracted using destructive sampling. In current times, where deforestation is considered as the leading threat for forest ecosystems, it is not prudent to adopt a traditional destructive sampling approach. Information generated from the remote sensing approach can be compared to the results generated using compiled harvest data, and other forest inventory data. These IFSAR data reflect the landscape conditions in 2013 when the imagery was taken. Other by-products generated like the CHM map and management zone mapping, are also reflective of the recent conditions.

This study has produced a digitized landcover map and original carbon map for the Mt. Apo Natural Park. The carbon storage computed from this study (258-418 Mg C ha<sup>-1</sup>) is within comparable range with global canopy maps of Saatchi et al (2011) and Baccini et al (2012) at 300 Mg C ha<sup>-1</sup> computed using LiDAR GLAS footprints. These maps can be considered as baseline information that will assist the forest management

agency in focusing their efforts for ecosystem management. A repeated forest inventory is recommended to assess land use changes and its effects on the biomass and carbon stocks. This temporal comparison can be done in three-year or longer intervals to capture any significant tree growth changes, and any disturbances in the forest health. The forested areas in the restoration and strict protection management zones need to be properly monitored to reduce human agricultural activities and eliminate deforestation activities inside the park. Further studies can be undertaken to characterize canopy cover across management zones and to aid in developing a vegetative cover in this park. This vegetation cover map can also add information relating to the carbon storage, and present policy implications for reforestation or afforestation activities.

## **CHAPTER V**

### **CONCLUSIONS**

This dissertation has produced a series of interrelated works that focused on the assessment of forest biomass in Mt. Apo Natural Park. The methodology utilized fieldwork, complemented with application of remote sensing technology and geospatial modeling.

In Chapter II, an attempt was made to provide a profiling for the various types of plant communities present in the lowland, midland and upland areas in the park. The results showed that both DBH and H are major predictors for estimating biomass. Wood density information was also added to characterize tree biomass content. Chave et al (2005) exhibited the best estimation results in both species-level and mixed-species level biomass estimation. This study also showed that IVI provided a good measure of ecosystem importance and as a quantifier for vegetation health. Ranking of species in terms of ecologically important species denoted that species importance is largely dependent on their stock density. This study also produced species-specific biomass estimates for 52 local species. Management zoning also provided insights on plot heterogeneity, which were helpful in assessing species dynamics and growth structure.

In Chapter III, a referenced plot-level biomass was estimated using an algorithm from Brown (1997). This approach showed a computation for plot biomass with large dbh interval using quadratic-mean-stem-diameter. Mt. Apo Natural Park contains the

hardwood tree species that has massive diameter sizes of 6.5-441 cm. The allometric equations considered in this study reported a good modeling fit with the dbh classes. The use of wood density information from allometries developed by Chave et al (2005) and Ketterings et al (2001) provided additional biomass information, in addition to height and dbh information. Chave et al (2005) proved to be the best estimation approach for relating tree mensuration and wood density information. Plot biomass was estimated using structural metrics derived from a terrestrial laser scanner. TLS-derived metrics like percentile heights and normalized height bins, showed the ability of TLS to capture accurate understory characteristics. It provided an insight to improve accuracy for estimating plot-level AGB. Normalized height bins offered a better approach in estimating plot biomass values. However, the use of multiple scans, did not show good results from merging scans. This could be further improved to allow extraction of individual tree metrics, by reducing the plot size, or by using more visible targets or reflectors during scanning.

In Chapter IV, the study demonstrated how IFSAR products (DSM, DTM and ORI) can be used to characterize biomass and carbon in a landscape level. This study demonstrated that IFSAR data reflects the landscape conditions in 2013 when the imagery was taken. It also revealed that other by-products generated like the CHM map and management zone mapping, are also reflective of the recent conditions. This study produced digitized baseline landcover, biomass and carbon maps for the Mt. Apo Natural Park.

The study recommends that these maps be considered as baseline information to assist the forest management agency in focusing their efforts for ecosystem management. A repeated forest inventory is also recommended to assess land use changes and its effects on the biomass and carbon stocks. This temporal comparison can be done in three-year or longer intervals, to capture any significant tree growth changes, and any disturbances in the forest health.

It is likewise recommended that the forested areas in the restoration and strict protection management zones need to be properly monitored. Monitoring will help reduce human agricultural activities, and eliminate deforestation activities inside the park. Further studies can be undertaken to characterize canopy cover across management zones and to aid in developing a vegetative cover in this park. This vegetation cover map can also add information relating to the carbon storage, and present policy implications for reforestation or afforestation activities.

Finally, this study has showed that the application of remote sensing technology and use of ecological modelling can aid policy makers in achieving compliance with UN REDD requirements. The use of these 2013 biomass and carbon maps can help the Philippine government in doing monitoring, verification and reporting activities for MANP. These maps can also assist in directing their conservation and management efforts for the protection of Mt. Apo Natural Park - a heritage for the Filipino people.

## REFERENCES

Achard, F., Eva, H. D., Stibig, H. J., Mayaux, P., Gallego, J., Richards, T., and Malingreau, J. P. (2002). Determination of deforestation rates of the world's humid tropical forests. *Science* 297, 999–1002.

Achard, F., Eva, H. D., Mayaux, P., Stibig, H. J., and Belward, A. (2004). Improved estimates of net carbon emissions from land cover change in the tropics for the 1990s. *Global Biochemistry Cycles*, 18, GB2008 doi:10.1029/2003GB002142

Amoroso, V.B., Acma, F.M., Marin, R.A., Tulod, A.M, Opiso, J.G., Baldo, R.R. (date accessed: 12/15/2013). Trees and shrubs found in 1-hectare permanent plot in Mt. Apo, EDC, Kidapawan, Cotabato. Central Mindanao University, Musuan, Maramag, Bukidnon.

Andersen, H., McGaughey, R., and Reutebuch, S. (2006). Assessing the Influence of flight parameters and interferometric processing on the accuracy of X-band IFSAR-derived forest canopy height models. Workshop on 3D Remote Sensing in Forestry, 14<sup>th</sup>-15<sup>th</sup> February.

Arsenio, J.J., Medecilo, M.P., Mercado, E.T., Salibay, Jr., E.T., and Valera, F.A.H. (2011). The vegetation of Mt. Maculot, Cuenca, Batangas, Philippines. *International Journal of Environmental Science and Development*, 2, 4.

Baccini, A., Goetz, S.J., Walker, W.S., Laporte, N.T., Sun, M., Sulla-Menashe, D., Hackler, J., Beck, P.S.A., Dubayah, R., Friedl, M.A., Samanta, S., and Houghton, R.A. (2012). Estimated carbon dioxide emissions from tropical deforestation improved by carbon-density maps. *Nature Climate Change* 2,182-185. Doi:10.1038/nclimate1354.

Bagarinao, T. (1998). Nature parks, museums, gardens and zoos for biodiversity conservation and environment education: The Philippines, *Ambio*, 27, 3,230-237.

Balzter, H., Rowland, C.S., and Saich, P. (2007). Forest canopy height and carbon estimation at Monks Wood National Nature Reserve, UK, using dual-wavelength SAR interferometry. *Remote Sensing of Environment*, 108, 224-239.

Basuki, T.M., van Laake, P.E., Skidmore, A.K., and Hussin, .Y.A. (2009). Allometric equations for estimating the above-ground biomass in tropical lowland Dipterocarpaceae forests. *Forest Ecology and Management*, 257, 1684-1694.



Bienert, A., Scheller, S., Keane, E., Mullooly, G. and Mohan, F. (2006). Application of terrestrial laser scanners for the determination of forest inventory parameters.

International Archives of Photogrammetry, Remote Sensing and Spatial Information Sciences, 36.

Brooks, T.M., Pimm, S.L., and Collar, N.J. (1997). Deforestation predicts the number of threatened birds in insular Southeast Asia. *Conservation Biology*, 11, 382-394.

Brooks, T.M., Pimm, S.L., and Oyugi, J.O. (1999). Time lag between deforestation and bird extinction in tropical forest fragments. *Conservation Biology*, 13, 5, 1140-1150

Brown, S. and Lugo, A.E. (1984). Biomass of tropical forests: a new estimates based on forest. *Science*, 223, 1290-1293.

Brown, I.F., Martinelli, L.A., Thomas, W.W., Moreira, M.Z., Ferreira, C.A. C. and Victoria, R. A. (1995). Uncertainty in the biomass of Amazonian forests: an example from Rondonia, Brazil. *Forest Ecology and Management*, 75,175-189.

Brown, S., Sathaye, J., Cannell, M., and Kauppi, P. (1996). Mitigation of carbon emissions to the atmosphere by forest management. *Commonwealth Forestry Review* 75:80-91.

Brown, S. (1997). Estimating biomass and biomass change of tropical forests: a primer. FAO Forestry Paper no. 134, Rome.

Canadell, J.G., Le Quere, C., Raupach, M.R., Field, C.B., Bultenhuis, E.T., Ciais, P., Conway, T.J., Gillett, N.P., Houghton, R.A., and Marland, G. (2007). Contributions to accelerating atmospheric CO<sub>2</sub> growth from economic activity, carbon intensity, and efficiency of natural sinks. *Proceedings of the National Academy of Sciences*. 104,47,18866-18870. [www.pnas.org/cgi/doi/10.1073.pnas.0702737104](http://www.pnas.org/cgi/doi/10.1073.pnas.0702737104)

Chapin III, F.S., Matson, P.A., and Vitousek, P.M. (2011). *Principles of Terrestrial Ecosystem Ecology*. Second edition. Springer Science. ISBN 978-1-4419-9503-2.

Chave, J., Andalo, C., Brown, S., Cairns, M. A., Chambers, J. Q., Eamus, D., Folster, H., Fromard, F., Higuchi, N., Kira, T., Lescure, J.P. B., Nelson W., Ogawa, H., Puig, H., Riera, B. and Yamakura, T. (2005). Tree allometry and improved estimation of carbon

stocks and balance in tropical forests. *Oecologia* 145, 87–99. DOI 10.1007/s00442-005-0100-x

Chen, Q., Gong, P., Baldocchi, D., and Tian, Y.Q. (2007). Estimating basal area and stem volume for individual trees from LiDAR data, *Photogrammetric Engineering & Remote Sensing*, 73(12): 1355 - 1365.

Danson, F. M., Hetherington, D., Morsdorf, F., Koetz, B., and Allgöwer, B. (2007). Forest canopy gap fraction from terrestrial laser scanning, *IEEE Geosciences and Remote Sensing Letters*, 4, 157 - 160.

DeFries, R.S., Houghton, R.A., Hansen, M.C., Field, C.B., Skole, D, and Townshend, J. (2002). Carbon emissions from topical deforestation and regrowth based on satellite observations for the 1980s and 1990s. *Proceedings of National Academy of Science*, 99, 14256-14261.

Drake, J.B., Dubayah, R.O., Clark, D.B., Knox, R.G., Blair, J.B., Hofton, M.A., Chazdon, R.L., Weishampel, J.F., Prince, S. D. (2002). Estimation of tropical forest

structural characteristics using large-footprint LiDAR. *Remote Sensing of the Environment*, 79, 305-319.

FAO (2005). *Global Forest Resources Assessment 2005. Progress towards sustainable forest management*. FAO Forestry Paper 147, Rome.

FARO, 2010. *FARO Laser Scanner Software Scene 4.8-User Manual*.

Foley, J.A., and Ramankutty, N. (2003). *A primer on the terrestrial carbon cycle: what we don't know, but should*. Center for Sustainability and the Global Environment (SAGE). University of Wisconsin.

FUSION/LDV: *Software for LiDAR Data Analysis and Visualization*. Robert J. McGaughey. United States Department of Agriculture Forest Service. Pacific Northwest Research Station. September 2012 –FUSION Version 3.20.

Gibbs, H.K. (2006). *Olson's major world ecosystem complexes ranked by carbon in live vegetation: an updated database using the GLC2000 land cover products NDP-017b*

available at <http://cdiac.ornl.gov/epubs/ndp/ndp017/ndp017b.html> from the Carbon Dioxide Information Center. Oak Ridge National Laboratory, Oak Ridge, TN.

Gibbs H.K., Brown, S., Niles, J.O., and Foley, J.A. (2007). Monitoring and estimating tropical forest carbon stocks: making REDD a reality. *Environmental Research Letters*, 2, 1-13.

Gibbs, H.K. and Brown, S. (2007a). Geographical distribution of woody biomass carbon stocks in tropical Africa: an updated database for 2000. Available at <http://cdiac.ornl.gov/epubs/ndp/ndp068/ndp068b.html> from the Carbon Dioxide Information Center. Oak Ridge National Laboratory, Oak Ridge, TN.

Gibbs, H.K. and Brown, S. (2007b). Geographical distribution of biomass carbon stocks in tropical southeast Asian forests: an updated database for 2000. Available at <http://cdiac.ornl.gov/epubs/ndp/ndp068/ndp068b.html> from the Carbon Dioxide Information Center. Oak Ridge National Laboratory, Oak Ridge, TN.

Ginsberg, J. (1999). Global conservation priorities. *Conservation Biology*, 13, 5.

Goetz, S.J., Baccini, A., Laporte, N.T., Johns, T., Walker, W., Kellndorfer, J., Houghton, R.A., and Sun, M. (2009). Mapping and monitoring carbon stocks with satellite

observations: a comparison of methods. Carbon Balance and Management, 4,2,  
doi:10.1186/1750-0680r-r4-2

Golden Surfer 9, Golden Software, LLC. [www.goldensoftware.com](http://www.goldensoftware.com). Date accessed:  
8/15/2014

GPS III plus Manual, Garmin Corp. [www.garmin.com](http://www.garmin.com). Date accessed: 7/10/2013.

Grainger, A. (2008). Difficulties in tracking the long-term global trend in tropical forest  
area. Proceedings of National Academy of Sciences, 105,2,818-823.  
[www.pnas.org/cgi/doi/10.1073/pnas.0703015105](http://www.pnas.org/cgi/doi/10.1073/pnas.0703015105)

Grainger, A., and Obersteiner, M. (2010). A framework for structuring the global forest  
monitoring landscape in the REDD+ era. Environmental Science and Policy, 14,2,127-  
139. Doi:10.1016/j.envsci.2010.10.006

Hagberg, J., Ulander, L., and Askne, J. (1995). Repeat-pass SAR interferometry over  
forested terrain. IEEE Transactions on Geoscience and Remote Sensing, 33, 2, 331-340.

Han, S.R., Woo, S.Y., and Lee, D.K. (2010). Carbon storage and flux in aboveground vegetation and soil of sixty-year old secondary natural forest and large leafed mahogany (*Swietenia macrophylla* King) plantation in Mt. Makiling, Philippines. *Asia Life Sciences*, 19, 2, 357-372.

Harmon, M.E., and Sexton, J. (1996). Guidelines for measurements of woody detritus in forest ecosystems US LTER Publication No. 20 US LTER Network Office, University of Washington, Seattle, WA

Heaney L.R. (2004). Philippines. Pp. 179-183 in *Hotspots revisited* (R.A. Mittermeier, et al, 2004, eds.) CEMEX, Mexico City, Mexico.

Hertel, D., Moser, G., Culmsee, H., Erasmi, S., Horna, V., Schuldt, B., and Leuschner, C. (2009). Below- and above-ground biomass and net primary production in a paleotropical natural forest (Sulawesi, Indonesia) as compared to neotropical forests. *Forest Ecology and Management*, 258, 1904-1912.

Hofmann, D.J., Butler, J.H., Dlugokencky, E.J., Elkins, J.W., Masaire, K., Montzka, S.A., and Tans, P. (2006). The role of carbon dioxide in climate forcing from 1979 to 2004: introduction of the annual greenhouse gas index. *Tellus*, 58,5,614-619. Doi: 10.1111/j.1600-0889.2006.00201.x

Houghton, R.A., Davidson, E.A., and Woodwell, G.M. (1998). Missing sinks, feedbacks, and understanding the role of terrestrial ecosystems in the global carbon balance. *Global Biogeochemical Cycles*, 12,1,24-34.

Houghton, R.A. (1999). The annual net flux of carbon to the atmosphere from changes in land use 1850-1990. *Tellus B*,51, 298-313.

Houghton, R.A, Lawrence K.T., Hacker, J.L., and Brown, S. (2001). The spatial distribution of forest biomass in the Brazilian Amazon; a comparison of estimates. *Global Change Biology*, 7, 731-746.

IPCC (2003a). Good practice guidance for land use, land-use change and forestry (GPG-LULUCF). Penman, J., Gytarsky, M., Krug, T., Kruger, D., Pipatii, R., Buendia, L., Miwa, K., Ngara, T., Tanabe, K, and Wagner, F. (eds). IPCC-IGES, Kanagawa.



IPCC (2003b). IPCC meeting on current scientific understanding of the processes affecting terrestrial carbon stocks and human influences on them. Manning, M., and Schimel, D (eds). Boulder, USA.

IPCC 2006. IPCC Guidelines for National Greenhouse Gas Inventories. Prepared by the National Greenhouse Gas Inventories Programme.

IUCN (1992). Conserving Biological Diversity in Managed Tropical Forests. IUCN, Gland, Switzerland and Cambridge, UK. xi + 244 pp.

Jensen, C. (2003). Development Assistance to Upland Communities in the Philippines. Published by World Agroforestry Centre (ICRAF).Bogor, Indonesia.

Jensen, J. (2007). Remote Sensing of the Environment (2<sup>nd</sup> edition) Prentice Hall Series in Geographic Information Science.

Kellmann, M.C. (1970). Secondary plant succession in tropical montane Mindanao. Research School of Pacific Studies, Australian National University, Canberra.

Ketterings, Q.M., Coe, R., van Noordwijk, M., Ambagau, Y., and Palm, C.A. (2001). Reducing uncertainty in the use of allometric biomass equations for predicting above-ground tree biomass in mixed secondary forests, *Forest Ecology and Management*, 146,199-209.

Ku, N, S. Popescu, R.J. Ansley, H.L. Perotto-Baldevieso, A.M. Filippi (2012). Assessment of available rangeland woody plant biomass with terrestrial LiDAR system. *American Society for Photogrammetry and Remote Sensing*, 78,4. Doi: 10.14358/PERS.78.4.349

Kunwar, R.M., and Sharma, S.P. (2004). Quantitative analysis of tree species in two community forests of Dolpa district, mid-west Nepal. *Himalayan Journal of Science*, 2(3): 23-28.

Lasco, R.D., and Pulhin, F.P. (1998). Philippine forestry and CO<sub>2</sub> sequestration: Opportunities for mitigating climate change. *Environmental Forestry Programme (ENFOR)*, UPLB College of Forestry and Natural Resources, Laguna, Philippines. 24 pp.

Lasco, R.D., Visco, R.G., and Pulhin, J.M. (2001). Secondary forests in the Philippines: formation and transformation in the 20th century. *Journal of Tropical Forest Science*, 13, 4, 652-670.

Lasco, R.D., Guillermo, I.Q., Cruz, R.V., Bantayan, N.C., and Pulhin, F.B. (2004). Carbon stocks assessment of a secondary forest in Mount Makiling Forest Reserve, Philippines. *Journal of Tropical Forest Science*, 16, 35-45.

Lasco, R.D., MacDicken, K.G., Pulhin, F.B., Guillermo, I.Q., Sales, R.F., and Cruz, R.V. (2006). Carbon stocks assessment of a selectively logged dipterocarp forest and wood processing mill in the Philippines. *Journal of Tropical Forest Science*, 18, 212-221.

LASTools. Created by Martin Isenburg. Efficient tools for LiDAR processing, [www.rapidlasso.com](http://www.rapidlasso.com). Date accessed: 9/20/2014

Lefsky, M.A., Cohen, W.B., Parker, G.G., and Hardin, D.J. (2002). LiDAR remote sensing for ecosystem studies, *BioScience*, 52(1):19 - 30.

Lefsky, M.A. (2010). A global forest canopy height map from the moderate resolution imaging spectroradiometer and the Geoscience Laser Altimeter System. *Geophysical Research letters*, 37, L15401.

Lewis, R.E. (1988). Mt. Apo and other national parks in the Philippines, *Oryx*, 22, 2,100-109.

Li, X., Baker, A.B., and Hutt, T. (2002). Accuracy of Airborne IFSAR Mapping. *American Society of Photogrammetry and Remote Sensing Proceedings*. 1-6 pp.

Li, W., Guo, Q., Jakubowski, M.K., and Kelly, M. (2012). A new method for segmenting individual trees from the LiDAR point cloud. *Photogrammetric Engineering & Remote Sensing*, 78 (1): 75 - 84.

Loudermilk, E.L., Hiers, J.J., O'Brien, J.J., Mitchell, R.J., Singhania, A., Fernandez, J.C., Cropper, Jr. W.P., and Slatton, K.C. (2009). Ground-based LIDAR: a novel approach to quantify fine-scale fuelbed characteristics. *International Journal of Wildland Fire*, 18(6): 676 - 685.

McNeely, J.A., Miller, K.R., Reed, W.V., Mitternmeier, R.A., and Werner, T.B (1990).  
Conserving the World's Biological Diversity. IUCN, Gland, Switzerland. 193 pp

Meher-Homji, V.M. (1991). Probable impact of deforestation on hydrological processes.  
Climatic Change 19.163-173.

Misbari, S., and Hashim, M. (2014). Total aboveground biomass (TAGB) estimation  
using IFSAR: speckle noise effect on TAGB in tropical forest. 8<sup>th</sup> International  
Symposium of the Digital Earth.

Mitchard, E.T.A., Saatchi, S.S., Baccini, A., Asner, G., Goetz, S. J., Harris, N.L., and  
Brown, S. (2013). Uncertainty in the spatial distribution of tropical forest biomass: a  
comparison of pan-tropical maps. Carbon Balance and Management, 8,10.

Mittermeier, R. A., Myers, N., Gil, P. R. & Mittermeier, C. G. (1999). Hotspots: Earth's  
Biologically Richest and Most Endangered Terrestrial Ecoregions (Cemex, Conservation  
International and Agrupacion Sierra Madre, Monterrey, Mexico).

Mittermeier, R. A., Gil, P.R., Hoffmann, M., Pilgrim, J., Brooks, T., Mittermeier, C.G.,

Lamoreux, J., da Fonseca, G.A.B. (2004). Hotspots Revisited. Earth's Biologically Richest and Most Endangered Ecoregions. Mexico City (Mexico) CEMEX.

Montesano, P.M., Nelson, R.F., Dubayah, R.O., Sun, G., Cook, B.D., Ranson, K.J.R., Naesset, E., and Kharuk, V. (2014). The uncertainty of biomass estimates from LiDAR and SAR across a boreal forest structure gradient. Remote Sensing of Environment, <http://dx.doi.org/10.1016/j.rse.2014/01.027>.

Morel, A.C., Saatchi, S., Malhi, Y., Berry, N.J., Banin, L., Burslem, D., Nilus, R., and Ong, R. (2011). Estimating aboveground biomass in forest and oil palm plantation in Sabah, Malaysian Borneo using ALOS PALSAR data. Forest Ecology and Management, 262, 1786-1798.

Mount Apo Protected Area Act of 2003 (Republic Act No. 9237). Republic of the Philippines.

Mt. Apo Natural Park Management Plan 2000. Department of Environment and Natural Resources. Region XI and XII. Philippines.

Myers, N. (1988). Threatened biotas: “hot spots in tropical forests. The Environmentalist, 8,3, 187-208

Myers, N. (1990). The biodiversity challenge: expanded hotspots analysis. Environmentalist 10, 243-256

Myers, N., Russell A. Mittermeier, Ç, Cristina G. Mittermeier, Gustavo A. B. da Fonseca & Jennifer Kent (2000). Biodiversity hotspots for conservation priorities. Nature, 403: 853-858.

Myers, N. (2003). Biodiversity hotspots revisited. BioScience, 53,10.  
National Integrated Protected Area System (NIPAS) Act of 1992 (Republic Act No. 7586).

Olander, L.P., Gibbs, H.K., Steininger, M., Swenson, J.J., and Murray, B.C. (2008). Reference scenarios for deforestation and forest degradation in support of REDD: a review of data and methods. Environmental Research Letters, 3. doi:10.1088/1748-9326/3/2/025011

Olson, J.S., Watts, J.A., and Allison, L.J. (1983). Carbon in live vegetation of major world ecosystems. ORNL-5862 (Oak Ridge, TN: Oak Ridge National Laboratory).

Olson, D.M., Dinerstein, E., Wikramanayake, E.D., Burgess, N.D., Powell, G.V.N., Underwood, E.C., D'Amico, J.A., Itoua, I., Strand, H.E., Morrison, J.C., Loucks, C.J., Allnutt, T.F., Ricketts, T.H., Kura, Y., Lamoreux, J.F., Wettengel, W.W., Hedao, P., and Kassem, K.R. (2001). Terrestrial ecoregions of the world: a new map of life on earth. *BioScience* 933.

Penman, J., Gytarsky, M., Hiraishi, T., Krug, T., Kruger, D., Pipatti, R., Buendia, L., Miwa, K., Ngara, T., Tanabe, K., Wagner, F. (2003). Good practice guidance for land use, land use change and forestry. IPCC National Greenhouse Gas Inventories Programme and Institute for Global Environmental Strategies, Kanagawa, Japan. Available at: <http://www.ipcc-nggip.iges.or.jp/public/gpplulucf/gpplulucf.htm>

Philippines Country Study Guide, 2008. International Business Publications, USA.

Popescu, S.C., Wynne, R.H. and Nelson, R.F. (2003). Measuring individual tree crown diameter with LiDAR and assessing its influence on estimating forest volume and biomass, *Canadian Journal of Remote Sensing*, 29(5):564 - 577.



Popescu, S.C., and Wynne, R.H. (2004). Seeing the trees in the forest: using LiDAR and multispectral data fusion with local filtering and variable window size for estimating tree height, *Photogrammetric Engineering & Remote Sensing*, 70(5):589 - 604.

Prendergast, J. R., Quinn, R. M. & Lawton, J. H. (1999). The gaps between theory and practice in selecting nature reserves. *Cons. Biol.* 13, 484±492

Pressey, R. L., Humphries, C. J., Margules, C. R., Vane-Wright, R. I. & Williams, P. H. (1993). Beyond opportunism: key principles for systematic reserve selection. *Trends Ecol. Evol.* 8, 124-128

Pueschel, P. (2013). The influence of scanner parameter on the extraction of tree metrics from FARO Photon 120 terrestrial laser scans. *ISPRS Journal of Photogrammetry and Remote Sensing*, 78, 58-68.

Quick Terrain Modeler. LiDAR Exploitation Software by Applied Imagery.

[www.appliedimagery.com](http://www.appliedimagery.com). Date accessed: 7/1/2014

Ramankutty, N., Gibbs, H.K. Achard, F., DeFries, R., Foley, J.A. and Houghton, R.A. (2007). Challenges to estimating carbon emissions from tropical deforestation. *Global Change Biology*, 13, 51-66.

Ramos, L.T., Torres, A.M., Pulhin, F.B., and Lasco, R.D. (2012). Developing a georeferenced database of selected threatened tree species in the Philippines. *Philippine Journal of Science* 141 (2), 165-177.

Revilla, A.V. (1997). Working paper for the forestry policy agenda for the incoming administration. UPLB. College of Forestry and Natural Resources, Laguna, Philippines. 13 pp.

Ribeiro, N.S., Saatchi, S.S., Shugart, H.H., and Washington-Allen, R. A. (2008). Aboveground biomass and leaf-area index mapping for Niassa Reserve, northern Mozambique. *Journal of Geophysical Research*, 113. G02S02, doi:10.1029/2007JG000550

Ribeiro, N.S, Shugart, H., and Washington-Allen, R.A. (2008). The effects of fire and elephants on species composition and structure of the Niassa Reserve, northern Mozambique. *Forest Ecology and Management*, 255,1626-1636.

Ribeiro, N.S., Matos, C., Moura, I., Washington-Allen, R.A., and Ribeiro, A. (2013).  
Monitoring vegetation dynamics and carbon stock density in miombo woodlands.  
Carbon Balance and Management, 8:11

Running, S.W., Nemani, R.K., Heinsch, F., Zhao, M., Reeves, M., and Hashimoto, H.  
(2004). A continuous satellite-derived measure of global terrestrial primary production.  
BioScience 54, 6, 14 pp.

Saatchi, S.S., Houghton, R.A, Dos Santos Alvala, R.C., Soares, J.V., and Yu, Y. (2007).  
Distribution of aboveground live biomass in the Amazon basin. Global Change Biology,  
13, 816-837.

Saatchi, S.S., Harris, N.L., Brown, S., Lefsky, M., Mitchard, E.T.A., Salas, W., Zutta,  
B.R., Buermann, W., Lewis, S.L., Hagen, S., Petrova, S., White, L., Silman, M., and  
Morel, A. (2011). Benchmark of forest carbon stocks in tropical regions across three  
continents. Proceedings of the National Academy of Science 108 (24), 9899-9904. Doi:  
10.1073/pnas.1019576108.

Saket, M., Altrell, D., Brnathomme, A., and Vuorinen, P. (2005). FAO's approach to  
support national forest assessments for country capacity building. Rome, Italy.

Shimada, M., and Isoguchi, O. (2002). JERS-1 SAR mosaic of Southeast Asia using calibrated path images. *International Journal of Remote Sensing*, 23,7, 1507-1526.

Srinivasan, S., Popescu, S. Eriksson, M., Sheridan, R.D., and Ku, N. (2014). Multi-temporal terrestrial laser scanning for modelling tree biomass change. *Forest Ecology and Management*, 318,304-317. doi: 10.1016/j.foreco.2014.01.038

Tighe, M. L., and Baker, A. B. (2000). Topographic line map production using high resolution airborne interferometric SAR. *Proceedings of the 19<sup>th</sup> ISPRS Congress and Exhibition, Amsterdam, The Netherlands, 16-22 July, 2000.*

Uhl, C., Buschbacher, R., and Serro, E.A.S. (1988). Abandoned pastures in eastern Amazonia. Pattern of plant succession. *Journal of Ecology*, 76, 663-681.

Verburg, P.H., K.P. Overmars, M.G.A. Huigen, W.T de Groot, and A. Veldkamp (2006). Analysis of the effects of land use change on protected areas in the Philippines. *Applied Geography*, 26,153-173.

Westlake, D.F. (1966). The biomass and productivity of glyceria maxima: I. Seasonal changes in biomass. *Journal of Ecology*, 54, 745-753.

Wijaya, A., and Gloaguen, R. (2009). Fusion of ALOS Palsar and Landsat ETM data for land cover classification and biomass modeling using non-linear methods. *Geoscience and Remote Sensing Symposium, 2009 IEEE International, IGARSS*, 3, 581-584.

Websites and other Sources:

ArcGIS Help. ESRI. (<http://resources.arcgis.com/en/help>), Retrieved on July 1– August 15, 2014

Association of Southeast Asian Nations (<http://www.asean.org/resources/category/asean-statistics>). Retrieved on October 23, 2014.

BirdLife International, Sites-Important Bird and Biodiversity Areas (IBAs) (<http://www.birdlife.org/datazone/sitefactsheet.php?id=9801>). Retrieved on October 23, 2014.

Center for International Forestry Research (CIFOR), Info brief, 16, November 2008, ([www.cifor.cgiar.org](http://www.cifor.cgiar.org)). Retrieved on October 24, 2014

Conservation International,

(<http://www.conservation.org/NewsRoom/pressreleases/Pages/The-Worlds-10-Most-Threatened-Forest-Hotspots.aspx#ranking.>) Retrieved on October 23, 2014.

Co's Digital Flora of the Philippines. Created by Pieter Pelsler. The interactive outpost of [www.philippineplants.org](http://www.philippineplants.org). Retrieved on 12/20/2014

Department of Environment and Natural Resources - Biodiversity Management Bureau  
Protected Areas, DENR-BMBPA

([http://bmb.gov.ph/index.php?option=com\\_wrapper&view=wrapper&Itemid=291](http://bmb.gov.ph/index.php?option=com_wrapper&view=wrapper&Itemid=291) ).

Retrieved on October 20, 2014.

Energy Development Corporation ([www.energy.com.ph](http://www.energy.com.ph)). Retrieved on June 6, 2014.

Google Earth ([www.googleearth.com](http://www.googleearth.com)). 2013 Digital Globe. Retrieved on October 27, 2014.

Intergovernmental Panel on Climate Change, IPCC ([www.ipcc.ch](http://www.ipcc.ch)). Retrieved on October 20, 2014.

Intermap Technologies Product Handbook & Quick Start Guide, Standard edition, v4.4

JMP 8 User Guide accessed on September 10, 2015 ([www.jump.com](http://www.jump.com))

Mt. Apo Foundation, Inc., (a) Historical Perspective and Land Area

([http://mafi.org.ph/mount\\_apo\\_park/mad\\_op01.html](http://mafi.org.ph/mount_apo_park/mad_op01.html)). Retrieved on June 20, 2014.

Mt. Apo Foundation, Inc. (b) Biological Features

([http://mafi.org.ph/mount\\_apo\\_park/mad\\_op04.html](http://mafi.org.ph/mount_apo_park/mad_op04.html)). Retrieved on June 20, 2014.

Mt. Apo Foundation, Inc. (c) Population in the Park

([http://mafi.org.ph/mount\\_apo\\_park/mad\\_op05.html](http://mafi.org.ph/mount_apo_park/mad_op05.html)). Retrieved on October 24, 2014.

Mt. Apo Foundation, Inc. (d) Vegetative Cover Map

([http://mafi.org.ph/mount\\_apo\\_park/ref\\_maps/Vegetative\\_Cover\\_Map.html](http://mafi.org.ph/mount_apo_park/ref_maps/Vegetative_Cover_Map.html)). Retrieved on June 13, 2014.

Mt. Apo Foundation, Inc. (e) Management Zone Map

([http://mafi.org.ph/mount\\_apo\\_park/ref\\_maps/Management\\_Zones\\_Map.html](http://mafi.org.ph/mount_apo_park/ref_maps/Management_Zones_Map.html)).

Retrieved on June 12, 2014.

Mount Apo Natural Park ASEAN Heritage Park

(<http://protectedplanet.net/sites/901240#>). Retrieved on October 20, 2014.

Reducing Emissions from Deforestation and Degradation, REDD ([www.un-redd.org](http://www.un-redd.org)).

United Nations. Retrieved on October 25, 2014.

Simulation and Econometrics to Analyze Risk (SIMETAR). Simetar, Inc. Woodlake Drive, College Station, TX.

United Nations Food and Agriculture Organization, UN-FAO ([www.fao.org](http://www.fao.org)). Retrieved on July 4, 2014.

United Nations Framework Convention on Climate Change, UNFCCC

(<http://newsroom.unfccc.int/>). Retrieved on November 2, 2014.



The United Nations Collaborative Programme on Reducing Emissions from Deforestation and Forest Degradation in Developing Countries, UN-REDD ([http://www.un-redd.org/Key\\_results\\_achievements\\_Philippines/tabid/106627/Default.aspx](http://www.un-redd.org/Key_results_achievements_Philippines/tabid/106627/Default.aspx)). Retrieved on October 25, 2014.

United States Environmental Protection Agency, US EPA (<http://www.epa.gov/climatechange/ghgemissions/gases.html>). Retrieved on October 21, 2014

United Nations Educational, Scientific and Cultural Organization (UNESCO) Tentative List (<http://whc.unesco.org/en/tentativelists/5485>). Retrieved on October 21, 2014.

United States Geological Survey (USGS). Retrieved on 7/1/2014 ([www.earthexplorer.usgs.gov](http://www.earthexplorer.usgs.gov))

World Agroforestry (ICRAF) accessed on June 20, 2014 (<http://db.worldagroforestry.org>)

World Wildlife Fund, WWF

([http://www.panda.org/about\\_our\\_earth/ecoregions/about/habitat\\_types/habitats/tropical\\_forests/](http://www.panda.org/about_our_earth/ecoregions/about/habitat_types/habitats/tropical_forests/)). Retrieved on October 27, 2014.

## APPENDIX A

### FIGURES



Figure 1-1. Location of Mt. Apo Natural Park research site in Mindanao island in the southern Philippines. Downloaded from Google Earth (<http://www.google.com/earth/>)

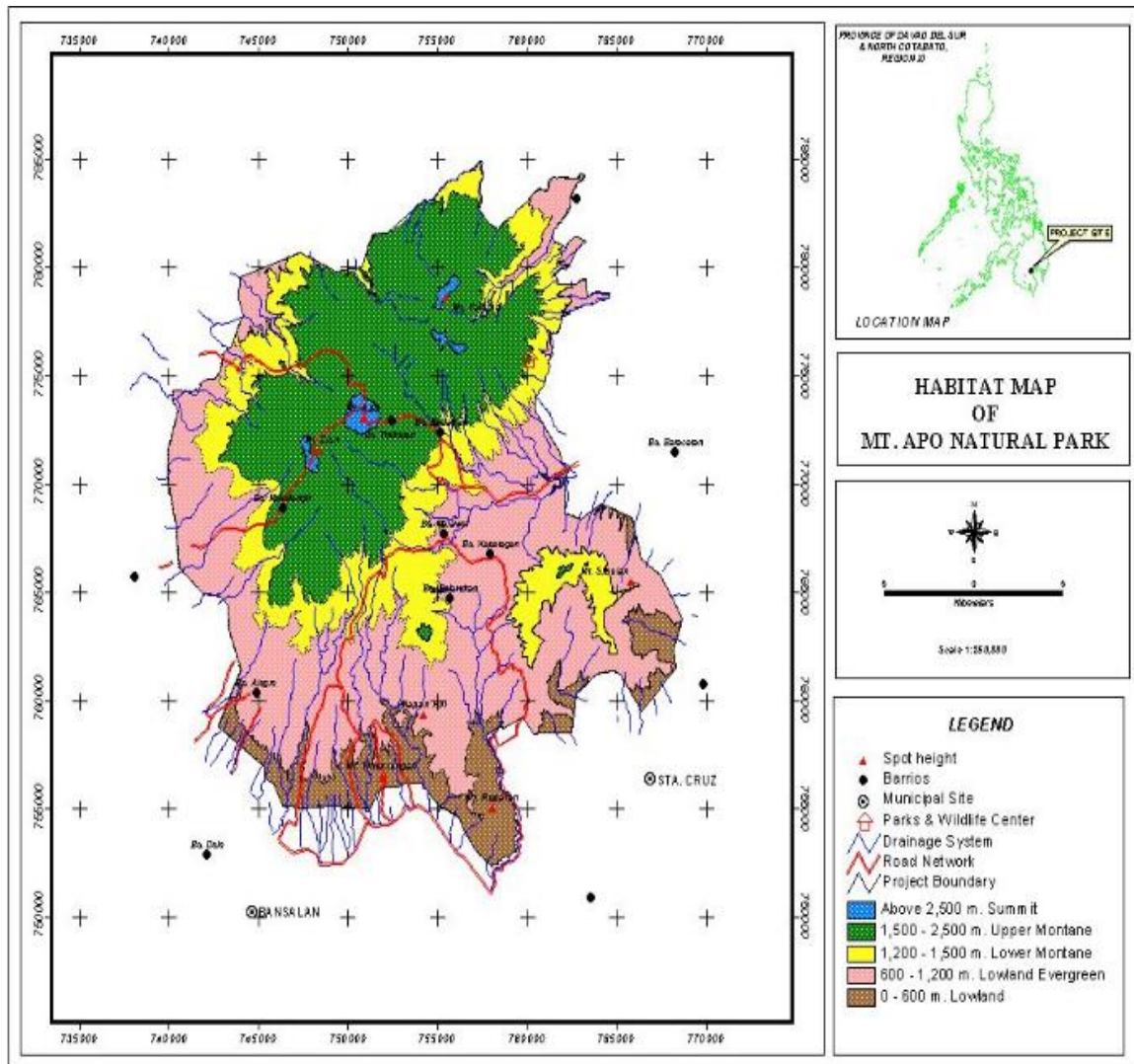


Figure 1-2. The habitat and elevation map of Mt. Apo Natural Park in Mindanao, Philippines. This map was prepared by the Mt. Apo Foundation, Inc. (<http://mafi.org.ph/>). Reprinted with permission.

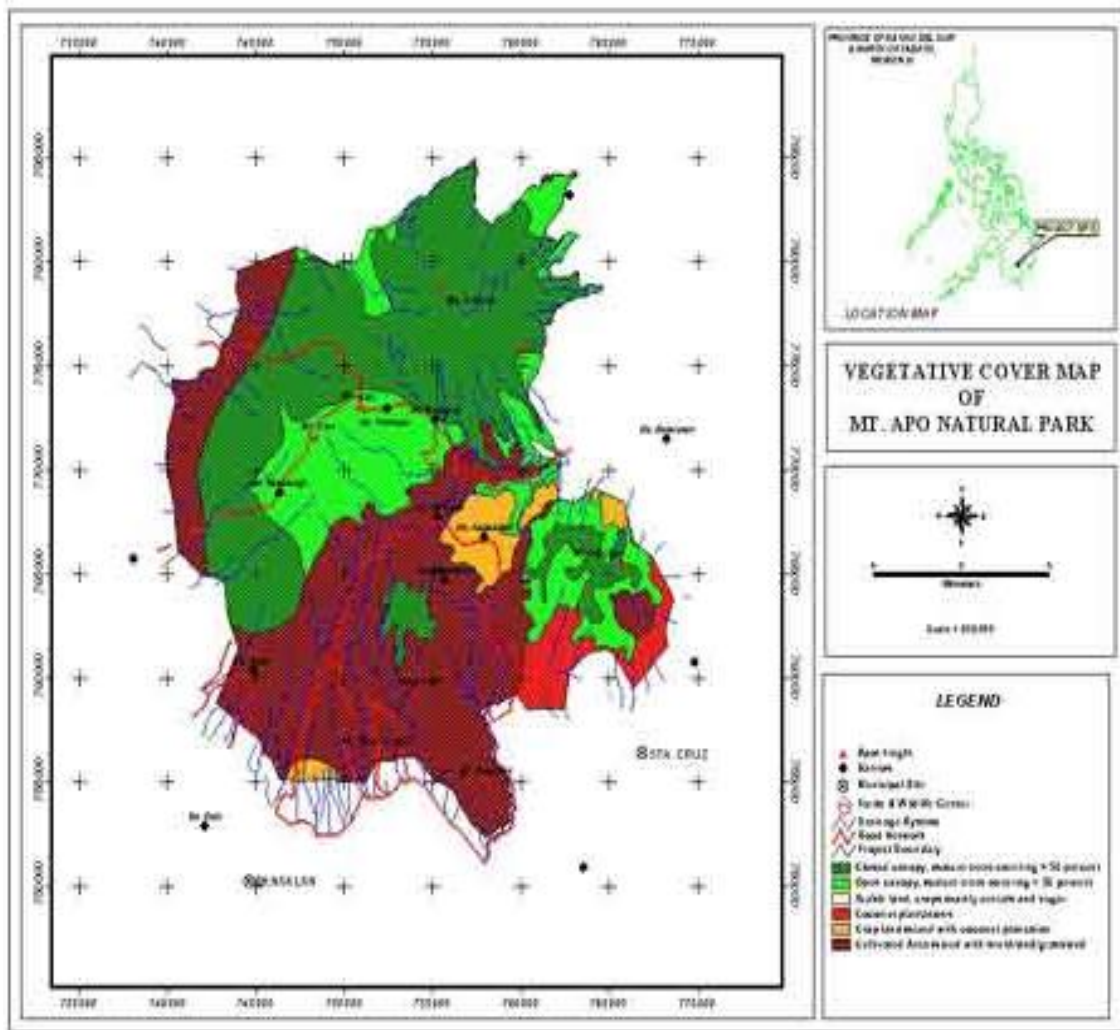


Figure 1-3. The vegetative cover map of Mt. Apo Natural Park in Mindanao, Philippines. This map was prepared by the Mt. Apo Foundation, Inc. (<http://mafi.org.ph/>). Reprinted with permission.

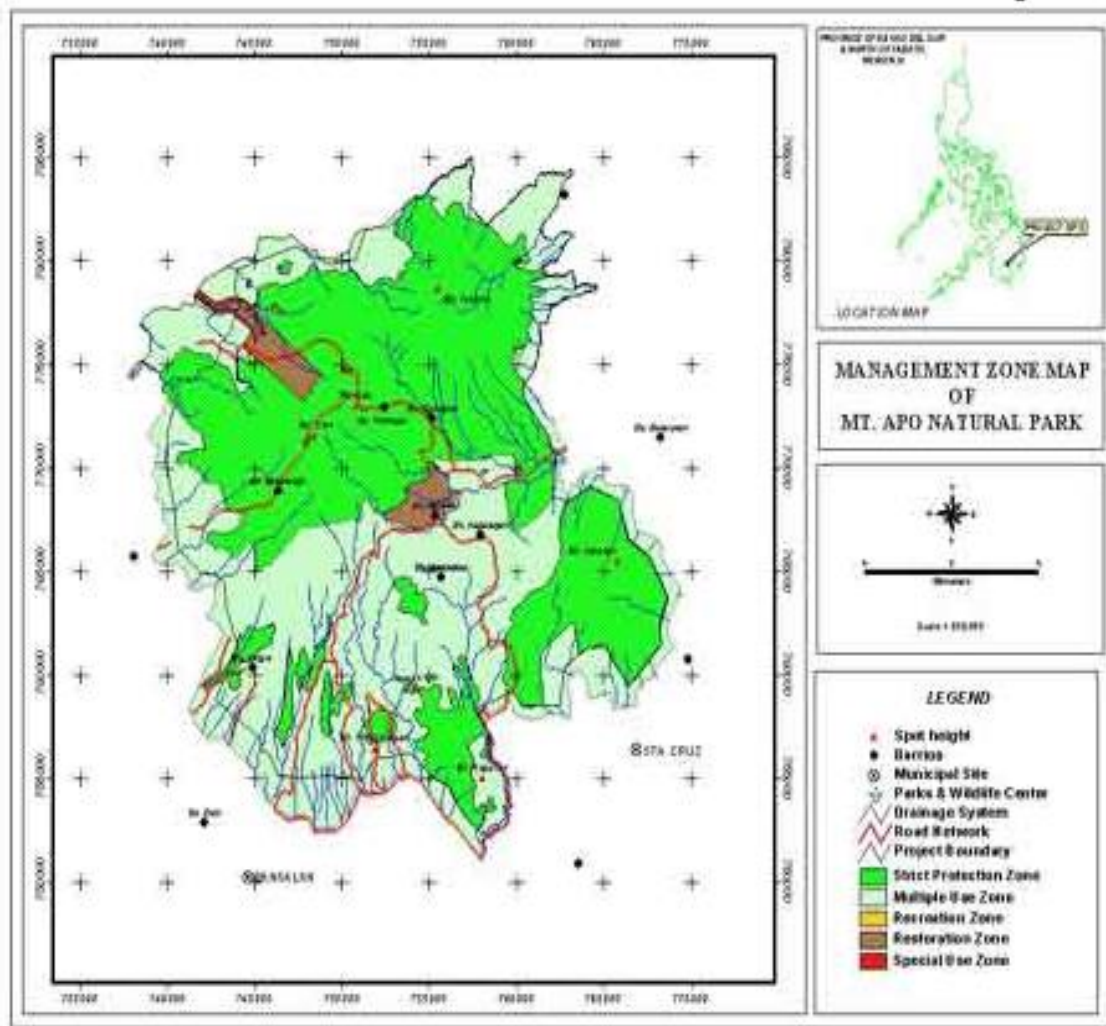


Figure 1-4. The Management Zone or land use map of Mt. Apo Natural Park in Mindanao, Philippines. This map was prepared by the Mt. Apo Foundation, Inc. (<http://mafi.org.ph/>). Reprinted with permission.

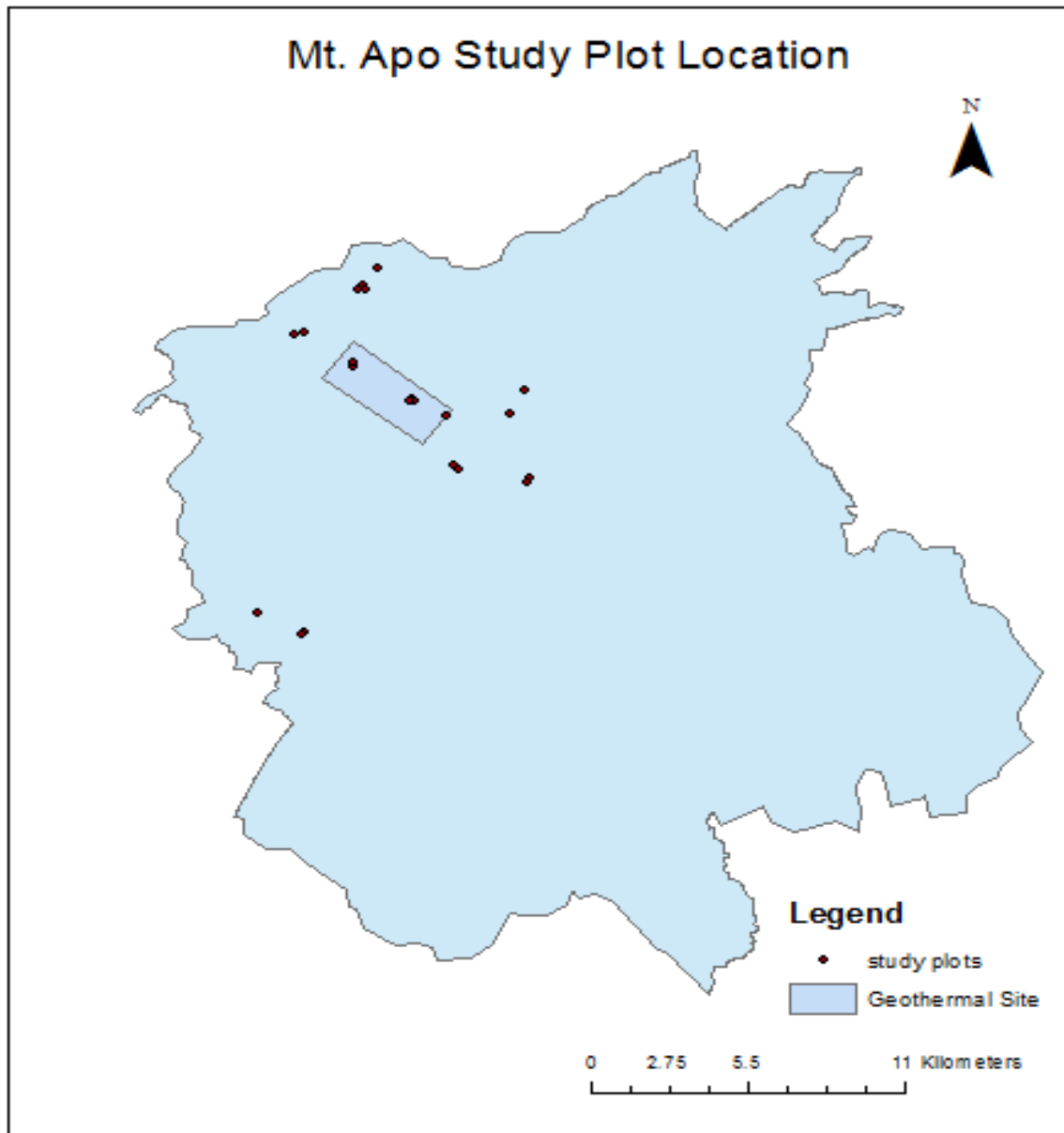


Figure 2-1. Location of 26 study plots inside Mt. Apo Natural Park

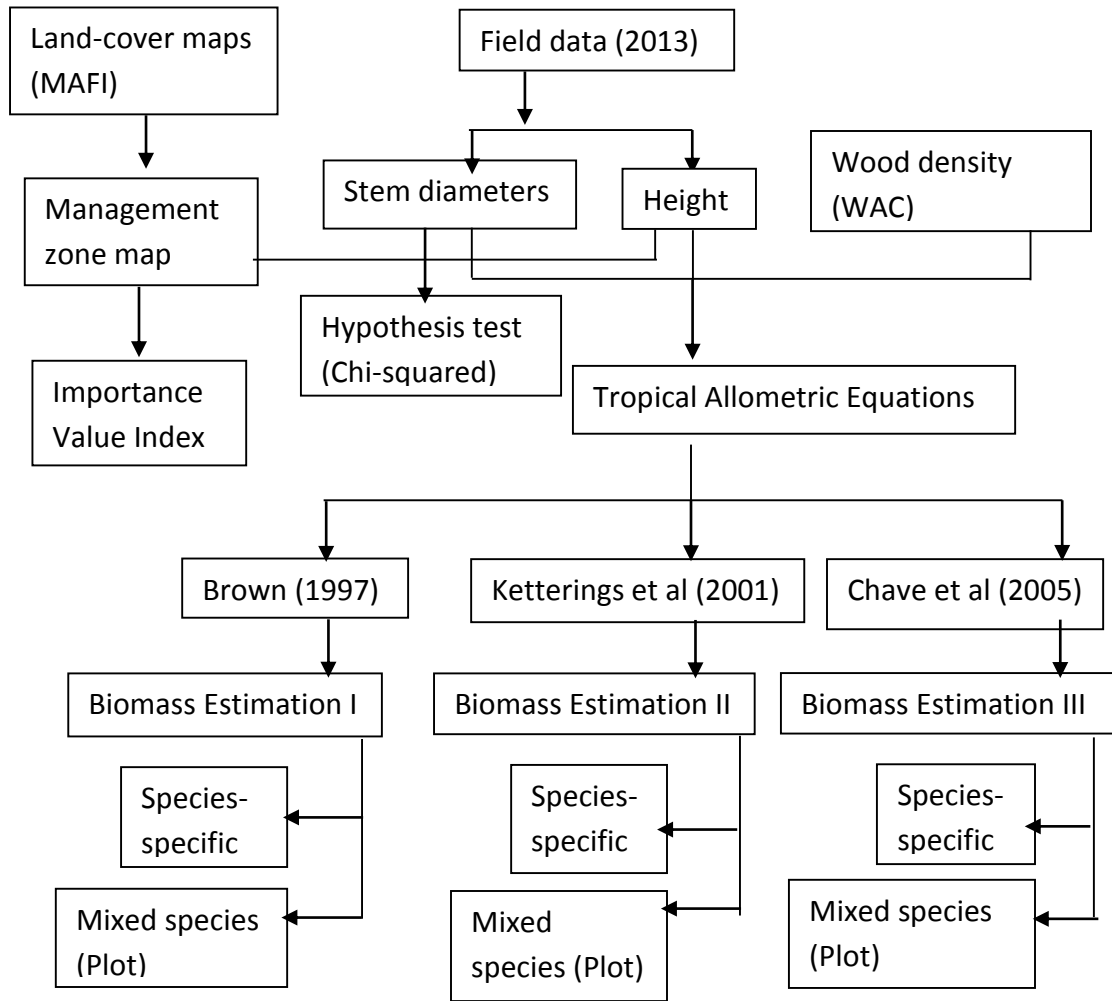


Figure 2-2. Data processing flowchart for biomass estimation



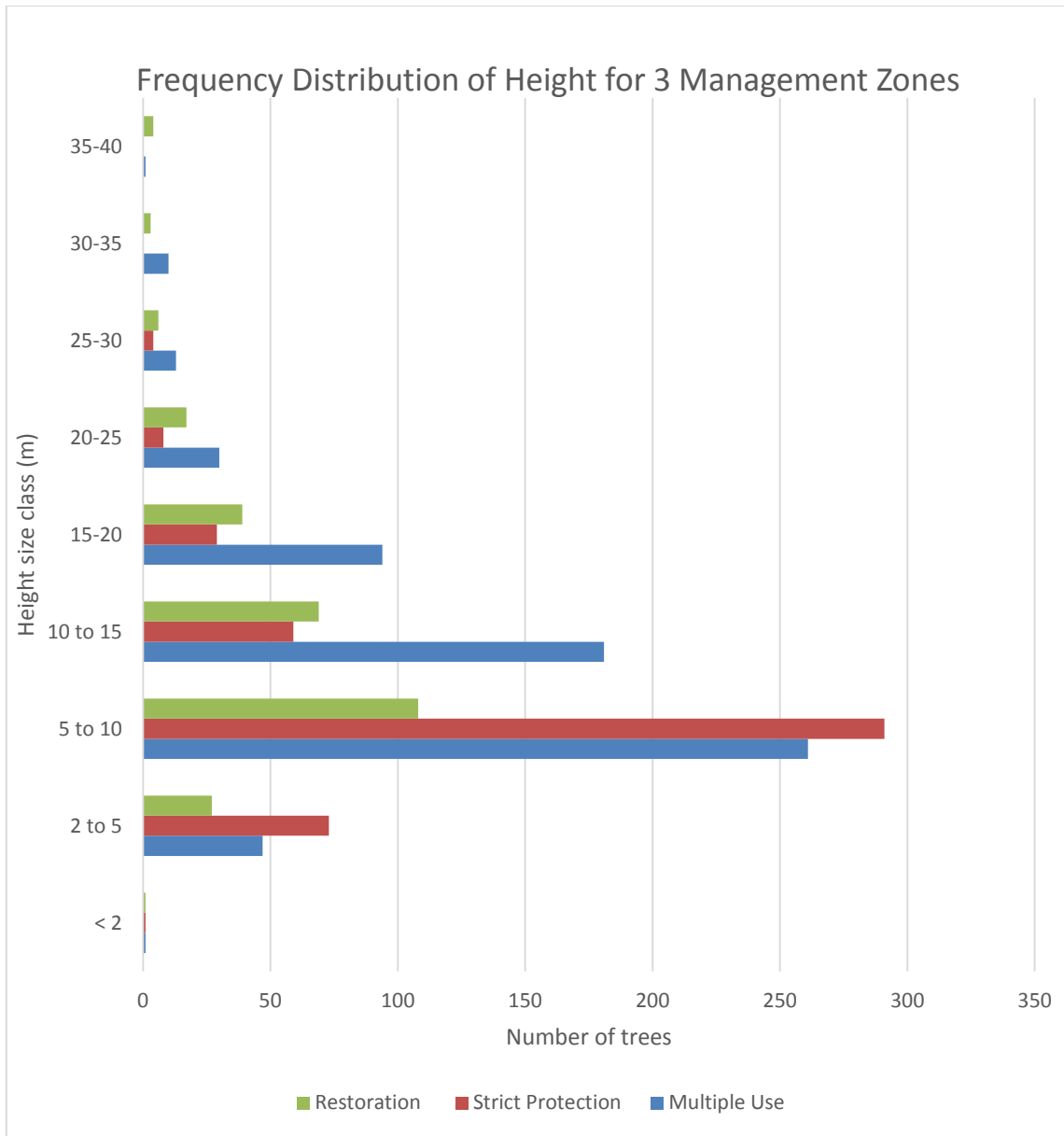


Figure 2-3. Frequency distribution of tree height class by management zones

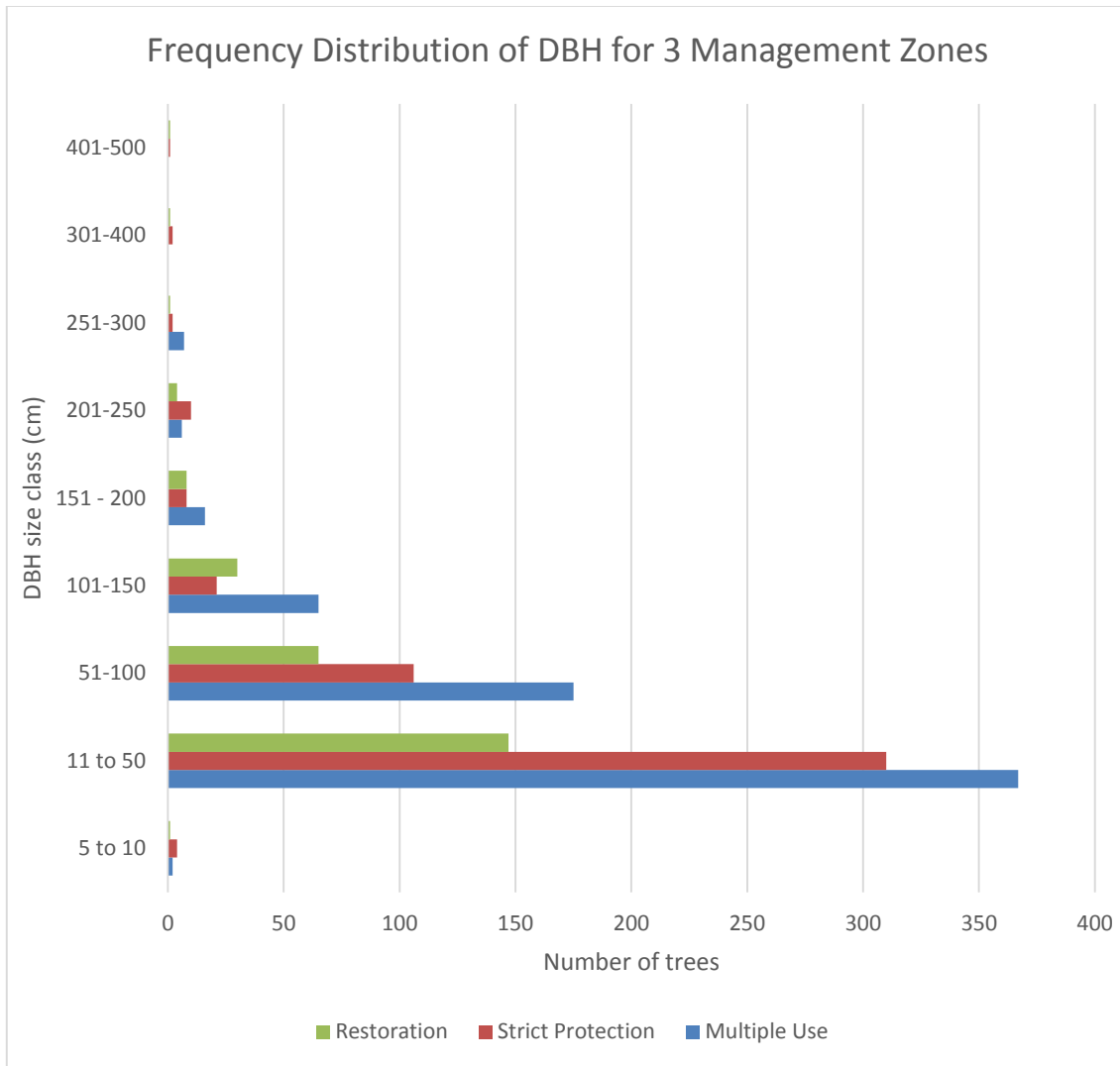


Figure 2-4. Frequency distribution of stem diameter class by management zones

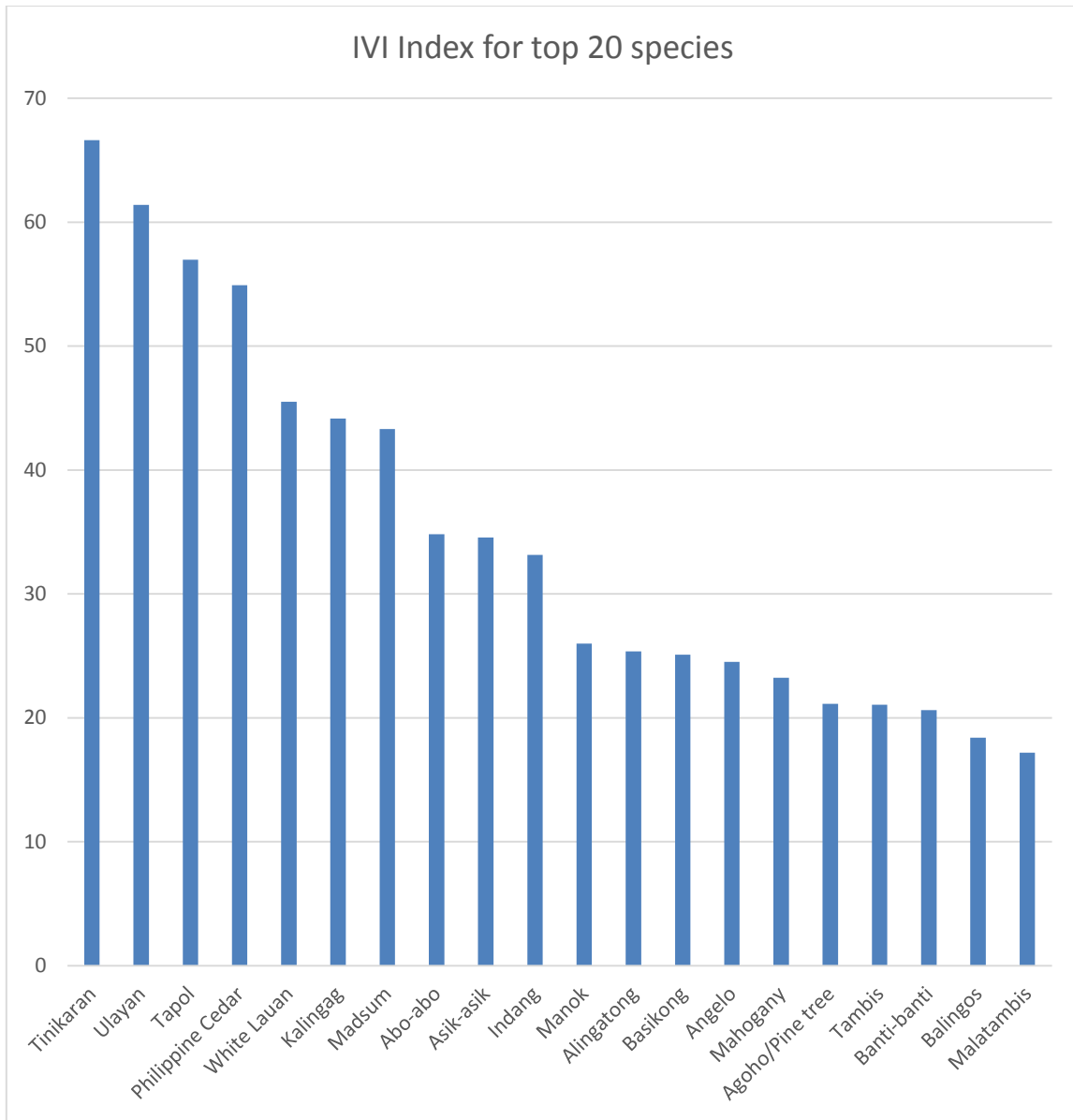


Figure 2-5. Importance Value Index (IVI) for top 20 ecologically important species

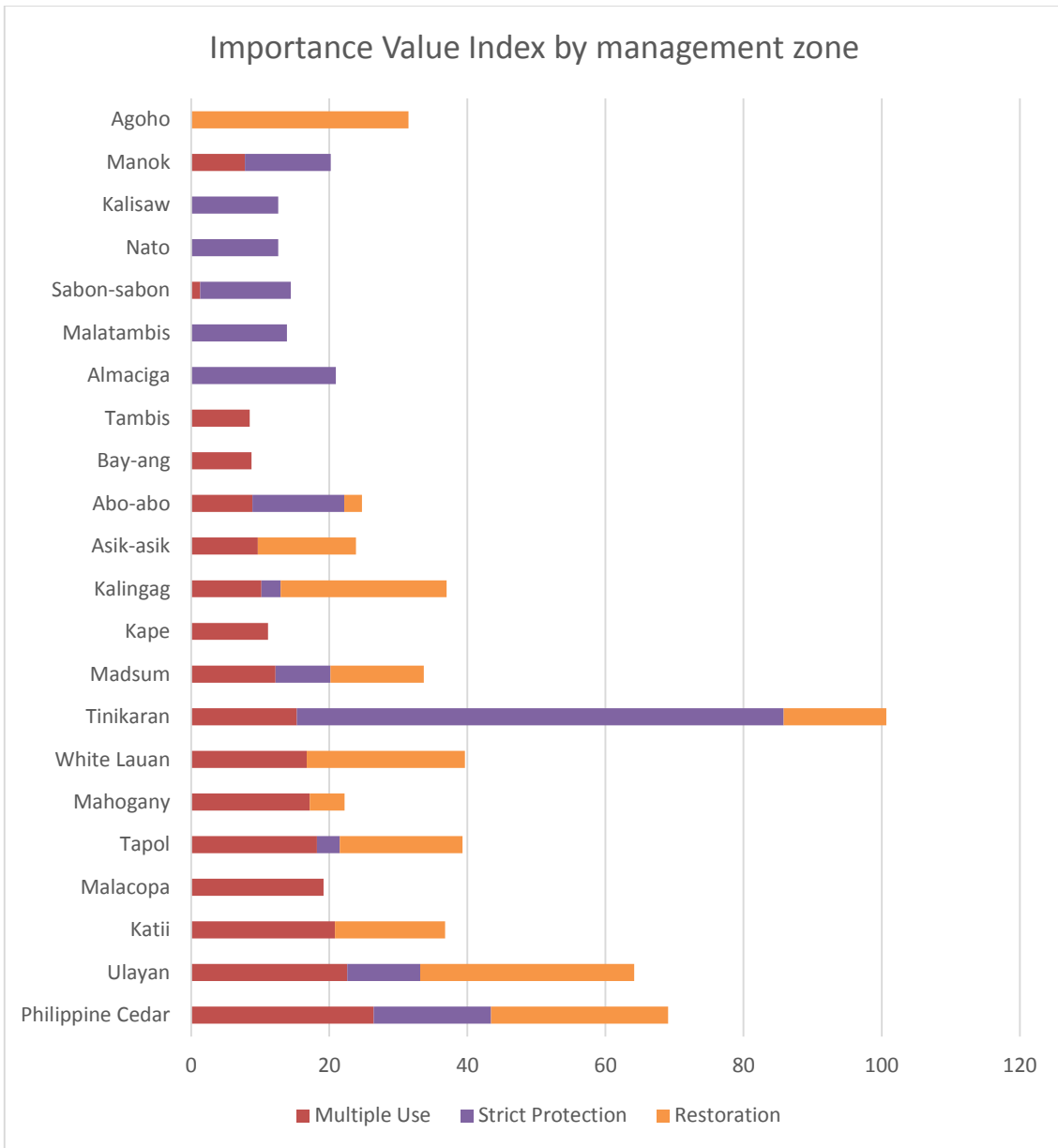


Figure 2-6. Importance Value Index (IVI) by management zone

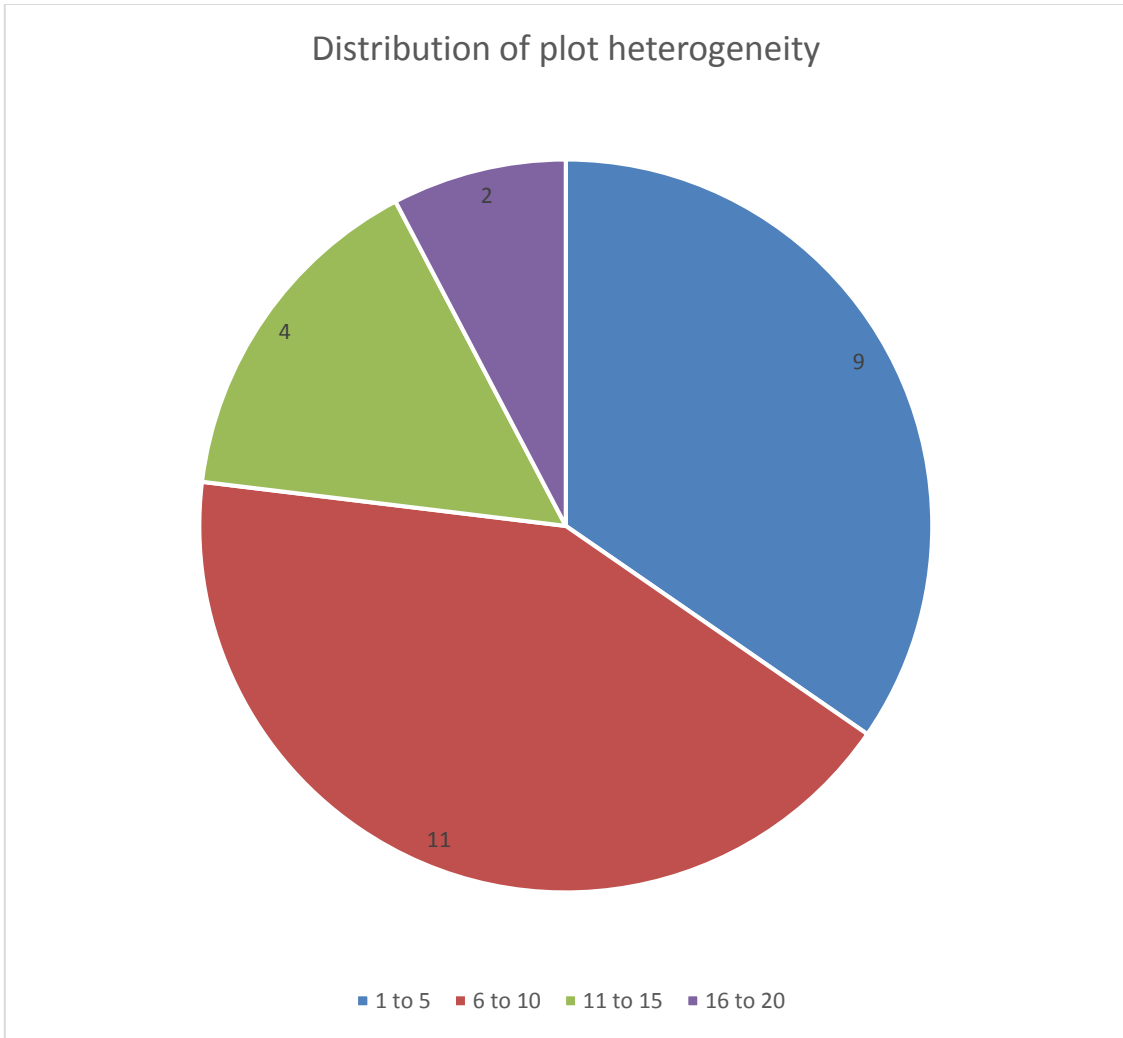


Figure 2-7. Distribution of number of tree species or plot heterogeneity. Number of plots containing with 1-5 species, up to 16-20 species.

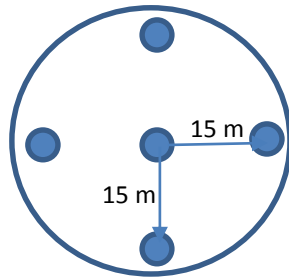


Figure 3-1. Sampling plot design at 15-m radius

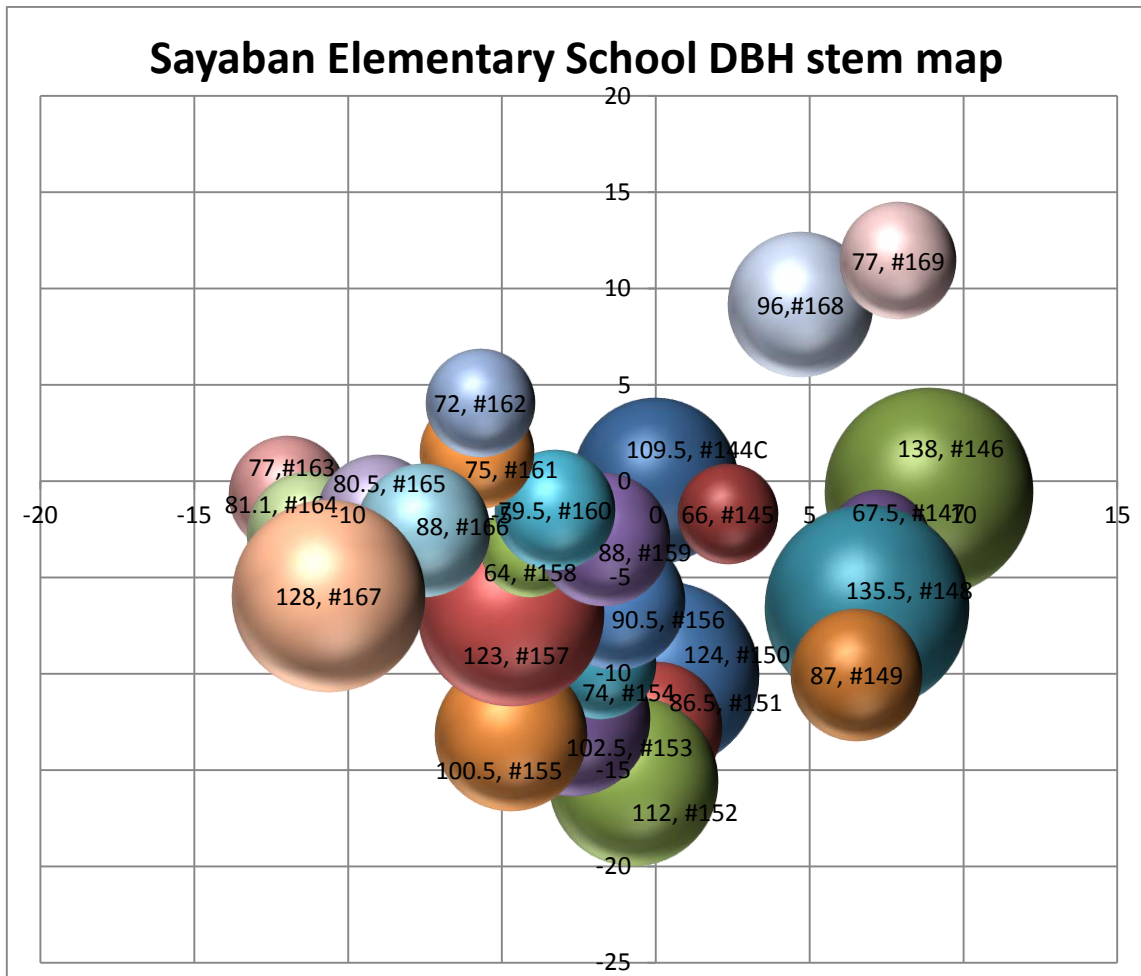


Figure 3-2. Sayaban Elementary School DBH stem map. Middle tree has (0,0) polar coordinates.

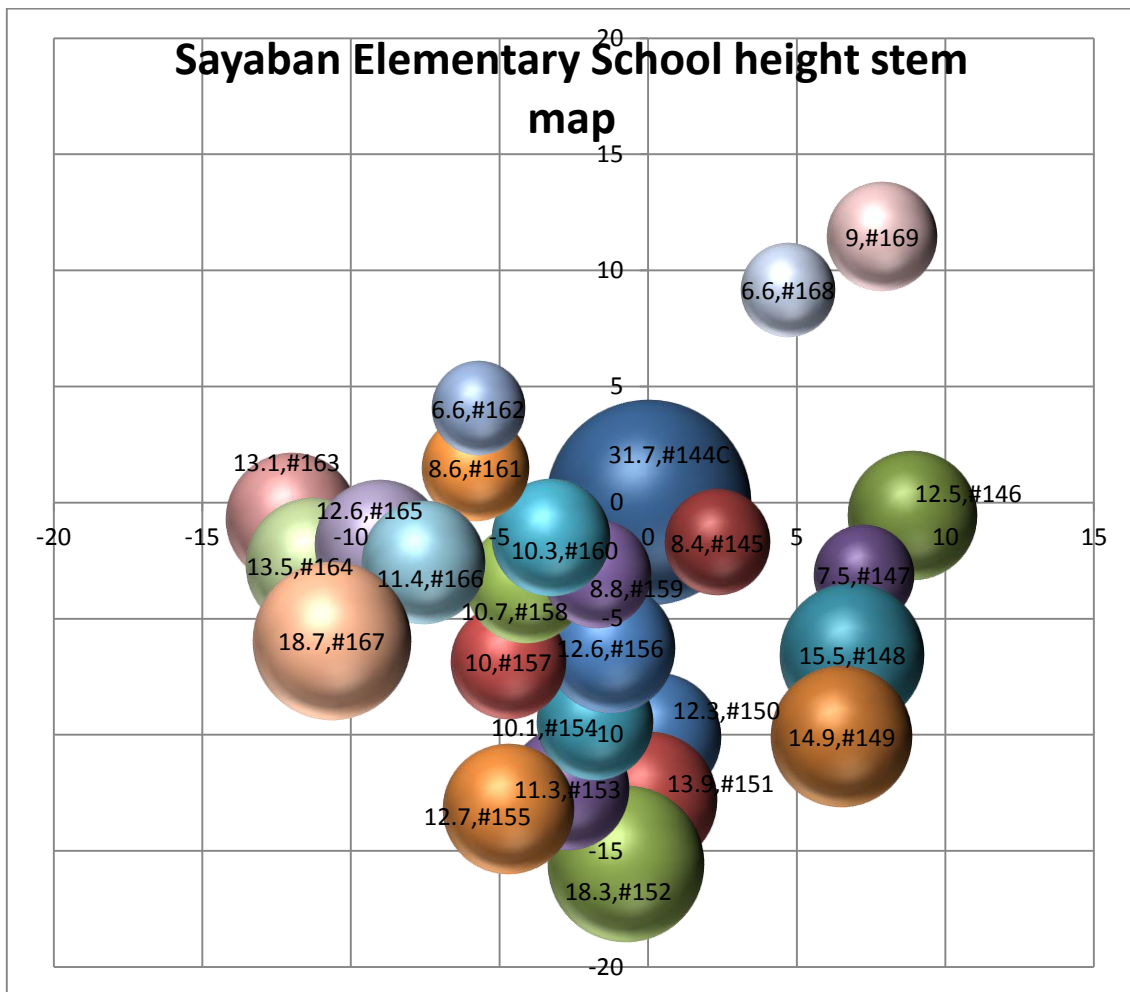


Figure 3-3. Sayaban Elementary School height stem map (mahogany plantation). Middle tree has (0,0) polar coordinates.

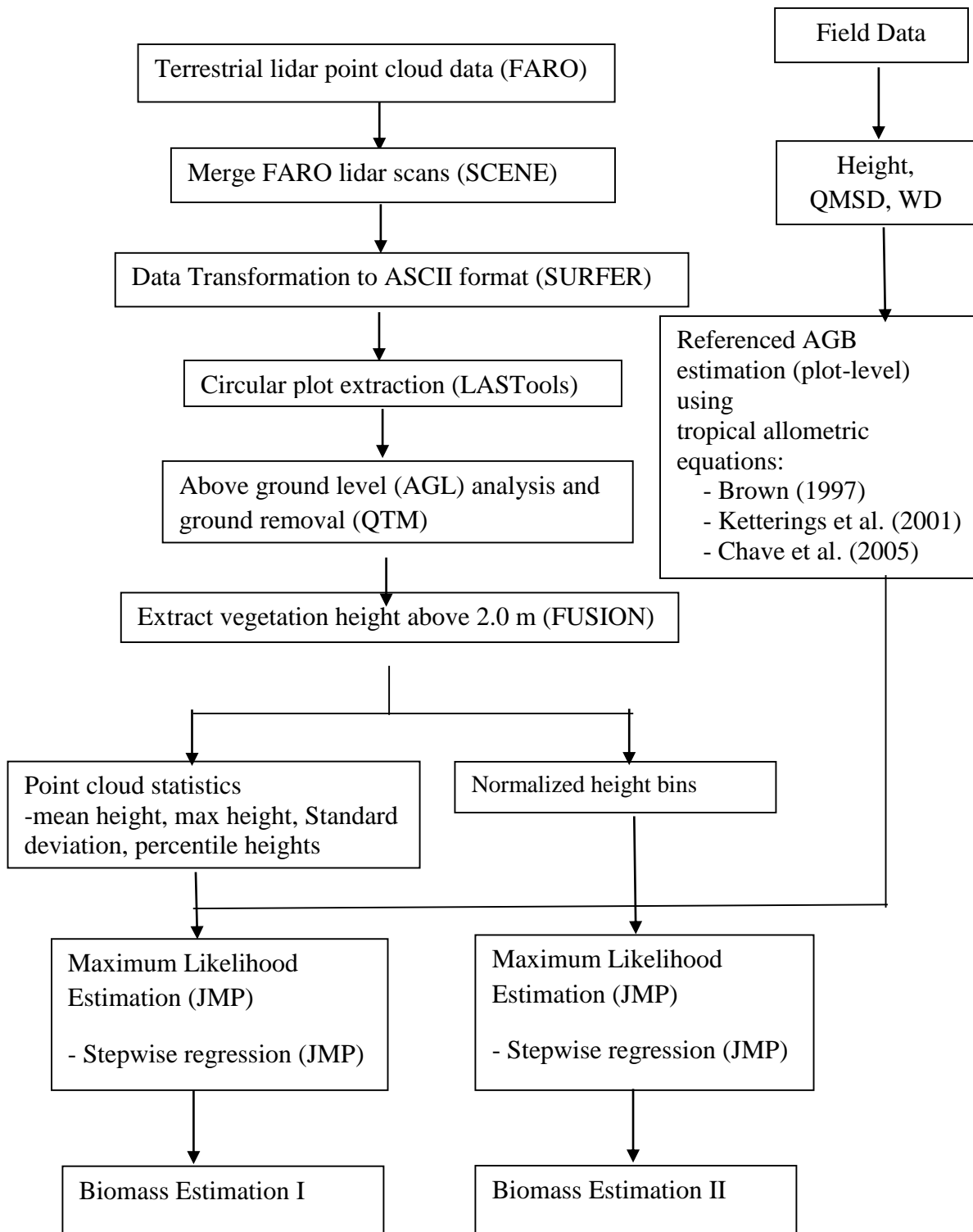


Figure 3-4. Data processing flowchart for terrestrial laser scan data



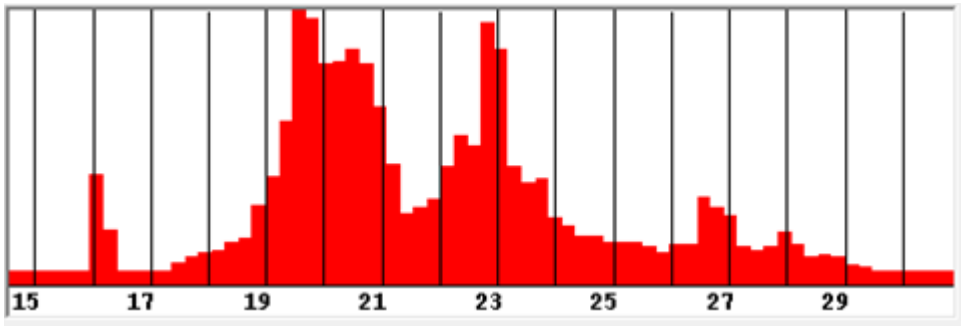


Figure 3-5. Height histogram of Sayaban Elementary School (multiple use zone). Height (in m) in x-axis. Tree frequency in y-axis.

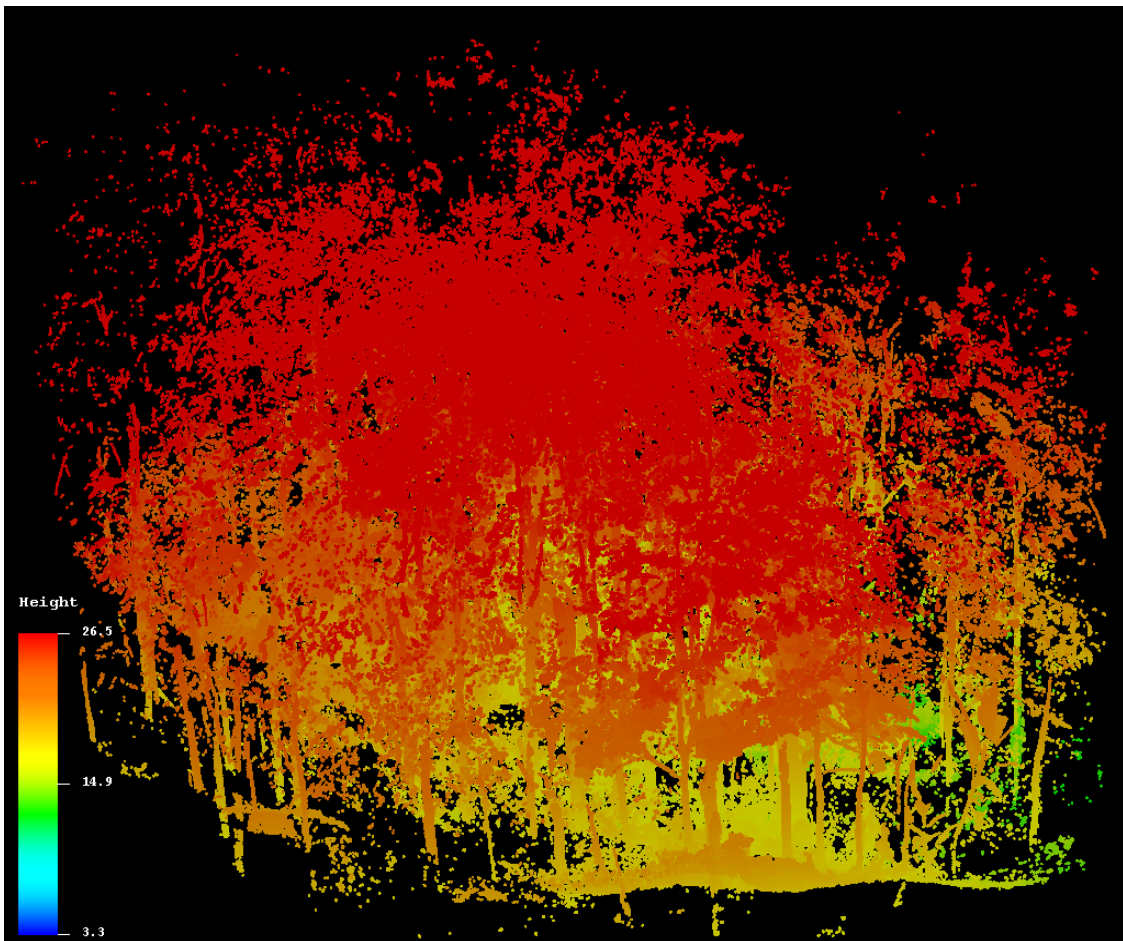


Figure 3-6. Point cloud image of Sayaban Elementary School (multiple use zone). Inset is height legend (in m).

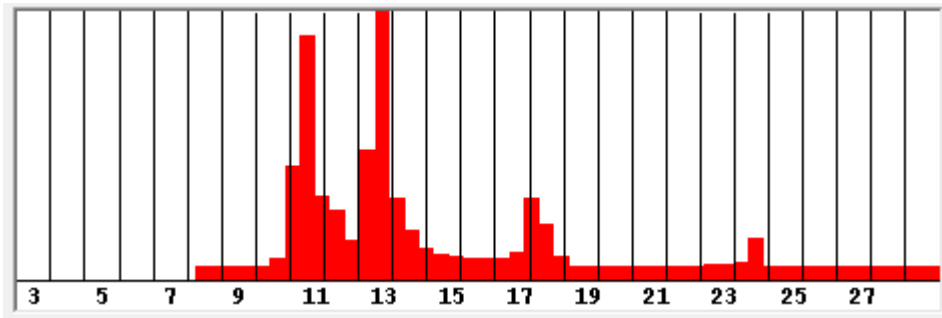


Figure 3-7. Height histogram of Matiaw 1 (restoration zone). Height (in m) in x-axis. Tree frequency in y-axis.

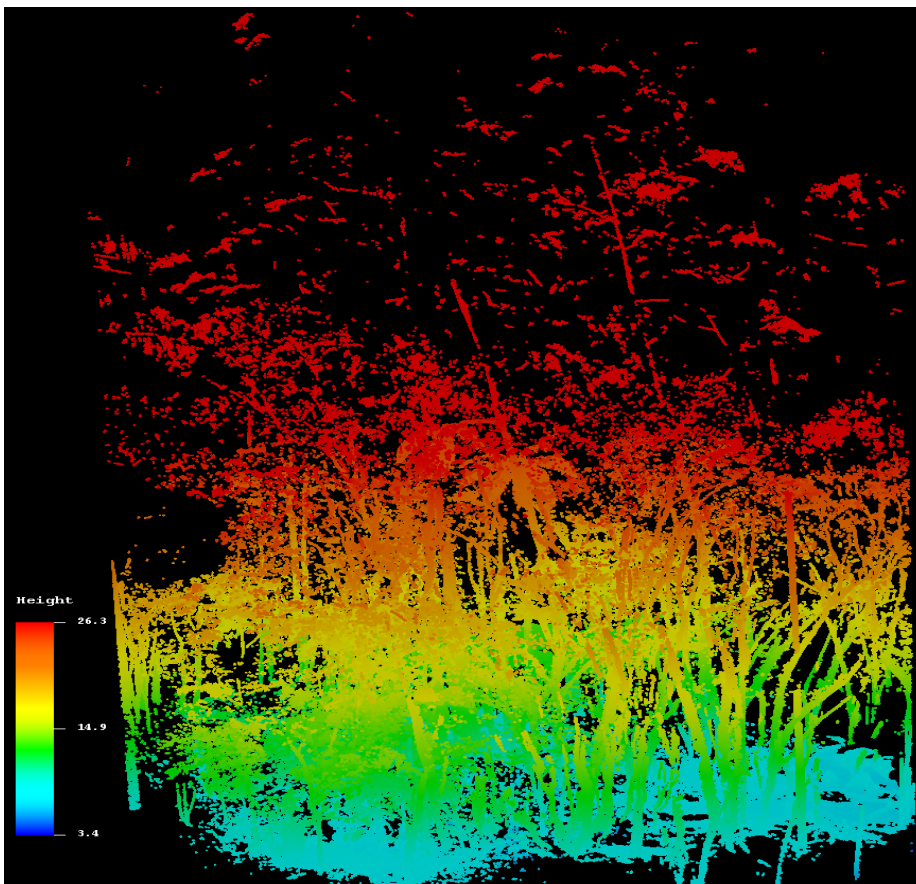


Figure 3-8. Point cloud image of Matiaw 1 (restoration zone). Inset is height legend.

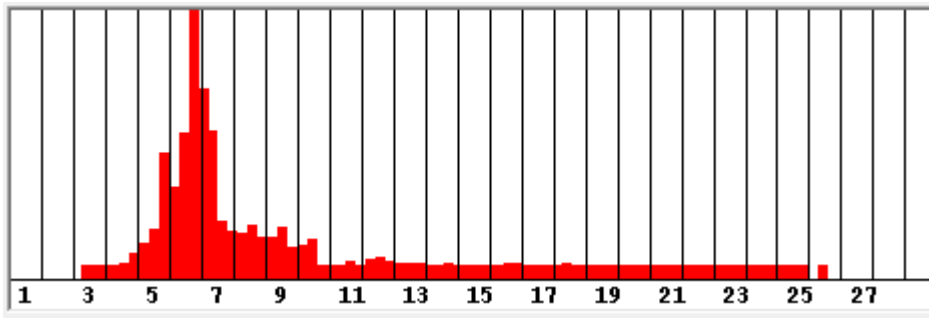


Figure 3-9. Height histogram of Lake Venado 2 (strict protection zone). Height (in m) in x-axis. Tree frequency in y-axis.

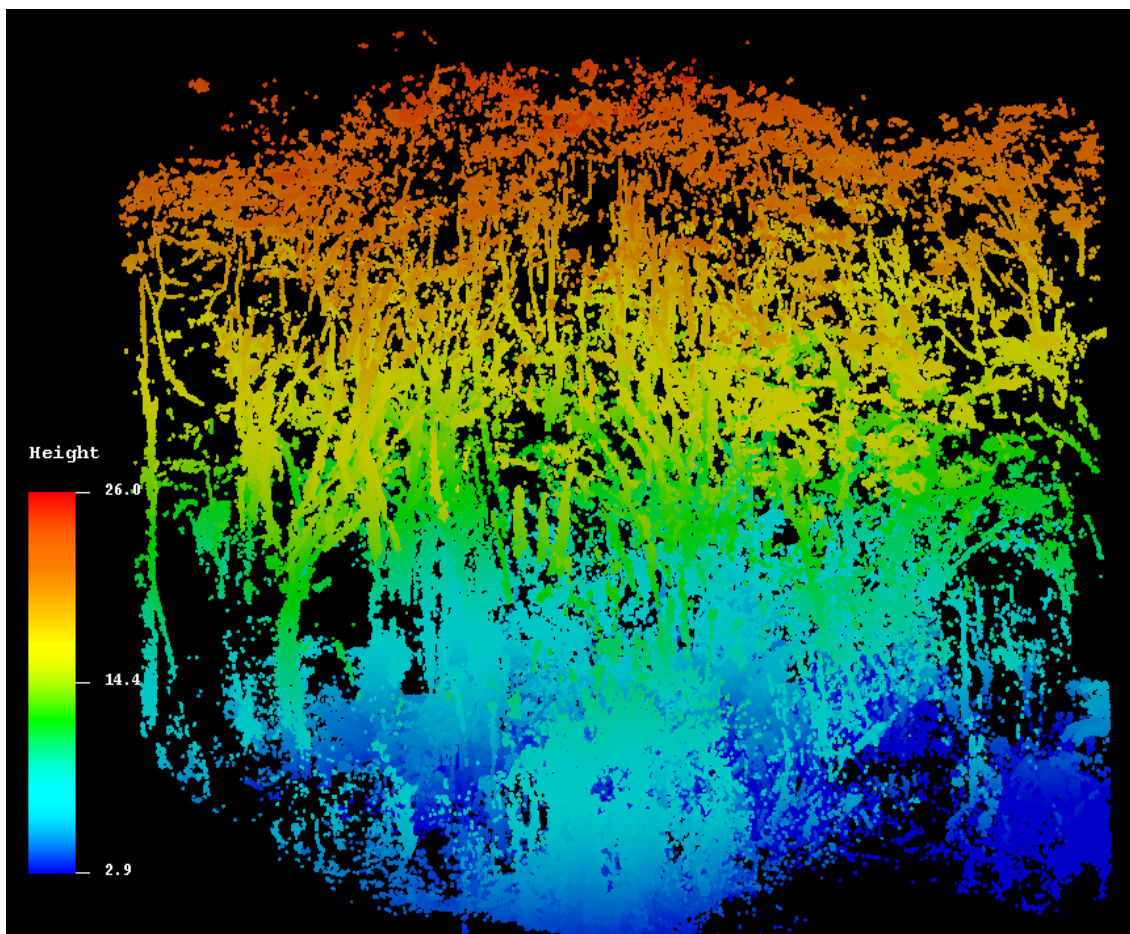


Figure 3-10. Point cloud image of Lake Venado 2 (strict protection zone). Inset is height legend (in m).

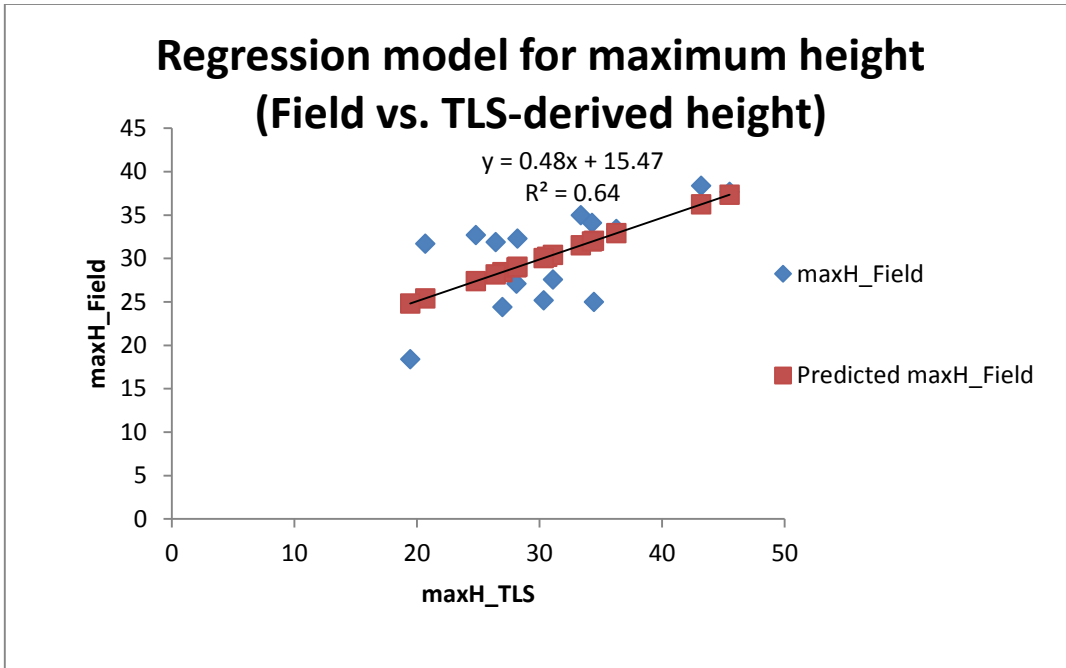


Figure 3-11. Regression model for maximum height from field and TLS data

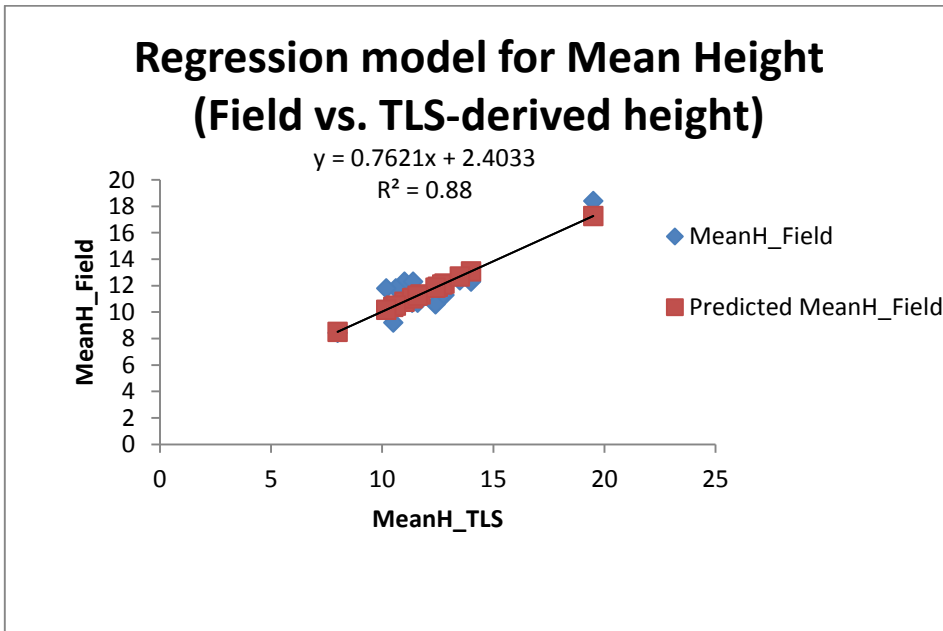


Figure 3-12. Regression model for mean height from field and TLS data

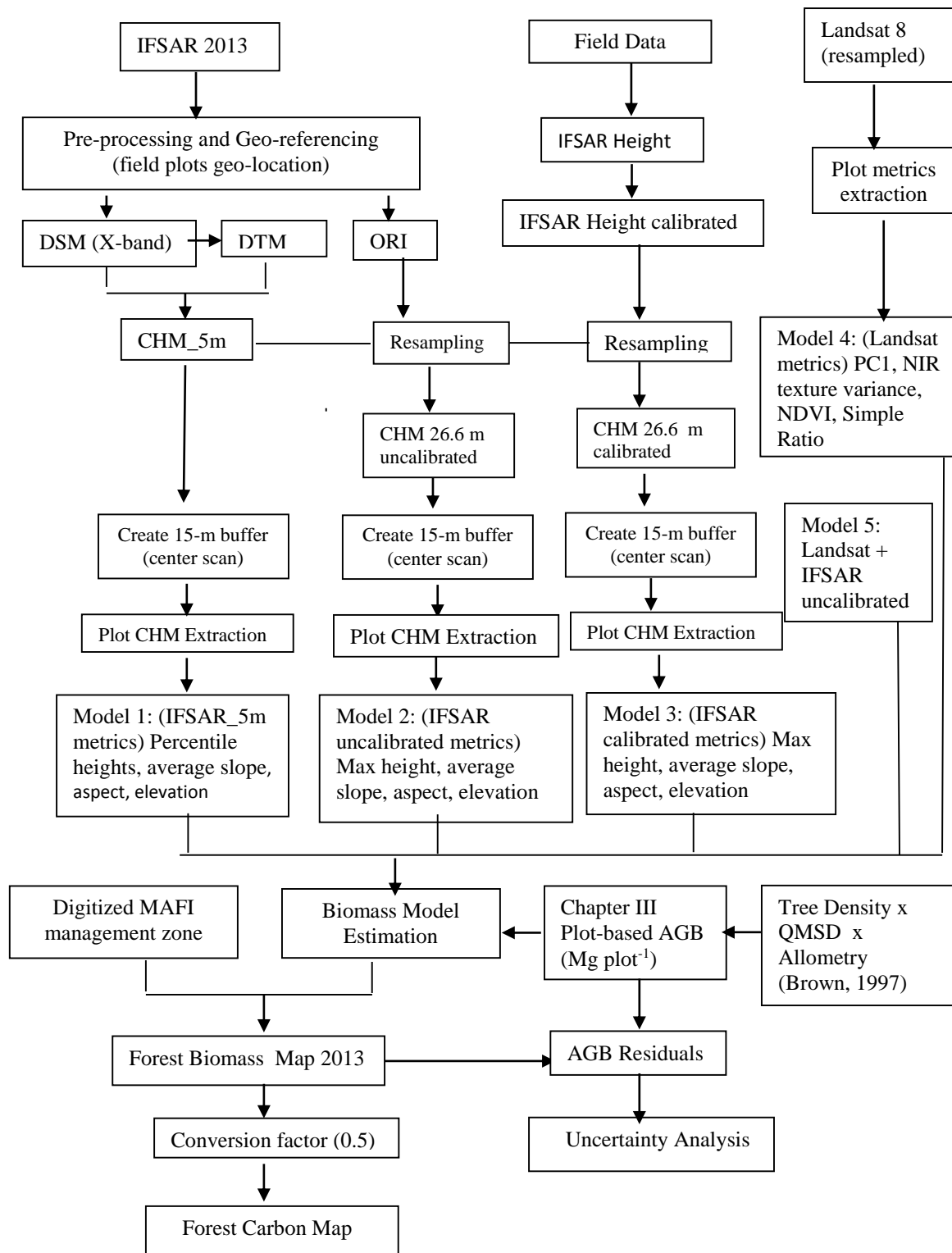


Figure 4-1. Flowchart for IFSAR image and data processing

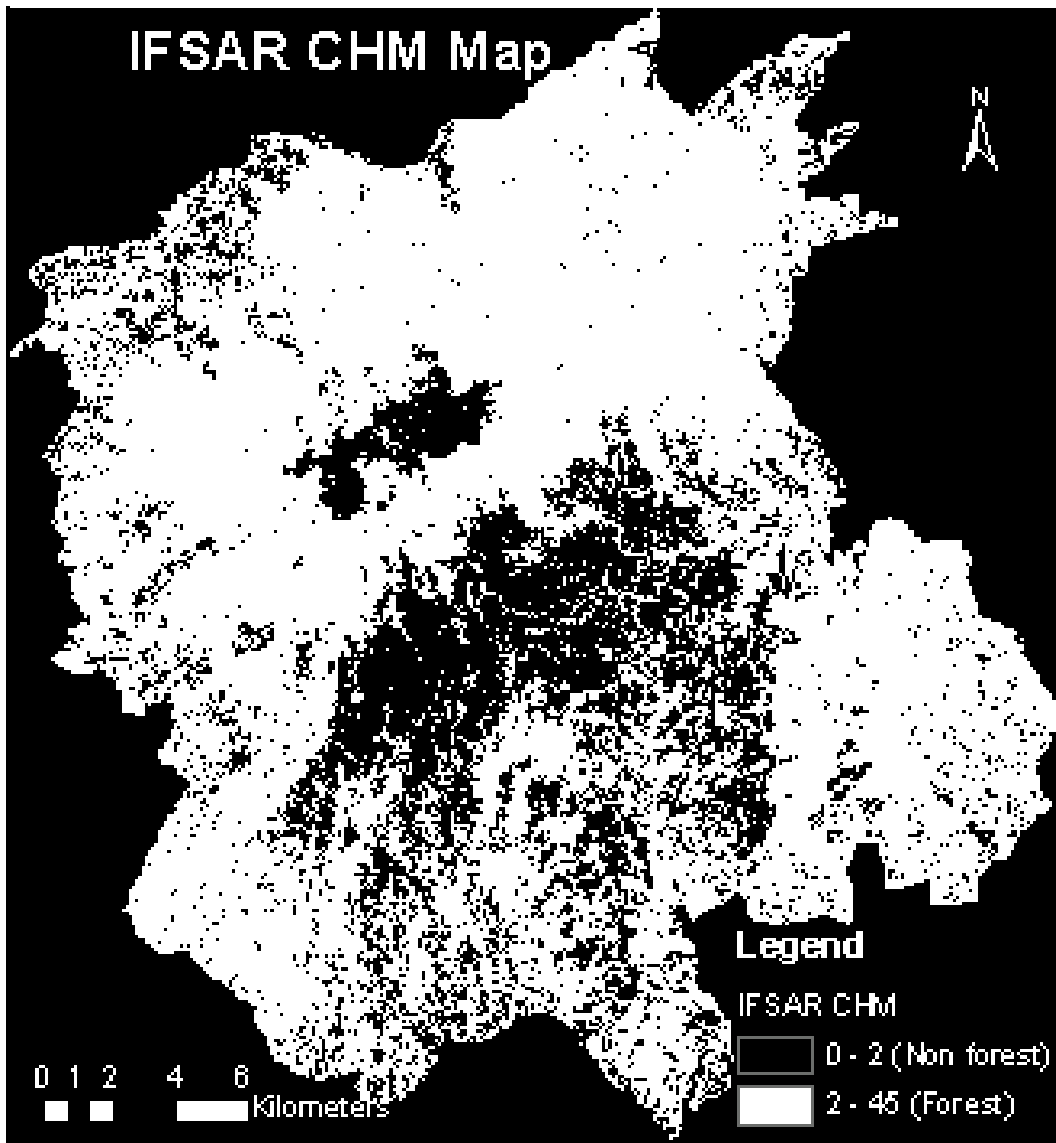


Figure 4-2. IFSAR canopy height model (CHM) distribution map

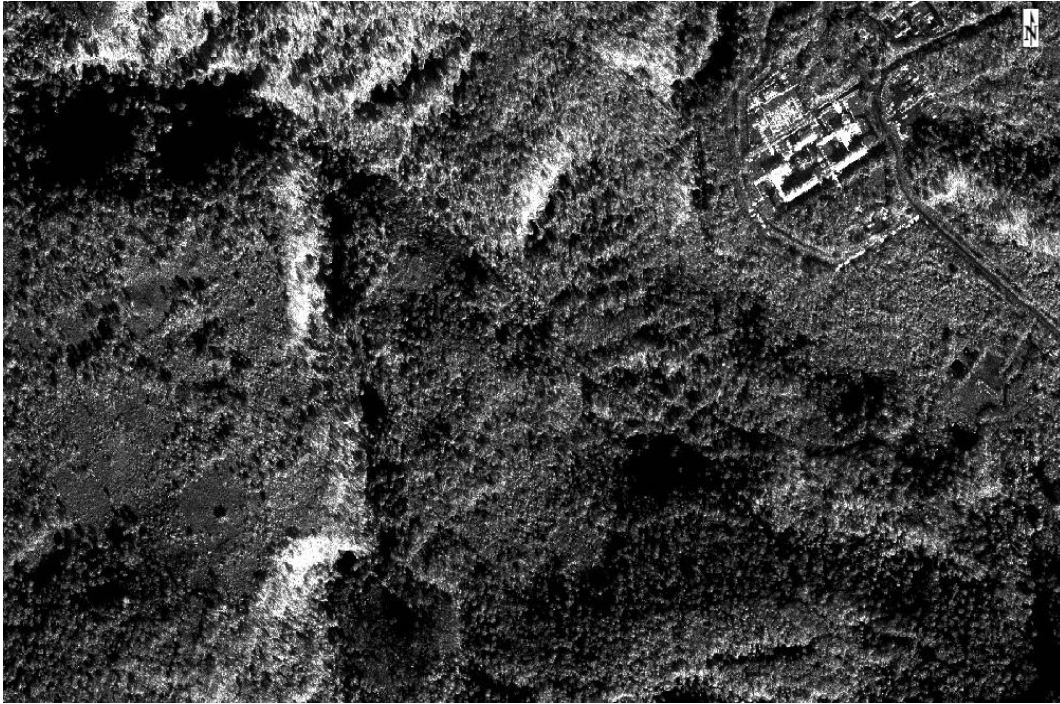


Figure 4-3. Areas within the restoration zone

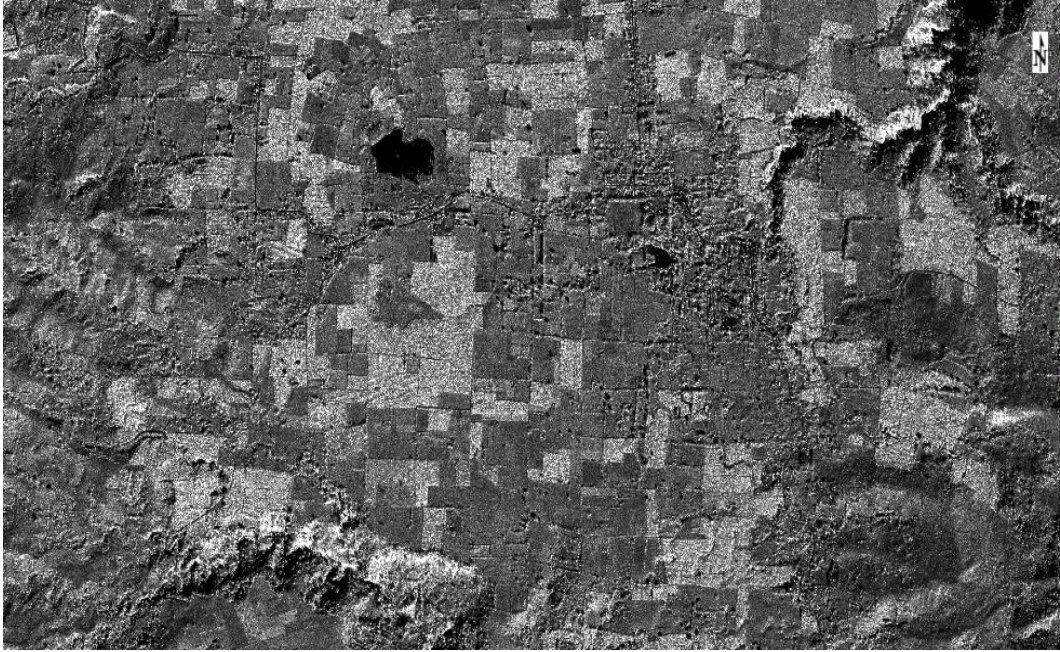


Figure 4-4. Areas within multiple use zone

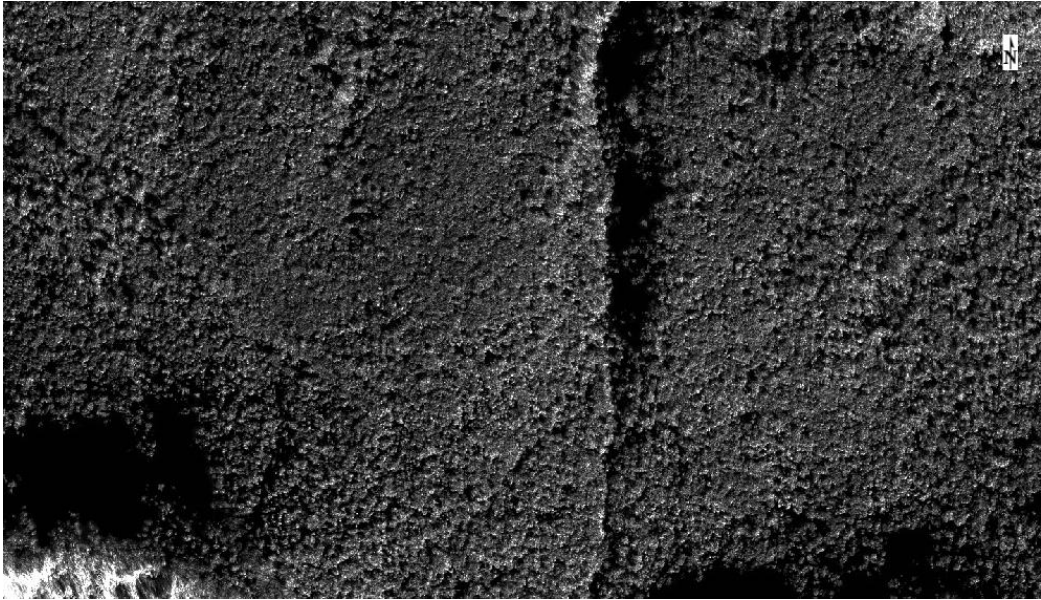


Figure 4-5. Areas within strict protection zone



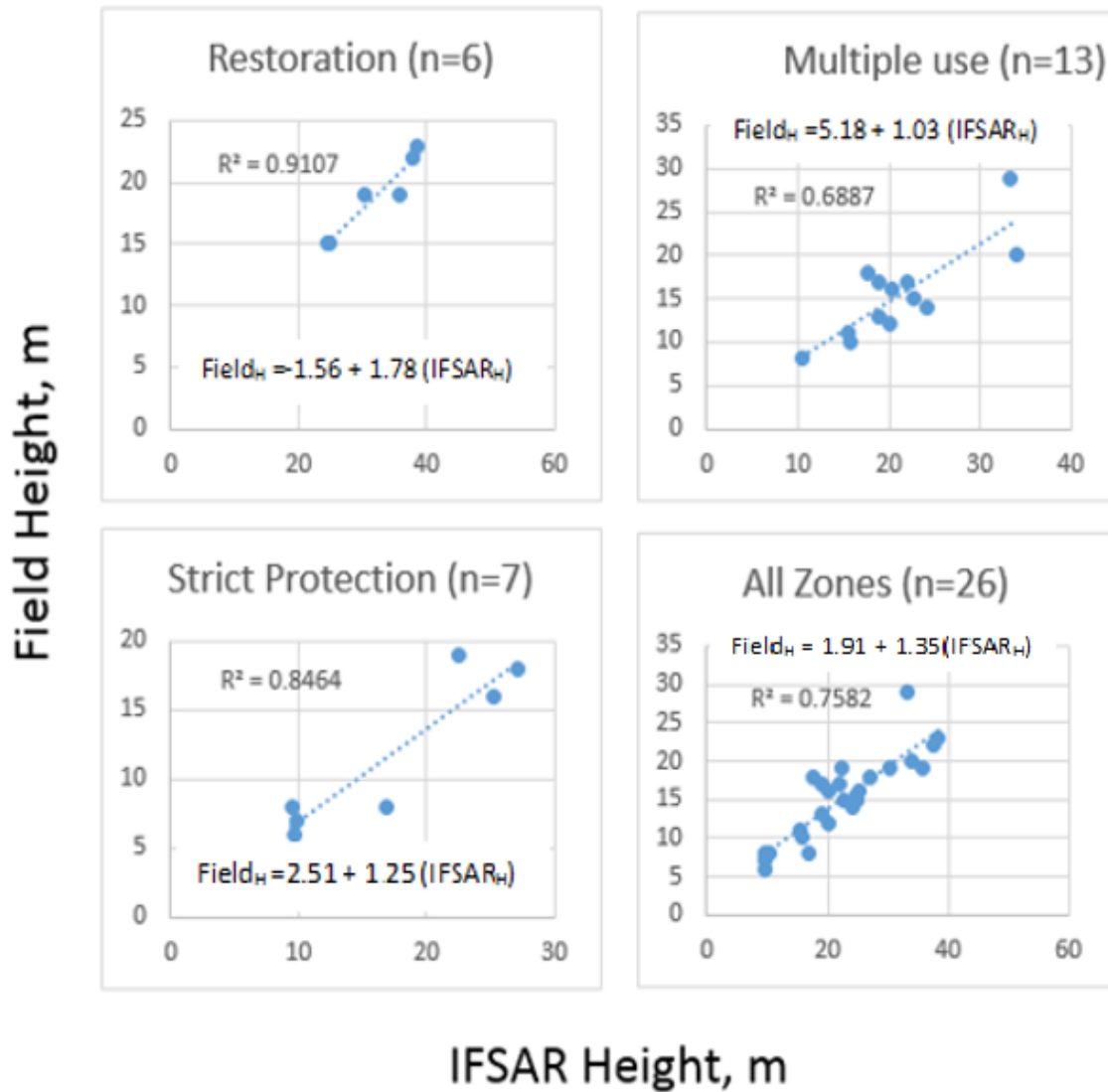


Figure 4-6. Scatterplot chart showing the empirical models to relate maximum IFSAR height (x-axis) and field-derived height (y-axis).

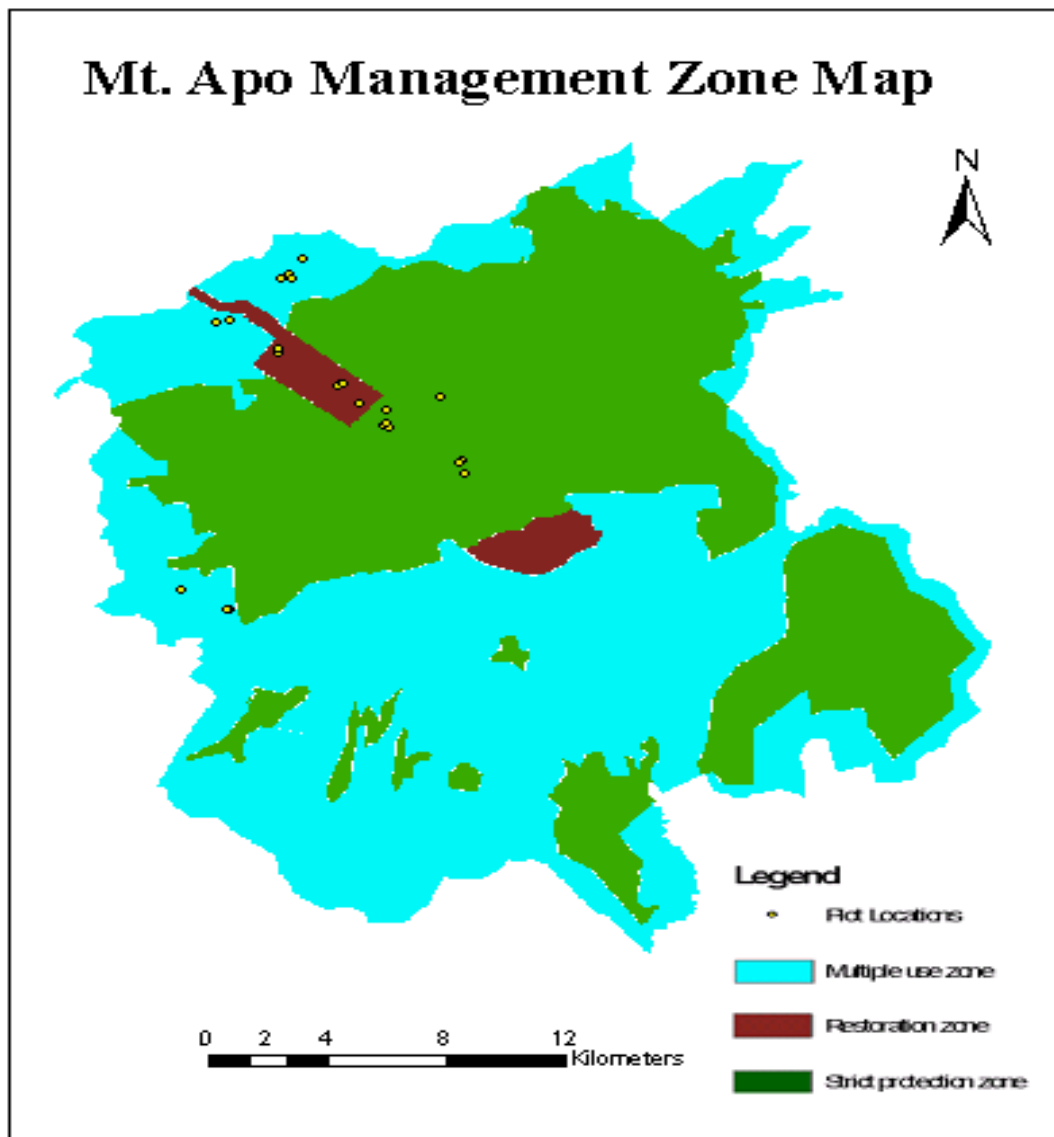


Figure 4-7. Mt. Apo management zone map overlaid with study plots

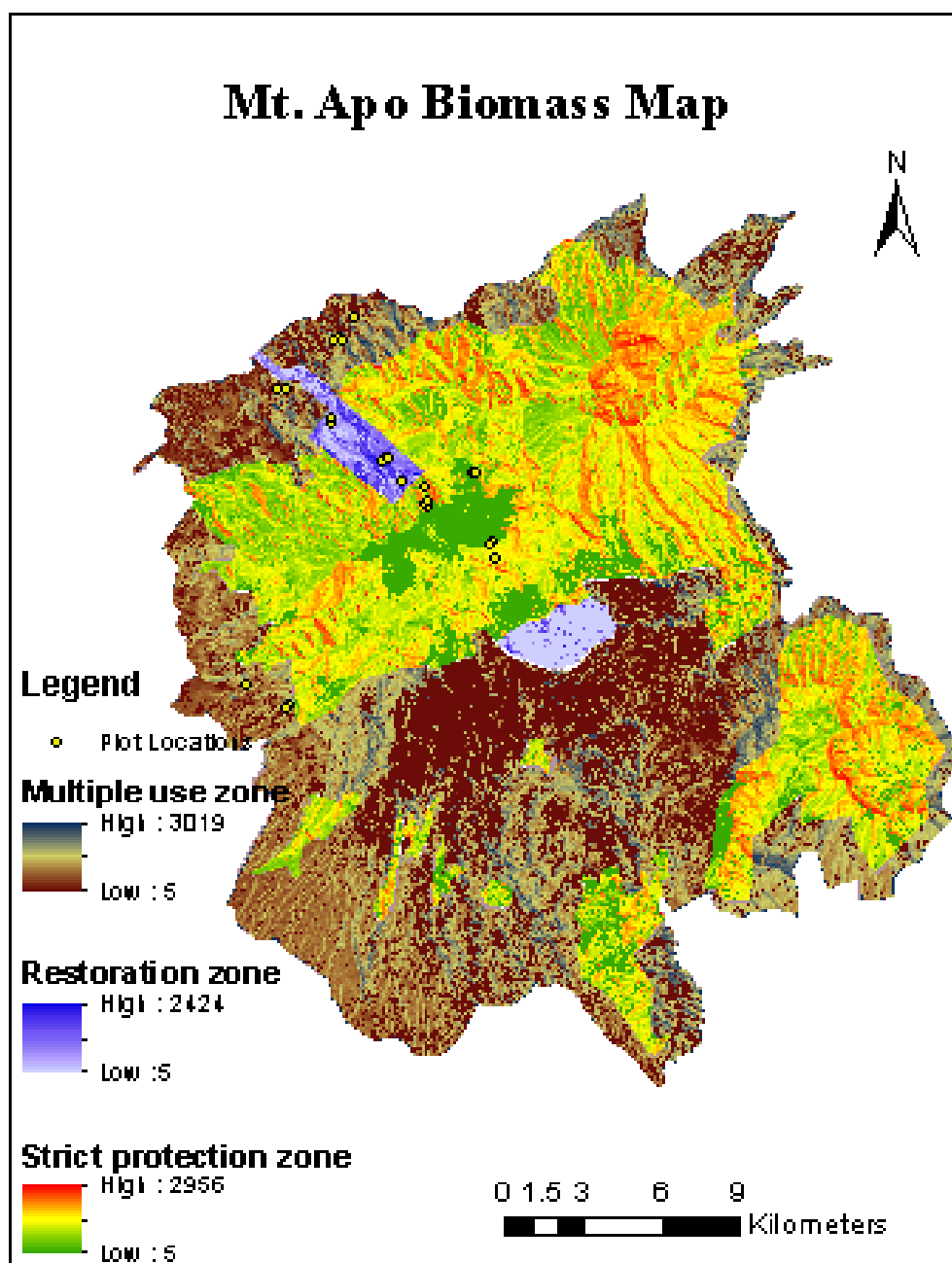


Figure 4-8. Mt. Apo biomass map measured in  $\text{Mg ha}^{-1}$

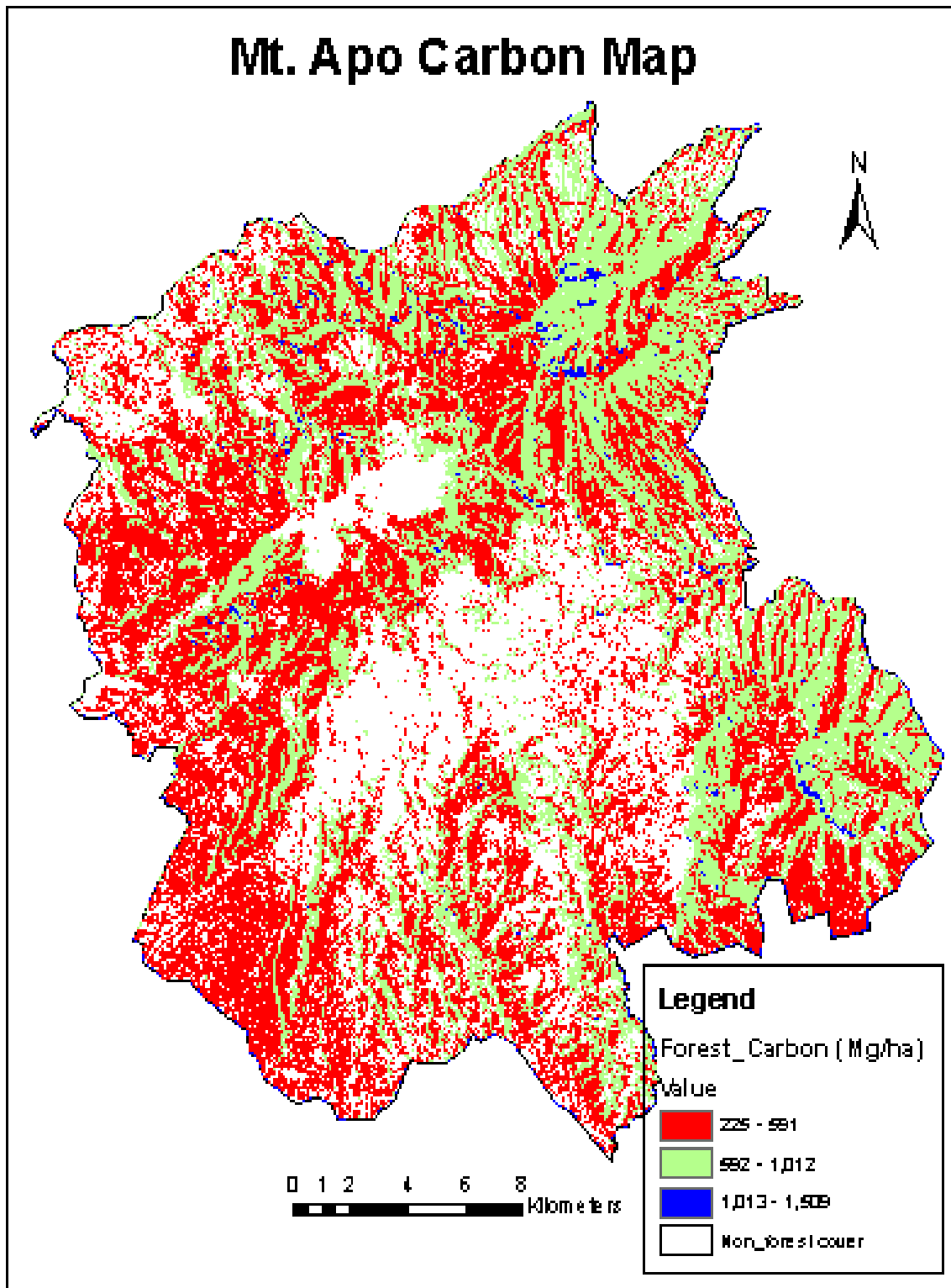


Figure 4-9. Mt. Apo forest and non-forest carbon map

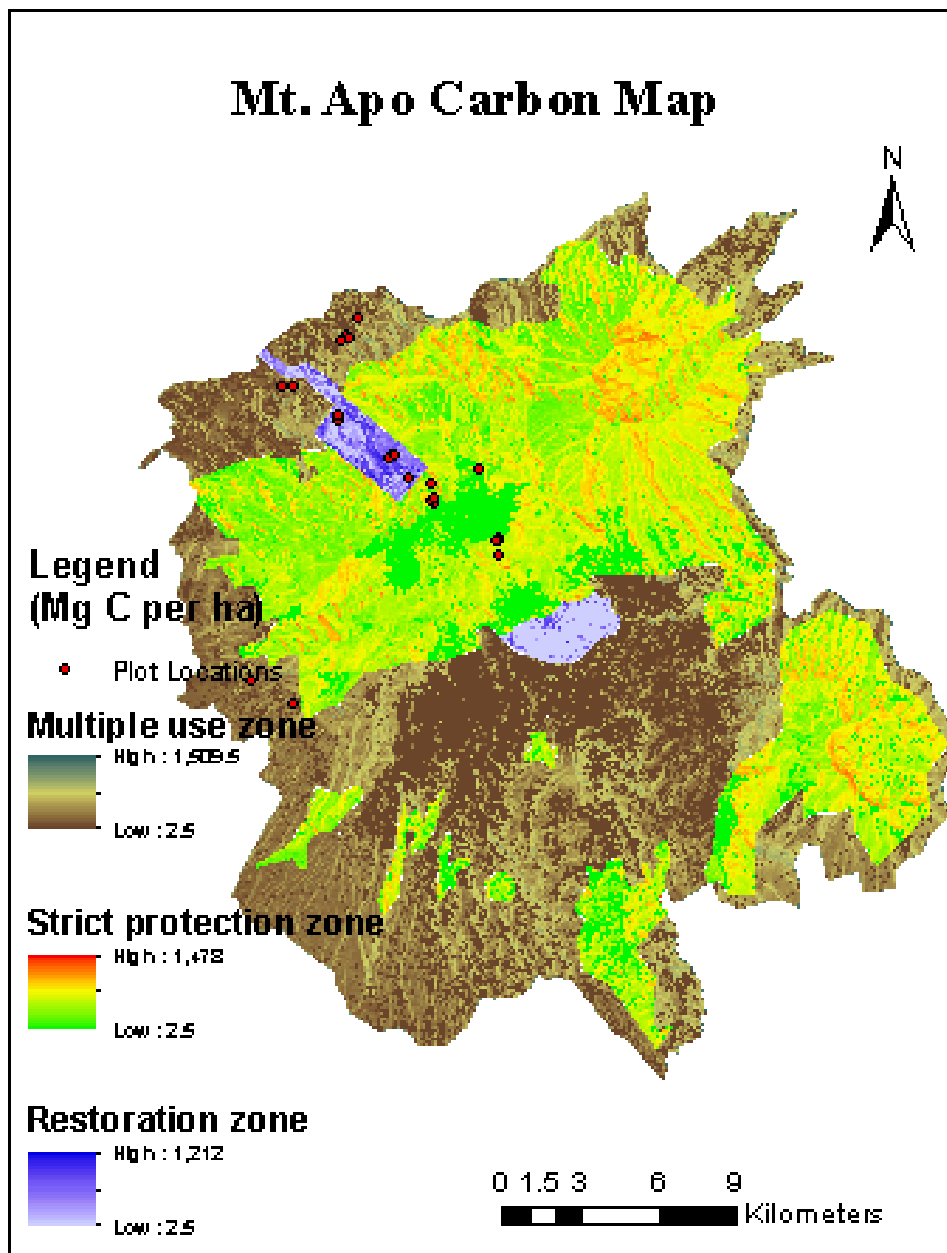


Figure 4-10. Mt. Apo carbon stocks on management zone map

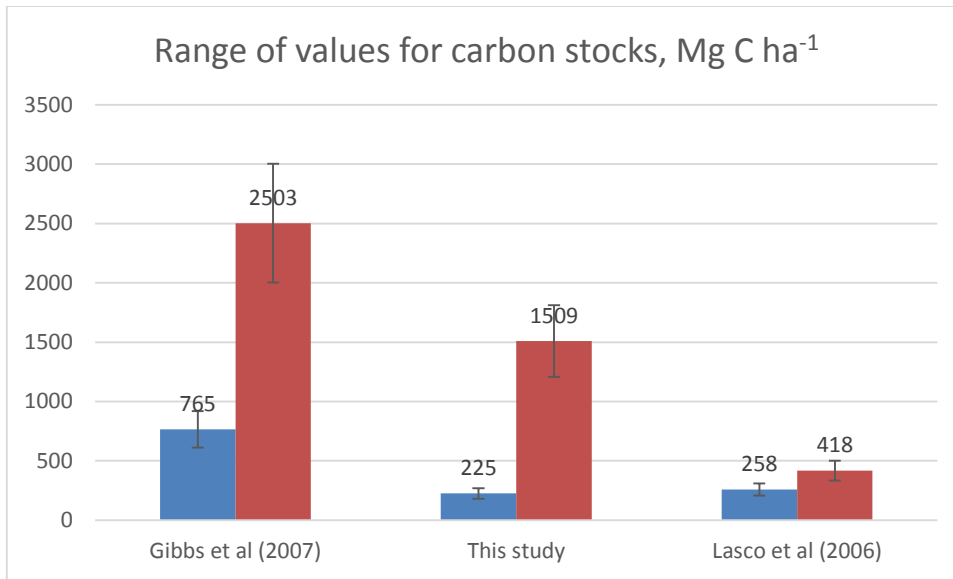


Figure 4-11. Comparing Philippines forest carbon values from this study to published materials

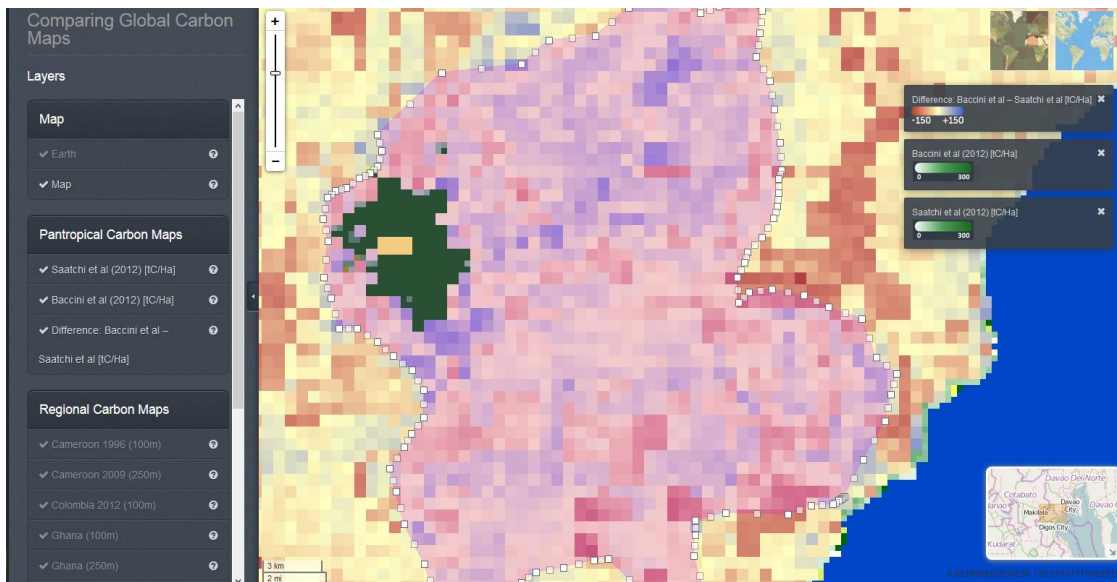


Figure 4-12. Global canopy maps from Saatchi et al. (2011) and Baccini et al. (2012)

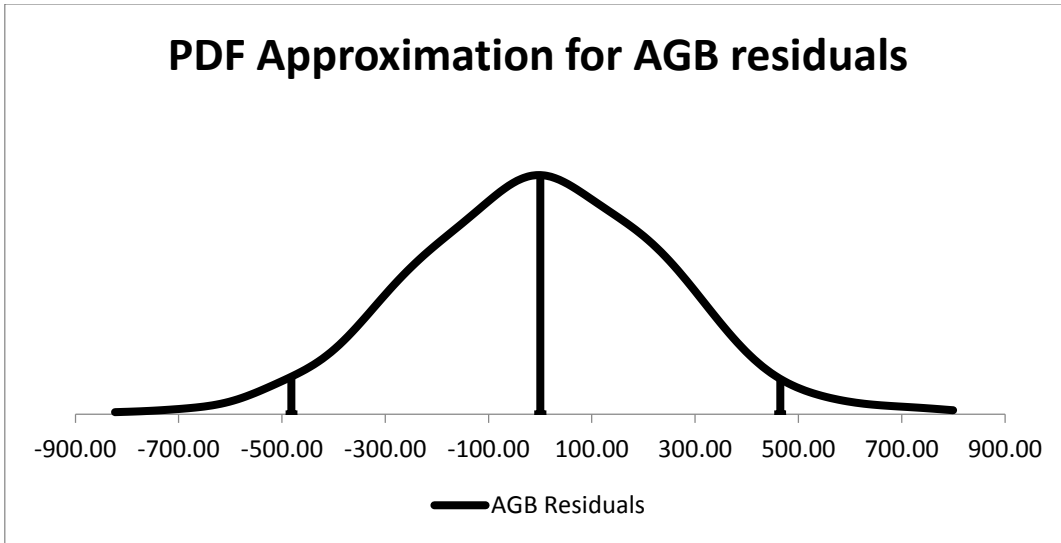


Figure 4-13. PDF approximation for AGB residuals

## APPENDIX B

### TABLES

Table 1-1. Compiled results of the total estimated carbon stocks in the Philippines. A compilation by Gibbs et al. (2007)

Compiled Harvest Data			Forest Inventory		
Source	Source	Source	Source	Source	Range of values
Olson et al. (1983) and Gibbs (2006): 869 Mt C	Houghton (1999) and DeFries et al. (2002): 765 Mt C	IPCC (2006): 2503 Mt C	Brown (1997), Achard et al. (2002, 2004) : 1213 Mt C	Gibbs and Brown (2007a,2007b) :1530 Mt C	765-2503 Mt C

Table 1-2. Scientific paper examined on carbon storage in selected areas in the Philippines

Author	Area, Method	Location description	Estimated Carbon stocks
Han et al. (2010)	Mt. Makiling Forest Reserve Destructive sampling, Soil respiration rate, bacteria count	60-year old secondary natural forest stand (1 ha) and large-leafed mahogany plantation (0.6 ha)	Carbon storage = 313.12 Mg C ha <sup>-1</sup> (natural forest stand), 185.28 Mg C ha <sup>-1</sup> (mahogany plantation)  R <sup>2</sup> for tree biomass in mahogany plantation range from 0.91 to 0.99
Lasco et al. (2004)	Mt. Makiling Forest Reserve Non-destructive sampling	secondary natural forest stand	Carbon storage = 418 Mg C ha <sup>-1</sup> and sequester 5 Mg C ha <sup>-1</sup> year <sup>-1</sup>
Lasco et al. (2006)	Effect of logging on C stocks Surigao del Sur	Selectively logged Dipterocarp forest	C stocks = 258 Mg C ha <sup>-1</sup> (unlogged forest), 34% is in SOC



Table 2-1. Profile of study plots by land cover type

Land cover type	No. of plots	Number of species sampled	Proportion of species (%)
Closed-canopy forest	11	32	61
Open- canopy forest	9	27	52
Cultivated area	6	21	40
Mt. Apo	26	52	

Table 2-2. Classification of the study plots by management zone

Management Zone	No. of plots	Individual Trees	No. of species sampled
Multiple Use	13	638	34
Strict Protection	7	465	28
Restoration	6	279	23
Mt. Apo	26	1382	52

Table 2-3. Distribution of study plots by elevation and habitat type

Elevation range (masl)	Habitat Type	Number of plots
0-600	Lowland	0
600-1200	Lowland evergreen	5
1200-1500	Lower montane	10
1500-2500	Upper montane	11
Above 2500	Summit	0
Total		26

Table 2-4. Descriptive statistics by management zone

	Multiple Use	Strict Protection	Restoration Zone
Height range (m)	2.1-35	2.3-27.1	2-38.4
DBH range (cm)	9.5-293	6.5-441	9-432
Elevation range (masl)	762-2194	1701-2373	1259-1500
Number of species, Total	34	28	23

Table 2-5. Test for Normality of Distribution for Height and DBH

Confidence Level	95.000%			
Procedure	Distribution	Test value	P-value	
Chi-Squared	Height	0.9872	0.3862	Fail to Reject the Ho that the samples are drawn from reference distribution*
Chi-Squared	DBH	0.8980	0.1521	Fail to Reject the Ho that the samples are drawn from reference distribution*
				*Based on approximate p-values

Table 2-6. Frequency distribution of 52 local tree species

Common Name	N	Scientific Name	Family Name
Tinikaran	319	Leptospermum flavescens	Myrtaceae
Philippine Cedar	193	Toona calantas	Meliaceae
Ulayan	119	Lithocarpus sulitii Soepadmo	Fagaceae
Tapol	88	Camellia sp	Theaceae
Mahogany	73	Swietenia mahogani Jacq.	Meliaceae
Kalingag	66	Cinnamomum mercadoi	Lauraceae
White lauan	59	Shorea contorta	Dipterocarpaceae
Madsum	50	Polyosma sp. 2	Escalloniaceae
Asik-asik	44	Flacourtia sp.	Flacourtiaceae
Abo-abo	36	Adinandra sp.	Theaceae
Sabon-sabon	36	Eurya sp	Theaceae
Kape	28	Coffea robusta L. Linden	Rubiaceae
Alingatong	24	Dendrocnide meyeniana	Urticaceae
Indang	23	Litsea perrottetii, B and H.	Euphorbiaceae
Basikong	16	Ficus botryocarpa Miq.	Moraceae
Tambis	16	Syzygium aqueum	Myrtaceae
Manok	15	Weinmannia sp.	Cunoniaceae
Angelo	13	Elaeagnus sp.	Elaeagnaceae
Banti-banti	13	Fagraea sp.	Loganiaceae
Katii	13	Castanopsis motleyana	Fagaceae
Kiramdam	11	Dacrycarpus imbricatu	Podocarpaceae
Balingos	10	Macaranga dipterocarpifolia Merrill	Euphorbiaceae
Kahoy-bungtod	10		
Malatambis	10	Syzygium hutchinsonii	Myrtaceae
Agoho	10	Casuarina equisetifolia	Casuarinaceae

Nato	9	Actinodaphne sp.	Fagaceae
Balete	8	Ficus balete Merr.	Moraceae
Binunga	8	Macaranga tanarius (L.) Muell. Arg.	Euphorbiaceae
Sinamomon	8	Astronia sp	Melastomataceae
Sangguyan	7	Syzygium sp.1	Myrtaceae
Mahabundoy	6	Lithocarpus sp. 2	Fagaceae
Sagawan	6	Perrottetia sp.	Cleastraceae
Gosip	4		
Almaciga	3	Agathis philippinensis	Araucariaceae
Sawraria	3	Polyosma philippinensis Merr.	Escalloniaceae
Aha	2	Elacocarpus sp.	Elaeocarpaceae
Dilat-manok	2	Gordonia lazonica	Theaceae
Dremis	2	Tasmannia piperita	Winteraceae
Langka	2	Artocarpus heterophyllus	Moraceae
Layapan	2	Prunus sp.	Rosaceae
Malacopa	2		
Rakrakan	2		
Tanguile	2	Shorea polysperma	Dipterocarpaceae
Bay-ang	1		
Buyo-buyo	1	Astronia macrophylla Blume	Piperaceae
Kalisaw	1	Ficus sp. 1	Moraceae
Katmon	1	Dillenia philippinensis	Dilleniaceae
Kulit-kulitan	1		
Malakawayan	1	Podocarpus rumphii Blume	Podocarpaceae
Malatadhan	1		
Marang	1	Artocarpus odoratissimus	Moraceae
Sagimsim	1	Syzygium sp.2	Myrtaceae

Table 2-7. Species-specific biomass estimates for ten leading common species

Common Name	N	Family Name	DBH (cm)	H (m)	WD (g cm <sup>-3</sup> )	Mean Biomass, kg tree <sup>-1</sup> (Brown 1997)	Mean Biomass, kg tree <sup>-1</sup> (Ketterin g et al. 2001)	Mean Biomass, kg tree <sup>-1</sup> (Chave et al. 2005)
Tinikaran	319	Myrtaceae	12-441	2.3-25.2	0.51	7391.6	2070.3	1623.8
Philippin	193	Podocarp	6.5-	2.6-	0.6	15519	4336.9	5364

e Cedar		aceae	376	34	5			
Ulayan	119	Fagaceae	12.5-432	3.5-34.1	0.71	16489.7	4582	6466
Tapol	88	Melastomataceae	9.5-101	2.3-23.1	0.71 <sup>a</sup>	1676.8	541	786.2
Mahogany	73	Meliaceae	11-138	4.3-31.7	0.69	7496	2287.8	2608
Kalingag	66	Lauraceae	9-229	2.1-22.6	0.65	6406.6	1846	1698
White lauan	59	Moraceae	15-343	4.6-35.7	0.77	20186.9	5556.7	10745.6
Madsum	50	Escalloniaceae	11.5-252	4.2-25	0.67	6470.9	1879	1738
Asik-asik	44	Staphylleaceae	10.5-120	2-23.6	0.71 <sup>a</sup>	1817	582.4	728.5
Abo-abo	36	Theaceae	17-246.5	4.7-32.3	0.7	8438	2405.8	2597.8

<sup>a</sup> used average WD of 0.71 g cm<sup>-3</sup> (Brown, 1997)

Table 2-8. Actual mean biomass by DBH class size

DBH class size (cm)	Mean biomass, kg tree <sup>-1</sup> (Brown, 1997)	Mean biomass, kg tree <sup>-1</sup> (Ketterings et al., 2001)	Mean biomass, kg tree <sup>-1</sup> (Chave et al., 2005)
5 - 50	11,141.04	4,453.54	4,422.18
51-100	100,515.34	37,183.98	46,337.96
101-150	375,767.40	127,312.97	157,821.94
151-200	671,351.29	212,606.90	302,893.99
201-250	774,869.26	245,102.79	256,987.11
251-300	681,269.63	199,789.14	212,810.74
>301	1,354,072.30	382,252.78	432,868.82

Table 2-9. Plot-level mean biomass

Plot	Location	N (Total Trees)	N (Species)	DBH (cm)	H (m)	Mean Biomass, kg tree <sup>-1</sup> (Brown, 1997)	Mean Biomass, kg tree <sup>-1</sup> (Ketterings et al. 2001)	Mean Biomass, kg tree <sup>-1</sup> (Chave et al. 2005)
1	Hotmud	27	8	20-145	2.8-24.4	9,434.9	2,809	3,743.9
2	Antapan	28	8	21-432	2.9-30.2	41,731	11,062	12,955
3	Sayaban HS	89	7	15-136	3.1-18.4	3,492.5	1,100.6	1,145.8
4	Sayaban Elem School	26	2	64-138	6.6-31.7	12,581	3,786	4,294
5	Bongolano n	60	14	11.5-206	2.3-27.6	4,181	1,218	1,793
6	Tawasan1	51	8	13-252	4.7-32.3	9,076.5	2,549.5	2,681
7	Tawasan2	27	8	27-184	8.5-32.7	11,006	3,269.4	6,139.5
8	Tawasan3	61	10	15-200	4.4-31.9	4,777.6	1,402.7	2,090.5
9	New Israel1	73	15	9.5-280	2.1-35	5,798.7	1,661	3,291.8
10	New Israel2	52	17	13-196	3-34.1	7,163.3	2,101.9	3,932
11	New Israel3	18	6	15-233	5.3-33.4	17,033	4,795	9,103.8
12	Matiaw1	39	8	14-237	4.5-37.7	11,289.6	3,288.6	5,461
13	Matiaw2	33	9	13-161	6.4-25	6,355.7	1,928.8	2,720
14	Matiaw3	48	12	10-186	3.9-38.4	6,121	1,820.6	3,466
15	Coong-Matiaw	104	9	9-343	2-35.7	8,787	2,459	4,313
16	Lake Venado1	35	5	10-376	3-27.1	27,852	7,443.6	9,082
17	Lake Venado2	30	4	6.5-441	2.6-25.2	46,082.9	12,003.8	11,072.7
18	Baroring	84	7	14-293	5.3-	8,250.5	2,309	3,032.3

					34			
19	Godi-godi1	34	1	40.5-269.5	5-22.1	23,350.6	6,690.3	8,000.9
20	Godi-godi2	23	4	22.5-167	4.8-17.6	11,593	3,448.7	3,560.7
21	Godi-godi3	40	4	21.5-259	4-19	16,803	4,747	4,187.5
22	Makadak1	88	2	16.7-115.5	4.9-9.8	2,174	709	445.4
23	Makadak2	93	4	17.6-120	2.3-9.7	1,925	626	335.4
24	Makadak3	86	2	17-80.3	3-9.5	1,455	481	279
25	EDC-H1	77	13	14.4-246.5	3.9-22.5	10,576.7	3,003.5	2,876.9
26	EDC-H2	56	16	15-207.5	3-16.8	10,728	3,148.8	3,069

Table 2-10. Carbon stock estimates by management zone

Management zone	N (Plots)	N (Total Species)	Mean Carbon, kg C tree <sup>-1</sup> (Brown, 1997)	Mean Carbon, kg C tree <sup>-1</sup> (Ketterings et al. 2001)	Mean Carbon, kg C tree <sup>-1</sup> (Chave et al. 2005)
Multiple use	13	34	5,196.4	1,503	2,048.2
Strict Protection	7	28	7,199.5	1,958.3	1,940.0
Restoration	6	23	6,976.6	1,947.3	2,721.6

Table 2-11. Carbon stock estimates by land cover type

Land cover type	N (Plots)	N (Total Species)	Mean Carbon, kg C tree <sup>-1</sup> (Brown, 1997)	Mean Carbon, kg C tree <sup>-1</sup> (Ketterings et al. 2001)	Mean Carbon, kg C tree <sup>-1</sup> (Chave et al. 2005)
Closed-canopy forest	11	37	8,529.5	2,335.2	3,142.8
Open-canopy forest	9	27	4,825.3	1,397.9	1,432.6
Cultivated area	6	21	3,759.6	1,110.5	1,511.9

Table 3-1. Selected studies on uncertainties of tropical AGB estimation

Sensor name	Index/method	Paper	Accuracy Assessment
Lidar	Quadratic mean stem diameter, basal area and AGBM	Drake et al (2002)	At plot-level: QMSD: $R^2 = 0.93$ BArea: $R^2 = 0.72$ AGBM = $R^2 = 0.93$
Lidar, MODIS, SRTM	Carbon density maps, bookkeeping model	Baccini et al (2012)	$R^2=0.83$ (L. America),0.78, (Africa),0.71 ( Asia)
Lidar, MODIS, SRTM, QSCAT	Aboveground carbon density map, MaxEntropy	Saatchi et al (2011)	Uncertainty levels: L.Amer:15.8%, sub-Saharan Africa:21.7%, SE Asia:25.1%

Table 3-2. Classification of field plots by management zone

Management zone	N (Plots)
Multiple use	9
Strict protection	2
Restoration	5
Mt. Apo	16

Table 3-3. Point cloud registration results

Plot #	Location	Minimum (m)	Maximum (m)	Mean (m)	Deviation (m)
1	Hotmud	0.0001	12.2158	2.3405	3.1247
2	Antapan	0.0001	4.8341	0.6358	1.0678
3	Sayaban HS	0.0001	8.4629	1.1304	1.9078
4	Sayaban Elem	0.0004	8.4939	2.6095	2.7882
5	Bongolanon	0.0000	4.3484	0.6979	1.4022
6	Tawasan 1	0.0015	7.8036	2.5139	2.4238
7	Tawasan 2	0.0000	0.1032	0.0302	0.0285
8	Tawasan 3	0.0002	2.6987	0.7994	0.9524
9	New Israel 1	0.0000	4.7924	1.0754	1.3484
10	New Israel 2	0.0000	6.5617	1.5914	1.8143
11	New Israel 3	0.0000	0.5142	0.0771	0.1110
12	Matiaw 1	0.0000	7.0231	1.1997	1.9605
13	Matiaw 2	0.0003	8.5910	3.0995	3.1673

14	Matiaw 3	0.0000	0.0678	0.0193	0.0231
15	Lake Venado 1	0.0000	5.7620	0.9128	1.3213
16	Lake Venado 2	0.0004	7.8611	2.4178	2.5442

Table 3-4. Lidar point cloud data of each plot

Plot ID	Point Density (points/m <sup>3</sup> ) above 2m	Max Height (m)	Mean Height (m)	Height Std Dev (m)
Antapan	1,636,983	30.62	4.43	2.62
Hotmud	3,327,032	26.97	5.33	3.17
SayabanHS	2,970,423	20.68	5.95	3.11
SayabanElem	2,090,367	19.45	6.08	3.04
Bongolanon	1,869,853	31.09	5.09	2.93
Tawasan1	4,631,692	28.2	4.54	2.27
Tawasan2	1,919,088	24.81	5.82	3.26
Tawasan3	4,126,042	26.42	4.17	2.09
NewIsrael1	6,018,564	33.36	4.83	2.47
NewIsrael2	4,297,043	34.28	5.31	3.78
NewIsrael3	1,647,630	36.27	6.91	3.75
Matiaw1	2,402,720	45.5	6.44	4.52
Matiaw2	3,327,233	34.42	4.21	2.77
Matiaw3	3,133,572	43.19	4.63	2.54
LV1	4,736,687	28.12	4.65	2.53
LV2	1,198,880	30.33	5.75	4.58

Table 3- 5. List of regression variables

Variable of Lidar metrics	Description
<b>I. Biomass Estimation I</b>	
Std Dev	Height standard deviation
Mean_h	Mean height
Per25_h	25 percentile height
Per50_h	50 percentile height
Per75_h	75 percentile height
Per90_h	90 percentile height
Per95_h	95 percentile height
Max_h	Maximum (100 percentile) height
<b>II. Biomass Estimation II</b>	
NHBin5	Normalized height bin from 2 to 5m
NHBin10	Normalized height bin from 5 to 10m
NHBin15	Normalized height bin from 10 to 15m
NHBin20	Normalized height bin from 15 to 20m



NHBin25	Normalized height bin from 20 to 25m
NHBin30	Normalized height bin from 25 to 30m
NHBin35	Normalized height bin from 30 to 35m
NHBin40	Normalized height bin from 35 to 40m
NHBin45	Normalized height bin from 40 to 45m

Table 3-6. Lake Venado 1 plot biomass using quadratic-mean-stem-diameter

	DBH class (cm)						
	5 to50	51-100	101-150	151-200	201-250	251-300	>301
Number of trees present in plot (1)	21	5	3	3	1	1	1
QMSD, Midpoint of class (cm) (2)	22.7	72.5	131.6	165.6	222	299	376
Biomass of tree at midpt (kg tree <sup>-1</sup> ) (Chave et al 2005) (3)	105.69	2,173.78	12,662.96	20,051.37	33,589.56	56,198.81	120,209.8
Biomass of all trees (Mg plot <sup>-1</sup> ) ([1*3]/1000)	2.21	10.86	37.98	60.15	33.58	56.19	120.21
Total AGB (Mg plot <sup>-1</sup> )	321.23						

Table 3-7. Referenced biomass from three allometric equations

Plot	Location	DBH (cm)	H (m)	Mean Biomass, Mg plot <sup>-1</sup> (Brown, 1997)	Mean Biomass, Mg plot <sup>-1</sup> (Ketterings et al. 2001)	Mean Biomass, Mg plot <sup>-1</sup> (Chave et al. 2005)
1	Hotmud	20-145	2.8-24.4	251.7635	88.1334	102.6893
2	Antapan	21-432	2.9-30.2	1165.997	360.1668	347.2175
3	Sayaban HS	15-136	3.1-18.4	323.2434	112.99	104.2796
4	Sayaban Elem School	64-138	6.6-31.7	325.359	112.84	112.494
5	Bongolanon	11.5-206	2.3-27.6	247.7589	85.5757	103.7921
6	Tawasan1	13-252	4.7-32.3	459.3474	155.3211	128.2037
7	Tawasan2	27-184	8.5-32.7	293.4051	103.4965	166.5663
8	Tawasan3	15-200	4.4-31.9	283.4871	100.3849	131.442
9	New Israel1	9.5-280	2.1-35	424.2322	160.8764	255.7743
10	New Israel2	13-196	3-34.1	380.9687	129.7652	200.8526
11	New Israel3	15-233	5.3-33.4	305.0471	114.6014	168.206
12	Matiaw1	14-237	4.5-37.7	435.9379	148.3309	215.9812
13	Matiaw2	13-161	6.4-25	206.5257	69.0125	87.1752
14	Matiaw3	10-186	3.9-38.4	289.4739	98.4986	159.7602
15	Lake Venado1	10-376	3-27.1	971.5203	281.4299	321.2298
16	Lake Venado2	6.5-441	2.6-25.2	1367.465	368.6408	371.8705

Table 3-8. Plot-level carbon stock estimates by management zone

Management zone	N (Plots)	Mean Carbon, Mg C plot <sup>-1</sup> (Brown, 1997)	Mean Carbon, Mg C plot <sup>-1</sup> (Ketterings et al. 2001)	Mean Carbon, Mg C plot <sup>-1</sup> (Chave et al. 2005)
Multiple use	9	169.0472	59.76951	76.20059
Strict Protection	2	584.7463	162.5177	173.2751
Restoration	5	234.9698	76.41422	91.28234

Table 3-9. Summary of regression results using percentile heights

	Stepwise		Generalized Linear Model		Model Selected
	R <sup>2</sup>	F-stat	AICc	Prob>X <sup>2</sup>	
<b>I. Brown's Equation</b>					
Linear model	0.49	0.5937	240	0.3080	
Log-log model	-		73.70	0.0351 <sup>a</sup>	GLM with lower AIC
<b>II. Chave's Equation</b>					
Linear model	0.50	0.5622	241.97	0.1890	
Log-log model	-		68.87	0.0560 <sup>b</sup>	GLM with lower AIC
<b>III. Kettering's Equation</b>					
Linear model	0.45	0.6706	244	0.2897	
Log-log model	-		71.31	0.0608 <sup>b</sup>	GLM with lower AIC

<sup>a</sup> model is significant at  $\alpha = 0.05$

<sup>b</sup> model is significant at  $\alpha = 0.10$

Table 3-10. GLM model regression results using percentile heights (Brown 1997)

Brown\_Percentile - Generalized Linear Model - JMP

**Generalized Linear Model Fit**

Overdispersion parameter estimated by Maximum Likelihood  
 Response: In\_AGB (Mg/plot)  
 Distribution: Normal  
 Link: Identity  
 Estimation Method: Maximum Likelihood  
 Observations (or Sum Wgts) = 16

**Whole Model Test**

	L-R			
Model	-LogLikelihood	ChiSquare	DF	Prob>ChiSq
Difference	8.27741775	16.5548	8	0.0351*
Full	4.85284977			
Reduced	13.1302675			

**Goodness Of Fit**

Fit Statistic	ChiSquare	DF	Prob>ChiSq	Overdispersion
Pearson	1.7183	7	0.9738	0.1074
Deviance	1.7183	7	0.9738	

AICc  
73.7057

**Effect Tests**

	L-R		
Source	DF	ChiSquare	Prob>ChiSq
In_MaxH	1	2.7863588	0.0951
In_MeanH	1	5.6965439	0.0170*
In_SDH	1	1.2404576	0.2654
In_Per25H	1	4.9868969	0.0255*
In_Per50H	1	5.8493449	0.0156*
In_Per75H	1	5.6859174	0.0171*
In_Per90H	1	1.3683012	0.2421
In_Per95H	1	5.6902631	0.0171*

**Parameter Estimates**

	L-R					
Term	Estimate	Std Error	ChiSquare	Prob>ChiSq	Lower CL	Upper CL
Intercept	5.5623559	5.115942	1.1405014	0.2855	-5.097776	16.222487
In_MaxH	-0.451361	0.258716	2.7863588	0.0951	-0.99045	0.0877278
In_MeanH	68.948532	26.358319	5.6965439	0.0170*	14.025479	123.87158
In_SDH	-4.413218	3.8859079	1.2404576	0.2654	-12.51032	3.683881
In_Per25H	-11.08602	4.5829155	4.9868969	0.0255*	-20.63548	-1.536559
In_Per50H	-17.09186	6.4318377	5.8493449	0.0156*	-30.49394	-3.689788
In_Per75H	-15.71304	6.0136035	5.6859174	0.0171*	-28.24364	-3.182446
In_Per90H	-6.116359	5.1174177	1.3683012	0.2421	-16.77957	4.5468476
In_Per95H	-11.17928	4.2765261	5.6902631	0.0171*	-20.09031	-2.268244

Table 3-11. GLM model regression results using percentile heights (Chave et al. 2005)

Chave\_Percentile - Generalized Linear Model - JMP

**Generalized Linear Model Fit**

Overdispersion parameter estimated by Maximum Likelihood  
 Response: ln\_AGB(Mg/plot)  
 Distribution: Normal  
 Link: Identity  
 Estimation Method: Maximum Likelihood  
 Observations (or Sum Wgts) = 16

**Whole Model Test**

Model	-LogLikelihood	L-R		
		ChiSquare	DF	Prob> ChiSq
Difference	7.58278011	15.1656	8	0.0560
Full	2.43942441			
Reduced	10.0222045			

**Goodness Of Fit**

Fit Statistic	ChiSquare	DF	Prob> ChiSq	Overdispersion
Pearson	1.2708	7	0.9892	0.0794
Deviance	1.2708	7	0.9892	

AICc  
68.8788

**Effect Tests**

Source	DF	L-R	
		ChiSquare	Prob> ChiSq
ln_MaxH	1	2.1219046	0.1452
ln_MeanH	1	2.3707281	0.1236
ln_SDH	1	0.1104749	0.7396
ln_Per25H	1	0.6200083	0.4310
ln_Per50H	1	4.1272512	0.0422*
ln_Per75H	1	1.4175213	0.2338
ln_Per90H	1	0.6744282	0.4115
ln_Per95H	1	6.0544462	0.0139*

**Parameter Estimates**

Term	Estimate	Std Error	L-R			
			ChiSquare	Prob> ChiSq	Lower CL	Upper CL
Intercept	10.045608	4.3996388	4.5126852	0.0336*	0.878043	19.213173
ln_MaxH	-0.335147	0.2224921	2.1219046	0.1452	-0.798756	0.1284615
ln_MeanH	36.235647	22.667787	2.3707281	0.1236	-10.99741	83.468707
ln_SDH	1.1126688	3.3418267	0.1104749	0.7396	-5.850724	8.0760614
ln_Per25H	-3.133667	3.9412435	0.6200083	0.4310	-11.34607	5.0787353
ln_Per50H	-12.00233	5.5312909	4.1272512	0.0422*	-23.52793	-0.476732
ln_Per75H	-6.296238	5.1716152	1.4175213	0.2338	-17.07238	4.479901
ln_Per90H	-3.652606	4.400908	0.6744282	0.4115	-12.82282	5.5176034
ln_Per95H	-9.976962	3.6777529	6.0544462	0.0139*	-17.64033	-2.313597

Table 3-12. GLM model regression results using percentile heights (Ketterings et al. 2001)

Kettering's\_Percentile - Generalized Linear Model - JMP

**Generalized Linear Model Fit**

Overdispersion parameter estimated by Maximum Likelihood  
 Response: ln\_AGB (Mg/plot)  
 Distribution: Normal  
 Link: Identity  
 Estimation Method: Maximum Likelihood  
 Observations (or Sum Wgts) = 16

**Whole Model Test**

Model	-LogLikelihood	L-R		
		ChiSquare	DF	Prob>ChiSq
Difference	7.45925724	14.9185	8	0.0607
Full	3.65763382			
Reduced	11.1168911			

**Goodness Of Fit**

Fit Statistic	ChiSquare	DF	Prob>ChiSq	Overdispersion
Pearson	1.4798	7	0.9830	0.0925
Deviance	1.4798	7	0.9830	

AICc  
71.3153

**Effect Tests**

Source	DF	L-R	
		ChiSquare	Prob>ChiSq
ln_MaxH	1	2.7352898	0.0982
ln_MeanH	1	4.9818683	0.0256*
ln_SDH	1	0.9625852	0.3265
ln_Per25H	1	4.0708233	0.0436*
ln_Per50H	1	5.2937993	0.0214*
ln_Per75H	1	4.756059	0.0292*
ln_Per90H	1	1.2889235	0.2562
ln_Per95H	1	5.1643573	0.0231*

**Parameter Estimates**

Term	Estimate	Std Error	L-R		
			ChiSquare	Prob>ChiSq	Lower CL Upper CL
Intercept	4.8938042	4.7477012	1.0287038	0.3105	-4.999021 14.786629
ln_MaxH	-0.414675	0.2400938	2.7352898	0.0982	-0.914961 0.0856101
ln_MeanH	59.136319	24.461072	4.9818683	0.0256*	8.1665768 110.10606
ln_SDH	-3.591986	3.6062039	0.9625852	0.3265	-11.10626 3.9222921
ln_Per25H	-9.156935	4.2530415	4.0708233	0.0436*	-18.01903 -0.294836
ln_Per50H	-14.95165	5.96888	5.2937993	0.0214*	-27.38905 -2.514243
ln_Per75H	-13.13376	5.5807499	4.756059	0.0292*	-24.76241 -1.505101
ln_Per90H	-5.502086	4.7490708	1.2889235	0.2562	-15.39776 4.3935932
ln_Per95H	-9.798135	3.9687057	5.1643573	0.0231*	-18.06776 -1.528509

Table 3-13. Summary of regression results using normalized height bins

	Stepwise		Generalized Linear Model		Model Selected
	R <sup>2</sup>	F-stat	AICc	Prob>X <sup>2</sup>	
I. Brown's Equation					
Linear model	0.52	0.0080 <sup>a</sup>	299.88	0.0159 <sup>a</sup>	Stepwise regression
Log-log model	-		-		
II. Chave's Equation					
Linear model	0.46	0.0175 <sup>a</sup>	259.06	0.0335 <sup>a</sup>	Stepwise regression
Log-log model	-		-		
III. Kettering's Equation					
Linear model	0.44	0.0226 <sup>a</sup>	260.87	0.0457 <sup>a</sup>	Stepwise regression
Log-log model	-		-		

<sup>a</sup> model is significant at  $\alpha = 0.05$

Table 3-14. Stepwise regression results using normalized height bins (Brown, 1997)

Response AGB (Mg/plot)

**Summary of Fit**

RSquare	0.523885
RSquare Adj	0.450636
Root Mean Square Error	262.7166
Mean of Response	483.2208
Observations (or Sum Wgts)	16

**Analysis of Variance**

Source	DF	Sum of Squares	Mean Square	F Ratio	Prob > F
Model	2	987283.4	493642	7.1522	
Error	13	897260.3	69020		
C. Total	15	1884543.7			0.0080*

**Parameter Estimates**

Term	Estimate	Std Error	t Ratio	Prob >  t	VIF
Intercept	312.17224	86.50163	3.61	0.0032*	.
NHBin25	188280.6	50004.58	3.77	0.0024*	2.1805303
NHBin30	-449860.3	149362.5	-3.01	0.0100*	2.1805303

Table 3-15. Stepwise regression results using normalized height bins (Chave et al., 2005)

<b>Fit Group</b>					
<b>Response AGB (Mg/plot)</b>					
<b>Summary of Fit</b>					
RSquare		0.463484			
RSquare Adj		0.380943			
Root Mean Square Error		72.69871			
Mean of Response		186.0959			
Observations (or Sum Wgts)		16			
<b>Analysis of Variance</b>					
		Sum of			
<b>Source</b>	<b>DF</b>	<b>Squares</b>	<b>Mean Square</b>	<b>F Ratio</b>	
Model	2	59353.79	29676.9	5.6152	
Error	13	68706.33	5285.1		<b>Prob &gt; F</b>
C. Total	15	128060.12			0.0175*
<b>Parameter Estimates</b>					
<b>Term</b>	<b>Estimate</b>	<b>Std Error</b>	<b>t Ratio</b>	<b>Prob&gt; t </b>	<b>VIF</b>
Intercept	137.55659	23.93666	5.75	<.0001*	.
NHBin25	45729.014	13837.22	3.30	0.0057*	2.1805303
NHBin30	-84949.44	41331.46	-2.06	0.0605	2.1805303

Table 3-16. Stepwise regression results using normalized height bins (Ketterings et al., 2001)

<b>Response AGB (Mg/plot)</b>					
<b>Summary of Fit</b>					
RSquare		0.441709			
RSquare Adj		0.355818			
Root Mean Square Error		76.17514			
Mean of Response		155.629			
Observations (or Sum Wgts)		16			
<b>Analysis of Variance</b>					
		Sum of			
<b>Source</b>	<b>DF</b>	<b>Squares</b>	<b>Mean Square</b>	<b>F Ratio</b>	
Model	2	59682.34	29841.2	5.1427	
Error	13	75434.47	5802.7		<b>Prob &gt; F</b>
C. Total	15	135116.81			0.0226*
<b>Parameter Estimates</b>					
<b>Term</b>	<b>Estimate</b>	<b>Std Error</b>	<b>t Ratio</b>	<b>Prob&gt; t </b>	<b>VIF</b>
Intercept	113.16684	25.0813	4.51	0.0006*	.
NHBin25	46345.876	14498.91	3.20	0.0070*	2.1805303
NHBin30	-109490.4	43307.91	-2.53	0.0252*	2.1805303



Table 4-1. Selected papers on biomass estimation in tropics using SAR technology

Sensor name	Index/method	Paper	Accuracy assessment
JERS-1, MODIS, QSCAT, SRTM	Decision tree, spline regression	Saatchi et al (2007)	OA = 88%
JERS-1	Calibration accuracy of high-resolution radar mosaic of SE Asia	Shimada and Isoguchi (2002)	Calibration accuracy = 1.1dB, Average geometric accuracy = 406 m
ALOS Palsar, Landsat ETM	AGB, SVM	Wijaya and Gloaguen (2009)	OA = 90.55%
InSAR	AGB	Neef et al (2005)	R2 = 0.89

Table 4-2. Intermap's STAR-3i technical specifications

Parameters	STAR-3i
Aircraft	Learjet 36A
Typical flight velocity	750 km/hour
Typical flight altitude above sea level	3-10 km
Ground swath width	3-10 km
Center frequency	9.57 GHz (X-band)
Range bandwidth	67.5 & 135 MHz, 270 MHz
Antenna elevation	30-60°
Polarization	HH
IFSAR baseline	0.9 m
Best image resolution	0.625 cm

Table 4-3. Specifications of Intermap's core products

STAR Product	Post Spacing/Pixel size	RMSE Accuracy	Datum Coordinate Systems	Format
DSM	5 m (nominal)	Type I: 0.5 m Type II: 1.0 m Type III:3.0 m	As required	32-bit,bil and header info
DTM	5 m (nominal)	Type I: 0.7 m Type II: 1.0 m	As required	32-bit,bil and header info
ORI	0.625 m, 1.25 m, or 2.5 m (nominal)	2.0 m	As required	8-bit GeoTiff

Table 4-4. 2013 IFSAR Product Accuracy

Product	RMSE	Pixel size
DSM (Type II) X band	1 m vertical, 2 m horizontal	5 m
DTM (Type II) L band	1 m vertical, 2 m horizontal	5 m
ORI	2 m	0.625 m

Table 4-5. Relating field height and CHM-derived height by management zones

Management zone	Number of plots	Regression results	R <sup>2</sup>	RMSE
Multiple use	13	F_Height = 5.18 + 1.03 (CHM_Height)	0.68	3.86
Strict protection	7	F_Height = 2.51 + 1.25 (CHM_Height)	0.85	3.33
Restoration zone	6	F_Height = -1.56 + 1.78 (CHM_Height)	0.91	2.09
All zones	26	F_Height = 1.91 + 1.35 (CHM_Height)	0.75	4.30

Table 4-6. Regression variables for 5 modelling tiers

Biomass Model	List of variables
I – IFSAR_5m	Percentile heights, average slope, average aspect, average elevation
II-IFSAR_resampled (uncalibrated)	Maximum height, average slope, average aspect, average elevation, ORI texture variance, CHM texture variance
III-IFSAR_resampled (calibrated)	Maximum height, average slope, average aspect, average elevation, ORI texture variance, CHM texture variance
IV- Landsat_resampled	PC1, NIR variance, NDVI, SR
V- Landsat_resampled and IFSAR_resampled (uncalibrated)	PC1, NIR variance, NDVI, SR Maximum height, average slope, average aspect, average elevation, ORI texture variance, CHM texture variance
Dependent variable	Aboveground biomass (Mg plot <sup>-1</sup> )

Table 4-7. Regression results using standard least squares in JMP software

Biomass Model	R <sup>2</sup>	RMSE (Mg plot <sup>-1</sup> )	F-stat	VIF
I – IFSAR_5m	0.85	398	0.0004 <sup>a</sup>	>10
II-IFSAR_resampled (uncalibrated)				
3.1. Nearest Neighbor	0.395	293	0.1059 <sup>a</sup>	<10
3.2. Bilinear interpolation	0.431	284	0.0675 <sup>b</sup>	<10
3.3. Cubic Convolution	0.434	283	0.0646 <sup>b</sup>	<10
III-IFSAR_resampled (calibrated)				
3.1. Nearest Neighbor	0.393	293	0.1077	<10
3.2. Bilinear interpolation	0.431	284	0.0674 <sup>b</sup>	<10
3.3. Cubic Convolution	0.434	283	0.0644 <sup>b</sup>	<10
IV- Landsat_resampled	0.09	327	0.6793	>10
V – Landsat resampled and IFSAR resampled (uncalibrated)				
5.1. Nearest Neighbor	0.27	320	0.2806	>10
5.2. Bilinear interpolation	0.39	329	0.0789 <sup>b</sup>	>10
5.3. Cubic Convolution	0.40	323	0.0695 <sup>b</sup>	>10

<sup>a</sup> model is significant at  $\alpha = 0.05$

<sup>b</sup> model is significant at  $\alpha = 0.10$

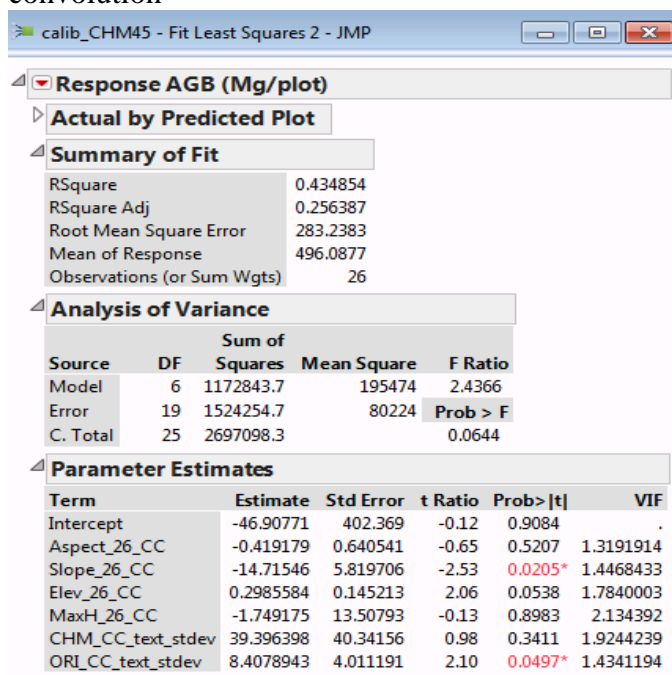
Table 4-8. Regression results using stepwise regression in JMP statistical software

Biomass Model	R <sup>2</sup>	RMSE (Mg plot <sup>-1</sup> )	F-stat	VIF
I – IFSAR_5m	0.32	365	0.0123 <sup>a</sup>	<10
II-IFSAR_resampled (uncalibrated)				
3.1. Nearest Neighbor	0.381	275	0.0128 <sup>a</sup>	<10
3.2. Bilinear interpolation	0.388	273	0.0115 <sup>a</sup>	<10
3.3. Cubic Convolution	0.395	272	0.0101 <sup>a</sup>	<10
III-IFSAR_resampled (calibrated)				
3.1. Nearest Neighbor	0.382	275	0.0128 <sup>a</sup>	<10
3.2. Bilinear interpolation	0.388	273	0.0115 <sup>a</sup>	<10
3.3. Cubic Convolution	0.395	272	0.0101 <sup>a</sup>	<10
IV- Landsat_resampled	0.12	314	0.0857	>10
V – Landsat resampled and IFSAR resampled (uncalibrated)				
5.1. Nearest Neighbor	0.31	318	0.0151 <sup>a</sup>	<10
5.2. Bilinear interpolation	0.29	328	0.0191 <sup>a</sup>	<10
5.3. Cubic Convolution	0.309	319	0.0141 <sup>a</sup>	<10

<sup>a</sup> model is significant at  $\alpha = 0.05$

<sup>b</sup> model is significant at  $\alpha = 0.10$

Table 4-9. Standard least squares regression model using calibrated IFSAR cubic convolution



**Response AGB (Mg/plot)**

**Actual by Predicted Plot**

**Summary of Fit**

RSquare	0.434854
RSquare Adj	0.256387
Root Mean Square Error	283.2383
Mean of Response	496.0877
Observations (or Sum Wgts)	26

**Analysis of Variance**

Source	DF	Sum of Squares	Mean Square	F Ratio
Model	6	1172843.7	195474	2.4366
Error	19	1524254.7	80224	Prob > F
C. Total	25	2697098.3		0.0644

**Parameter Estimates**

Term	Estimate	Std Error	t Ratio	Prob >  t	VIF
Intercept	-46.90771	402.369	-0.12	0.9084	.
Aspect_26_CC	-0.419179	0.640541	-0.65	0.5207	1.3191914
Slope_26_CC	-14.71546	5.819706	-2.53	0.0205*	1.4468433
Elev_26_CC	0.2985584	0.145213	2.06	0.0538	1.7840003
MaxH_26_CC	-1.749175	13.50793	-0.13	0.8983	2.134392
CHM_CC_text_stddev	39.396398	40.34156	0.98	0.3411	1.9244239
ORI_CC_text_stddev	8.4078943	4.011191	2.10	0.0497*	1.4341194

Table 4-10. Average biomass values in management zones

Management zone	Proportion (%)	Area (Ha)	No. of pixels (26.6 m <sup>2</sup> )	Average Biomass Level (Mg ha <sup>-1</sup> )
Strict Protection	45.9	25,201	413,426	118.6
Multiple use	51.5	28,340	464,917	94.8
Restoration	2.6	1,434	23,513	1,616.6
TOTAL	100	54,975	901,856	

Table 4-11. Compilation of results for the total estimated carbon stocks in the Philippines (Gibbs et al., 2007)

Compiled Harvest Data			Forest Inventory		
Source	Source	Source	Source	Source	Range of values
Olson et al (1983) and Gibbs (2006): 869 Mt C	Houghton (1999) and DeFries et al (2002): 765 Mt C	IPCC (2006): 2503 Mt C	Brown (1997), Achard et al (2002, 2004) : 1213 Mt C	Gibbs and Brown (2007a,2007b) :1530 Mt C	765-2503 Mt C

Table 4-12. Scientific paper examined on carbon storage in selected areas in the Philippines

Author	Area, Method	Location description	Estimated Carbon stocks
Han et al (2010)	Mt. Makiling Forest Reserve Destructive sampling, Soil respiration rate, bacteria count	60-year old secondary natural forest stand (1 ha) and large-leafed mahogany plantation (0.6 ha)	Carbon storage = 313.12 Mg C ha <sup>-1</sup> (natural forest stand), 185.28 Mg C ha <sup>-1</sup> (mahogany plantation)  R <sup>2</sup> for tree biomass in mahogany plantation range from 0.91 to 0.99
Lasco et al (2004)	Mt. Makiling Forest Reserve Non-destructive sampling	secondary natural forest stand	Carbon storage = 418 Mg C ha <sup>-1</sup> and sequester 5 Mg C ha <sup>-1</sup> year <sup>-1</sup>
Lasco et al (2006)	Effect of logging on C stocks Surigao del Sur	Selectively logged Dipterocarp forest	C stocks = 258 Mg C ha <sup>-1</sup> (unlogged forest), 34% is in SOC

Table 4-13. Comparison of methods for global carbon maps

	Carbon Maps	
	Saatchi et al (2011)	Baccini et al (2012)
Similarities	Chave et al (2005) allometric equation (D,H, WD)	Chave et al (2005) allometric equation (D,H)
Differences	<ul style="list-style-type: none"> <li>• 1 km resolution</li> <li>• 493 calibration field plots</li> <li>• 3 million canopy height estimates from GLAS satellite</li> <li>• MODIS/LAI/NDVI/VCT data</li> <li>• SRTM data (elevation)</li> <li>• QUICKSCAT data</li> <li>• MaxENT algorithm</li> </ul>	<ul style="list-style-type: none"> <li>• 500 m resolution</li> <li>• 283 calibration field plots</li> <li>• 5.5 million canopy height estimates from GLAS satellite</li> <li>• MODIS BRDF data (vegetation color)</li> <li>• SRTM data (elevation)</li> <li>• RandomForest algorithm</li> </ul>

Table 4-14. Hypothesis tests for distribution comparison of residuals and AGB residuals

<b>Distribution Comparison of Residuals &amp; AGB Residuals</b>				
Confidence Level		95.00%		
	Test Value	Critical Value	P-Value	
2 Sample t Test	-0.03	2.37	0.980	Fail to Reject the Ho that the Means are Equal
F Test	1.02	1.73	0.513	Fail to Reject the Ho that the Variances are Equal

Table 4-15. Hypothesis tests for normality of distribution for residuals

<b>Test for Normality of Distribution for Residuals</b>			
Confidence Level		95.0000%	
Procedure	Test Value	p-Value	
Shapiro-Wilks	0.968860145	0.593983098	Fail to Reject the Ho that the Distribution is Normally Distributed*
Anderson-Darling	0.307084914	0.539270633	Fail to Reject the Ho that the Distribution is Normally Distributed*
Cramer-von Mises	0.043598291	0.600159598	Fail to Reject the Ho that the Distribution is Normally Distributed*
Chi-Squared	3.461538462	0.94316171	Fail to Reject the Ho that the Distribution is Normally Distributed*
			*Based on approximate p-values

## **APPENDIX C**

### **PRE-RESEARCH ACTIVITIES**

This research undertaking involved a series of coordination with government officials and private entities in the Philippines.

On August 2011, I did an ocular visit to the research site together with my siblings. We paid the trekking permit at the Department of Tourism in Kidapawan City. We hired a tour guide to climb the Mt. Apo Natural Park, and camped for 2 nights.

In 2012, my research proposal was approved by the Research Committee.

#### **1.0.Coordination with Philippine Government**

In the 1<sup>st</sup> quarter of 2013, I initiated communication via email with the Regional Technical Director of Region XI - Department of Environment and Natural Resources (DENR). He is in charge of operations for the protected areas.

In his response, he listed the requirements for conducting research in the protected area. The requirements include: (1) submission of research proposal, (2) providing a letter of recommendation from the head of the department or college, and (3) obtaining approval from the Philippine Protected Area Management Board (PAMB) in a meeting. He also stated that the research permit would be issued after complying with these requirements.

## 2.0. Coordination with Military, Police and Local Government Units (LGUs)

Mt. Apo Natural Park is bounded by two regions, Region XI (Davao City and Davao del Sur) and Region XII (Central Mindanao).

### 2.1. LGU in Davao City

I wrote a letter to the City Mayor of Davao informing him about my research and our field work in park areas covering a portion of Davao.

### 2.2. LGU in Magpet, Cotabato

We met with the Chairman of Barangay Bongolanon and informed him of our research permit. He accompanied us to the Municipal Hall. We then completed some forms detailing the type of research we planned to conduct. I also wrote a letter to the Municipal Mayor. We then met with the Mayor, the Municipal Administrator and Tourism Officer.

### 2.3. LGU in Makilala, Cotabato

We submitted a letter to the Municipal Mayor of Makilala. In his lieu, the Municipal Administrator wrote a recommendation letter to the Barangay Chairman in New Israel.

### 2.4. LGU in Kidapawan City

We submitted a letter to the City Mayor. We also met with the City Tourism Officer.



## 2.5. LGU in Digos City

We submitted a letter to the City Mayor's office, but they referred me to the City Administrator's office. Unlike other LGUs, we were initially required to pay the climbing fees and to undergo medical tests. However, after providing additional explanations of our work, the climbing fees and medical exam requirements were waived. We were then issued individual ID cards.

## 3.0. Security Arrangement in Region XI

We met with the Philippine Army personnel in the Calinan District. He informed us that they were on a red alert status because of the reported sightings of rebels. He suggested that we wait for at least two weeks so they can clear the area and assign army soldiers to accompany us while conducting our fieldwork. We decided that we could not proceed with research work in the Calinan area.

After a month, we started another trip in the Kapatagan area. We were advised by the Barangay LGU to stop by the Philippine Army detachment in Sitio Mainit before starting our trekking. We met with the Army leader, and recorded our intended route in the area. He also provided us with his telephone number.

## 4.0. Security Arrangement in Region XII

We met the Provincial Director in Amas Provincial Police Headquarters in Kidapawan City. We were granted four civilian escort, each escort taking turns during our entire fieldwork.

## 5.0. Energy Development Corporation (EDC)

A request letter was also sent to the EDC office. We were accompanied by two EDC staff to our sampling plots in the EDC area. On our way out of the park, we dropped by the EDC office for a courtesy visit.